Earth-Science Reviews 231 (2022) 104073

Contents lists available at ScienceDirect

Earth-Science Reviews

journal homepage: www.elsevier.com/locate/earscirev

A persistent non-uniformitarian paleomagnetic field in the Devonian?

Annique van der Boon [a,*,1], Andrew J. Biggin [a], Daniele Thallner [a,2], Mark W. Hounslow [a,b], Richard Bono [a,3], Jerzy Nawrocki [c], Krystian Wójcik [d], Mariusz Paszkowski [d], Peter Königshof [e], Tim de Backer [f], Pavel Kabanov [g], Sofie Gouwy [g], Richard VandenBerg [g], Anne-Christine Da Silva [h]

[a] Geomagnetic Laboratory, Oliver Lodge Building, Department of Physics, Oxford Street, Liverpool L69 7ZE, United Kingdom
[b] Lancaster Environment Centre, Lancaster University, UK
[c] Faculty of Earth Sciences and Spatial Management, Maria Curie-Skłodowska University, Al. Kraśnicka 2cd, 20-718 Lublin, Poland
[d] Polish Geological Institute – National Research Institute, Rakowiecka 4, 00-975 Warszawa, Poland
[e] Senckenberg Research Institute and Natural History Museum, Senckenberganlage 25, 60325 Frankfurt, Germany
[f] Department of Geology, Ghent University, 9000, Ghent, Belgium
[g] Geological Survey of Canada, Calgary, AB T2L 2A7, Canada
[h] Université de Liège, Departement of Geology, Allée du Six Août, 12, 4000 Liège, Belgium

ARTICLE INFO

Keywords:
Magnetostratigraphy
Paleomagnetism
Non-dipolarity
Remagnetisation
Paleobiological crises

ABSTRACT

The Devonian has long been a problematic period for paleomagnetism. Devonian paleomagnetic data are generally difficult to interpret and have complex partial or full overprints– problems that arise in data obtained from both sedimentary and igneous rocks. As a result, the reconstruction of tectonic plate motions, largely performed using apparent polar wander paths, has large uncertainty. Similarly, the Devonian geomagnetic polarity time scale is very poorly constrained. Paleointensity studies from volcanic units suggest that the field was much weaker than the modern field, and it has been hypothesised that this was accompanied by many polarity reversals (a hyperreversing field). We sampled Middle to Upper Devonian sections in Germany, Poland and Canada which show low conodont alteration indices, implying low thermal maturity. We show that there are significant issues with these data, which are not straightforward to interpret, even though no significant heating or remineralisation appears to have caused overprinting. We compare our data to other magnetostratigraphic studies from the Devonian and review the polarity pattern as presented in the Geologic Time Scale. Combined with estimates for the strength of the magnetic field, we suggest that the field during the Devonian might have been so weak, and in part non-dipolar, that obtaining reliable primary paleomagnetic data from Devonian rocks is challenging. Careful examination of all data, no matter how unusual, is the best way to push forward our understanding of the Devonian magnetic field. Paleointensity studies show that the field during the Devonian had a similar low strength to the Ediacaran. Independent evidence from malformed spores around the Devonian-Carboniferous boundary suggests that the terrestrial extinction connected to the Hangenberg event was caused by increased UV-B radiation, supporting the weak field hypothesis. A fundamentally weak and possibly non-dipolar field during the Devonian could have been produced, in part, by true polar wander acting to maximise core-mantle heat flow in the equatorial region. It may also have influenced evolution and extinctions in this time period. There are a large number of paleobiological crises in the Devonian, and we pose the question, did the Earth's magnetic field influence these crises?

* Corresponding author.
E-mail address: AvanderBoon.work@gmail.com (A. van der Boon).
[1] Centre for Earth Evolution and Dynamics, University of Oslo, Norway
[2] Department of Geological Sciences, University of Florida, Gainesville, FL 32611, USA
[3] Department of Earth, Ocean and Atmospheric Science, Florida State University, Tallahassee, Florida, United States 32306

https://doi.org/10.1016/j.earscirev.2022.104073
Received 28 March 2022; Received in revised form 26 May 2022; Accepted 31 May 2022
Available online 3 June 2022

1. Introduction

The Devonian Period lasted for around 60 million years, and spanned the time from 419 to 359 million years ago (Becker et al., 2020). The Devonian was a key interval in which land-plant cover expanded from a ground-level green skin, localized in wet habitats, to extensive forests across humid regions (Le Hir et al., 2011). The first seed plants appeared in the middle Famennian (Prestianni and Gerrienne, 2010), and the first terrestrial tetrapods in the Eifelian (Niedźwiedzki et al., 2010). Life flourished in the oceans, and marine faunas attained their highest genus-level richness for the entire Paleozoic in the Givetian-Frasnian (e.g., Bambach et al., 2002). At the same time, reefs with a high diversity of metazoan organisms reached their peak abundance for the Paleozoic (Kiessling et al., 2003). Devonian paleogeography comprised three major continents. The largest of these, Gondwana, consisted of present-day South America, Africa, Madagascar, Arabia, India, Antarctica and Australia, and was positioned in the high latitudes of the southern hemisphere. Gondwana made up more than half of all landmass on Earth (Torsvik, 2019). Laurussia consisted of North America, Greenland and Baltica and was positioned in low latitudes, straddling the equator, while Siberia was positioned in the northern hemisphere (Torsvik and Cocks, 2013). During the Devonian, the terrestrial facies of the 'Old Red Sandstone' were deposited in large parts of present-day northwest Europe, Greenland and northeast North America. The climate during the Devonian is generally considered to be warm (Joachimski et al., 2009; Marcilly et al., 2021; Scotese et al., 2021). Throughout the Middle and Late Devonian, the atmospheric pO_2 rose from ~0.7 of the present-day atmospheric level (PAL) to present-day concentration, while pCO_2 has been interpreted to have dropped from 5.0-6.0 PAL to just slightly more than the pre-industrial Holocene level, based on modelling (Lenton et al., 2018). This major shift in Earth surface conditions is likely linked to the spread of land vegetation, including wetland forests (Le Hir et al., 2011; Strother et al., 2010). At the end of the Devonian, the climate cooled and gradually descended into the Late Paleozoic Ice Age, with a first glaciation event during the Famennian (Lakin et al., 2016). The Devonian was a time of many biotic crises in the marine realm, particularly in the Middle and Late Devonian. As reviewed by McGhee et al. (2013), the genus-level taxonomic loss identifies four Devonian extinctions (latest Eifelian, late Givetian, Frasnian-Famennian, Devonian-Carboniferous boundary) in the 10 most severe extinctions of the post-Cambrian Phanerozoic. These same events also enter the top-ten list based on estimates of their ecologic severity (McGhee et al., 2013). Other events during the Devonian were taxonomic radiations, a cascade of evolutionary innovations in marine faunas and sudden spreads of marine organisms linked to transgressions (Becker et al., 2016). Causes for nearly all of these perturbations are still heavily debated (e.g., Aretz, 2021; Boyer et al., 2021; Fields et al., 2020; Kaiho et al., 2021; Marshall, 2021; McGhee and Racki, 2021; Paschall et al., 2019). Many of the perturbations share similarities, as most are coincident with spreads of shelfal anoxia, manifested as deposits of black shale with a shallow, often photic-zone chemocline fluctuation in the water column (Kabanov and Jiang, 2020). Some of them also share anoxia-linked effects, such as narrowing benthic habitats and ocean acidification. The nature and magnitude of sea-level fluctuations during the Devonian is still a matter of debate (Carmichael et al., 2019; Kabanov and Jiang, 2020). Two of the Devonian perturbations are classified as major mass extinction events, firstly at the Frasnian-Famennian boundary (Kellwasser; see Carmichael et al., 2019) and secondly at the Devonian-Carboniferous boundary (Hangenberg; see Kaiser et al., 2016).

Since the early days of paleomagnetism, researchers have focused on obtaining paleopoles from Devonian rocks to reconstruct paleolatitudes and motions of the continents. However, Devonian paleomagnetic data have been troubling, with many later studies arguing that data from previous studies were unreliable due to remagnetisations (e.g., Abrajevitch et al., 2007; Aïfa, 1993; Aïfa et al., 1990; Bachtadse et al., 1987; Bachtadse and Briden, 1991; Bachtadse and Briden, 1990; Bachtadse and Briden, 1989; Briden et al., 1984; Huang et al., 2000; Schmidt et al., 1986; Smethurst and Khramov, 1992; Stearns et al., 1989). Although there is a wealth of studies that have attempted to obtain Devonian paleopoles, very few datasets are now considered of good quality (Van der Voo's Q >3; Van der Voo, 1990). This has resulted in a scarcity of reliable data for the reconstruction of apparent polar wander paths (Torsvik et al., 2012). This dearth of data also impacts the sparse knowledge of geomagnetic polarity changes during the Devonian (see Fig. 1). Although polarity patterns are presented for the Early Devonian and part of the Middle Devonian (Becker et al., 2012), and more recently also for the Late Devonian (Becker et al., 2020; Hansma et al., 2015; Ogg et al., 2016a), large portions of the Devonian are unresolved in detail (marked with grey in the timescale; Fig. 1). The magnetic polarity patterns have furthermore not been confirmed through studies of sections in different parts of the world, or are based on data that are poorly accessible (Lower and Middle Devonian; e.g., Guzhikov, 2019; Ogg and Smith, 2004). There is a strong need for many more magnetostratigraphic studies in the Paleozoic, and especially the Devonian. Studies on the strength of the magnetic field (paleointensity), show that it was very weak during the Devonian (e.g., Hawkins, 2018; Hawkins et al., 2021; Hawkins et al., 2019; Shcherbakova et al., 2021; Shcherbakova et al., 2017). Several studies have also hypothesised that the field was non-dipolar in some time intervals (Shatsillo and Pavlov, 2019; Shcherbakova et al., 2017).

1.1. This study

We set out to study several different Devonian sections of sedimentary rocks for magnetostratigraphy; to test reproducibility two sites with overlapping ages were chosen. Sections with low thermal maturity were selected, as indicated by a low conodont colour alteration index (CAI; Epstein et al., 1977; Rejebian et al., 1987) or T_{max} parameter (Peters and Cassa, 1994). CAI values of less than 3 indicate that sedimentary rocks were heated to an estimated maximum temperature of 200 °C (e.g., Königshof, 2003), which is below the resetting temperature of magnetic minerals that are typically ideal magnetic recorders. A T_{max} of less than 465°C is an indication that the kerogen thermal maturation did not proceed beyond the oil window (Peters and Cassa, 1994). Sections that do not show evidence for extensive remineralisation were explored, to maximise chances that these sections preserved a primary signal of the ancient magnetic field. We sampled four sections in Germany, Poland and Canada, in order to constrain the magnetostratigraphy of the Middle Devonian to the earliest Mississippian (see Fig. 2). A comparison of our data to the body of published paleomagnetic studies and review of the Devonian geomagnetic polarity timescale, paleopoles and paleointensity data was then performed. We discuss possible explanations for the prevalence of suboptimal data and controversial findings in this time period and present a hypothesis purporting that the paleomagnetic field was non-uniformitarian through some or all of the Devonian. A non-uniformitarian field may have contributed to a "Devonian paleomagnetic wasteland" as well as other geological phenomena reported at this time.

2. Geologic setting

2.1. Blankenheim, Germany

The Blankenheim section in the Eifel region of Germany (50.44104°N, 6.63705°E) comprises ca. 8 m of shales and carbonates (Junkerberg Fm and Freilingen Fm) of Eifelian age (Königshof et al., 2016). The section covers most of the *Tortodus kockelianus* conodont zone. Although the lower boundary of this conodont zone is unconstrained in the section, the top of the section contains the boundary between the *kockelianus* Zone and the overlying *Polygnathus ensensis* Zone (transition from the Junkerberg Fm to the Freilingen Fm; Fig. 3). Colour alteration indices for the Blankenheim section show very low

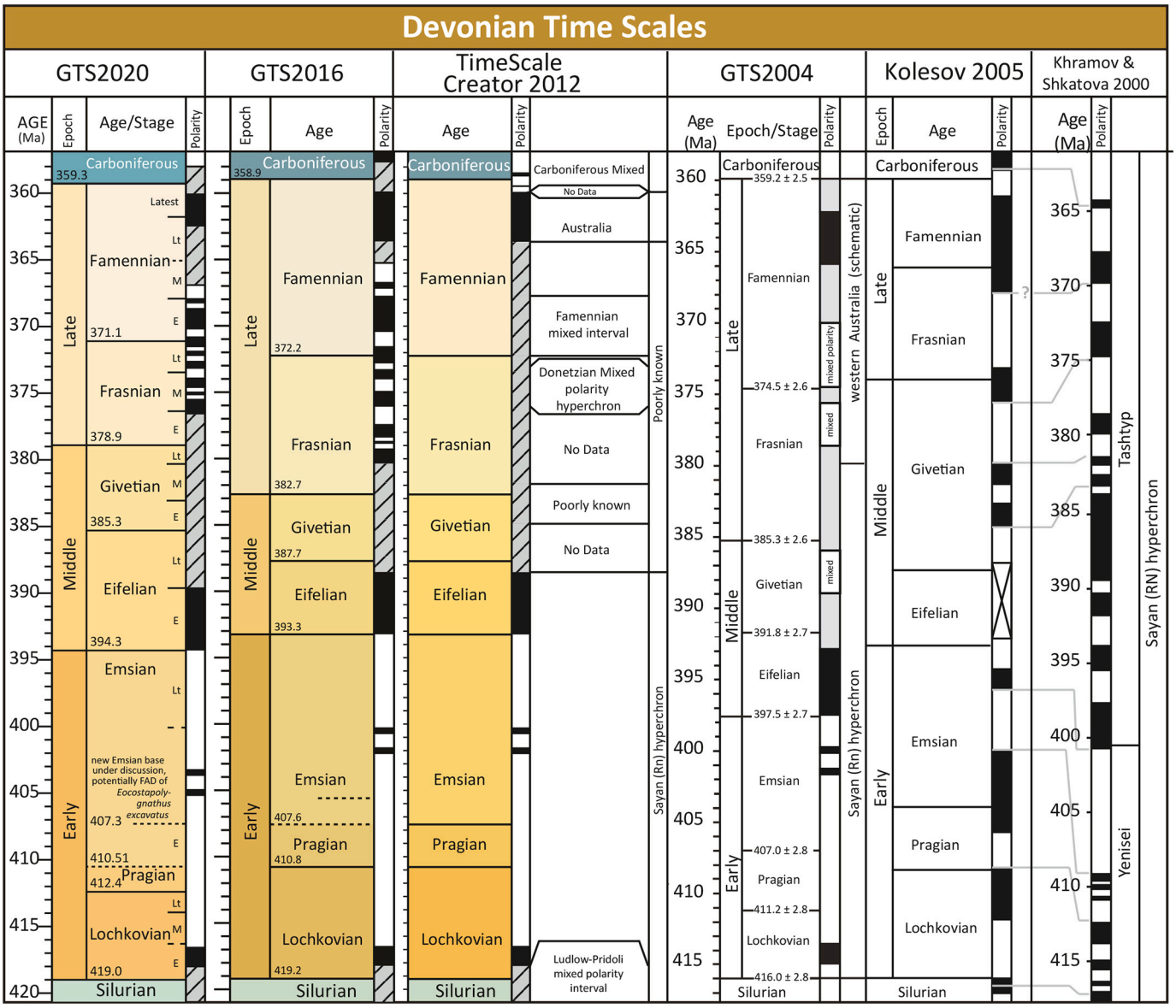

Fig. 1. A comparison between different geomagnetic polarity timescales from the Devonian. The GTS2020 timescale is from Becker et al. (2020). The GTS2016 timescale is from Ogg et al. (2016a), which is similar to the 2012 version of Becker et al. (2012) with the addition of the data from the Canning basin of Hansma et al. (2015) around the Frasnian-Famennian boundary. The 2012 timescale is made using TSCreator version 6.2 which is based on Becker et al. (2012). The GTS2004 timescale is from House and Gradstein (2004). The Russian time scale comparisons are modified after Kolesov (2005), who compares new results from outcrops from the Magadan, Sakha and Chukotka regions (far east Russia) to the timescale of Khramov and Shkatova (2000).

values for Devonian conodonts, around 1.5-2.0, indicating very low thermal maturity, equating to a maximum temperature of heating of ca. 80 °C (Königshof, 2003; Königshof et al., 2016).

2.2. Racławka and Czatkowice, Poland

The Racławka and Czatkowice sections are located in southern Poland, near the city of Krakow (Krzeszowice area). The Czatkowice section (50.15944° N, 19.64142° E) is the longer of the two, and is in a working quarry. The Racławka section is located in the Racławka Valley to the northeast of Czatkowice (50.17872° N, 19.68244° E). Both sections contain late Devonian-early Carboniferous limestones, which are correlated to sections in Belgium based on a foraminifer and coral biostratigraphy (Poty et al., 2007). The precise Devonian-Carboniferous level in the sections is not known, as the lithologies represent a shallow environment that lacks conodonts. Southern Poland was part of the Moravia-Silesia Basin during the Late Devonian and Mississippian, with the study region forming part of a carbonate platform that existed from the Eifelian (Middle Devonian) to the Viséan (a European stage correlating to the Middle Mississippian; Belka et al., 1996; Dvorák et al., 1995; Poty et al., 2007; Wójcik, 2012). The Devonian-Carboniferous succession in the Czatkowice Quarry and Racławka Valley was described by Paszkowski (in Dvorák et al., 1995), Łaptaś (1982) and Narkiewicz and Racki (1984). Paszkowski divided the lower part of the succession into 6 formations (from base to top): the Dubie Formation with the Góra Żarska Member at its top, Racławka Formation, Szklary Formation, Paczółtowice Formation, Pstrągarnia Formation and Przy Granicy Quarry Formation. The combined thickness of these formations is about 450 m. The succession of Carboniferous shallow-water limestones in the Czatkowice quarry is almost one kilometre thick, with the stratigraphic interval from the Czatkowice quarry in the Racławka Formation (containing the supposed Devonian-Carboniferous boundary level in the eastern quarry front), to the Czerna Formation of Viséan age (Paszkowski, in: Dvorák et al., 1995; Poty et al., 2007). Conodont

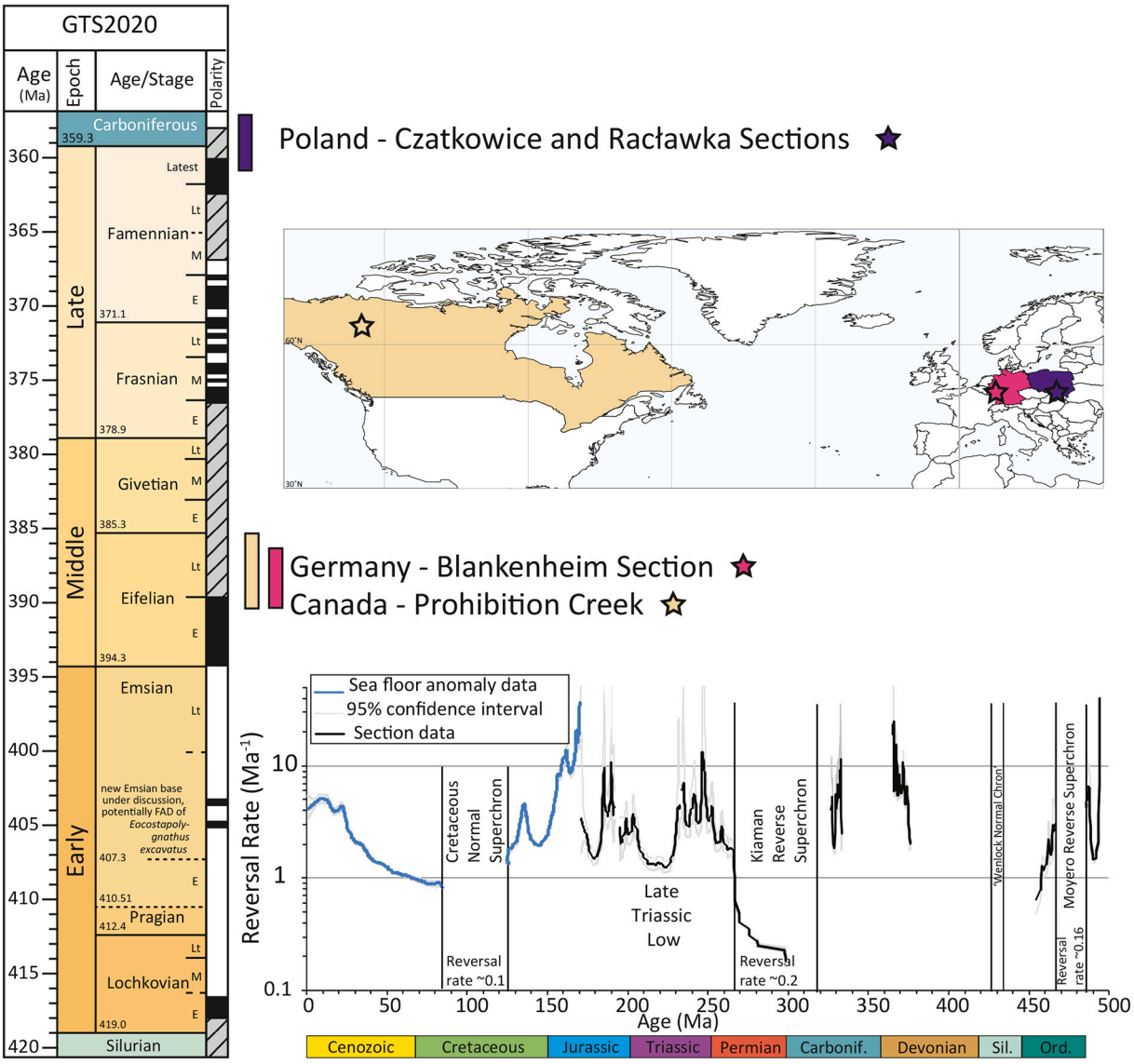

Fig. 2. The sampled sections with a map of their locations with the Devonian timescale from Becker et al. (2020) and estimated reversal rates for the timescale from 0-500 Ma (Hounslow et al., 2018).

biostratigraphy from the Przy Granicy Formation indicates an upper Tournaisian age (*Gnathodus cuneiformis* Zone; Appelt, 1998). Nearly 100 samples from 32 levels were collected from the Racławka Fm and Szklary Fm during several field campaigns from 2016-2018 (Fig. 4). CAI values at the sampled sections are around 1, although other localised areas closer to Permian intrusions have higher CAI (Belka, 1993).

2.3. Prohibition Creek, Canada

Prohibition Creek (65.18776° N, 126.22096° W) is located near Norman Wells, in the centre of the Sahtu First Nation Lands of the Northwest Territories in Canada. Prohibition Creek is a small creek that cuts the Norman Range of the Franklin Mountains and feeds into the Mackenzie River. Outcrops along Prohibition Creek range in age from Cambrian to Late Devonian (Fallas and McNaughton, 2013). We assessed the limestones of the Middle Devonian Hume Formation and the basinal mudrocks of the Middle Devonian Hare Indian and Frasnian Canol Formations (Kabanov, 2022). For an extended description of these units at Prohibition Creek, we refer to Kabanov et al. (2019). The Hare Indian and Canol shales were found too fissile to sample for paleomagnetic core plugs, therefore we focused on the limestones of the Hume Formation. Similar to the Blankenheim section, the Hume Formation covers the *Tortodus kockelianus* Zone of the Eifelian (Gouwy, 2022). In the Hume type section along the Hume River, the base of the Hume Fm is in the *Tortodus australis* Zone of earliest Late Eifelian age (Uyeno et al., 2017). The top of the Hume Fm, similar to the Blankenheim section, is in the *Polygnathus ensensis* Zone. The sampled interval in Prohibition Creek covers only the upper half of the Hume Fm. The lower part of the Hume Fm was not sampled, so comparisons of thickness between the Hume River and Prohibition Creek sections are difficult. The thickness of the Hume Fm is estimated to be 114.3 metres (Gouwy et al., 2021). The Prohibition Creek section was selected for its location in a zone of low thermal maturity where Tmax is within 426-465°C and where organic-matter biomarkers are well preserved (Kabanov and Jiang, 2020). Like the Blankenheim section, the CAI values in Prohibition Creek are very low (1.5-2.0; Gouwy, 2006). Because the Blankenheim section and the Prohibition Creek section both cover the same interval, they provide an excellent opportunity for comparison of paleomagnetic records from two different parts of the globe during the Eifelian. A lithological log of the section with sample positions is shown in Fig. 5.

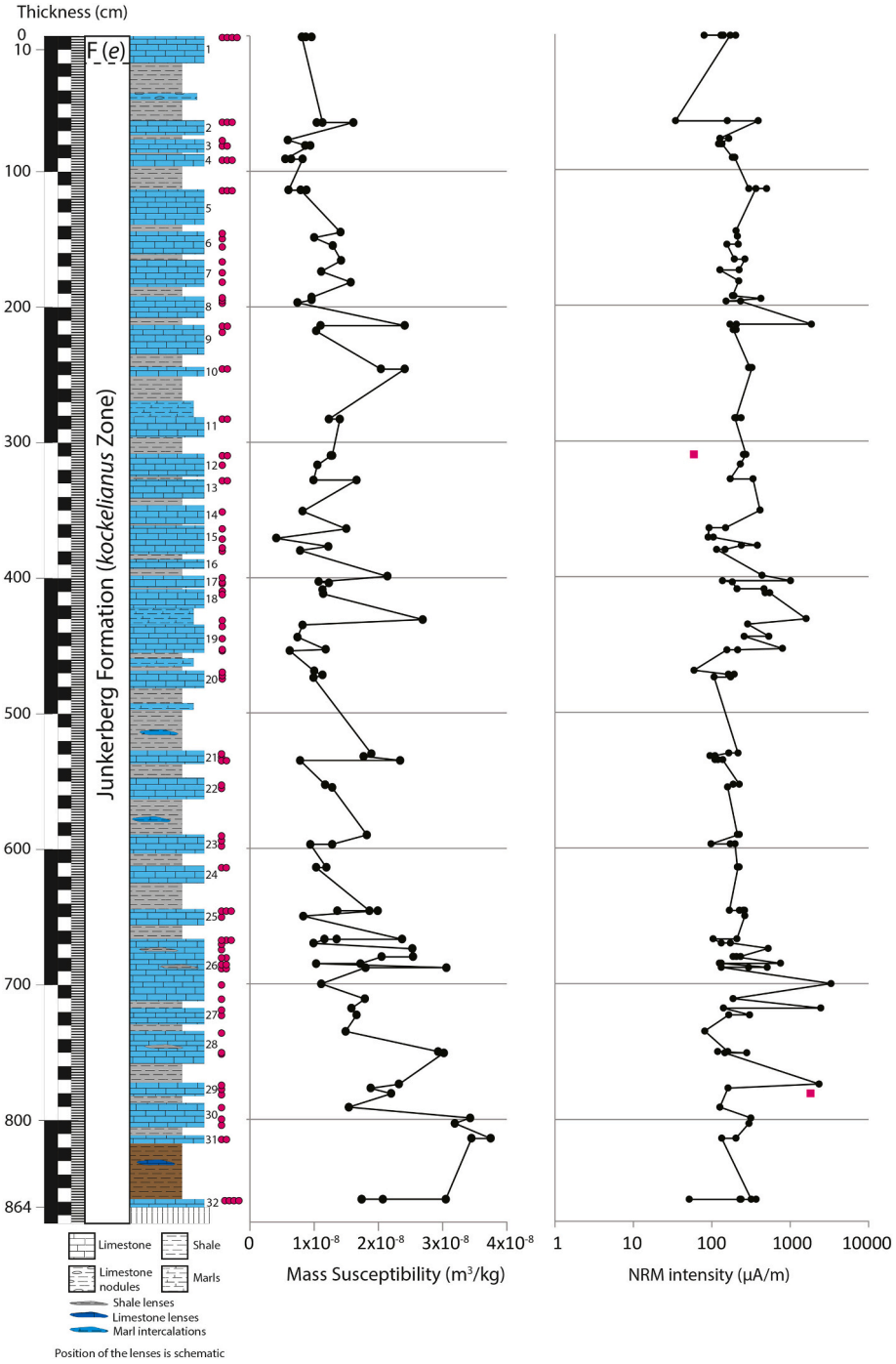

Fig. 3. Lithological log of the Blankenheim section with bed numbers, paleomagnetic sample positions (pink dots), bulk magnetic susceptibility and NRM intensity (measurements in pink squares have uncertainties of >20%). F(*e*) indicates the Freilingen Fm in the *ensensis* zone. The position of the boundary is inferred, based on correlation to Königshof et al. (2016).

3. Methods

3.1. Blankenheim, Germany

In July 2019, 100 samples were collected for magnetostratigraphy in the carbonates of the Blankenheim section. Standard paleomagnetic cores (25 mm Ø) were drilled using a gasoline-powered motor drill, and oriented using a magnetic compass. Shales in the section were too fissile to sample. Directions were corrected for a present-day declination (International Geomagnetic Reference Field; IGRF) of 2°. We provide a glossary of paleomagnetic acronyms in Table 1. Cores were subsequently cut into ca. 22 mm long specimens, and were processed at the University of Liverpool. A total of 39 specimens were subjected to stepwise thermal demagnetisation, 40 were demagnetised using three axis static alternating field (AF) demagnetisation, and another 29 specimens were demagnetised using a combination of thermal and AF demagnetisation. Thermal demagnetisation was performed by progressive heating in a shielded furnace with a hold time of one hour at peak temperature, in steps of 20-55 °C, up to 400 °C. AF demagnetisation was performed on the automated RAPID 2G-Entreprises Superconducting Rock Magnetometer (hereafter referred to as "RAPID"), equipped with three DC-SQUIDS (direct current-superconducting quantum interference

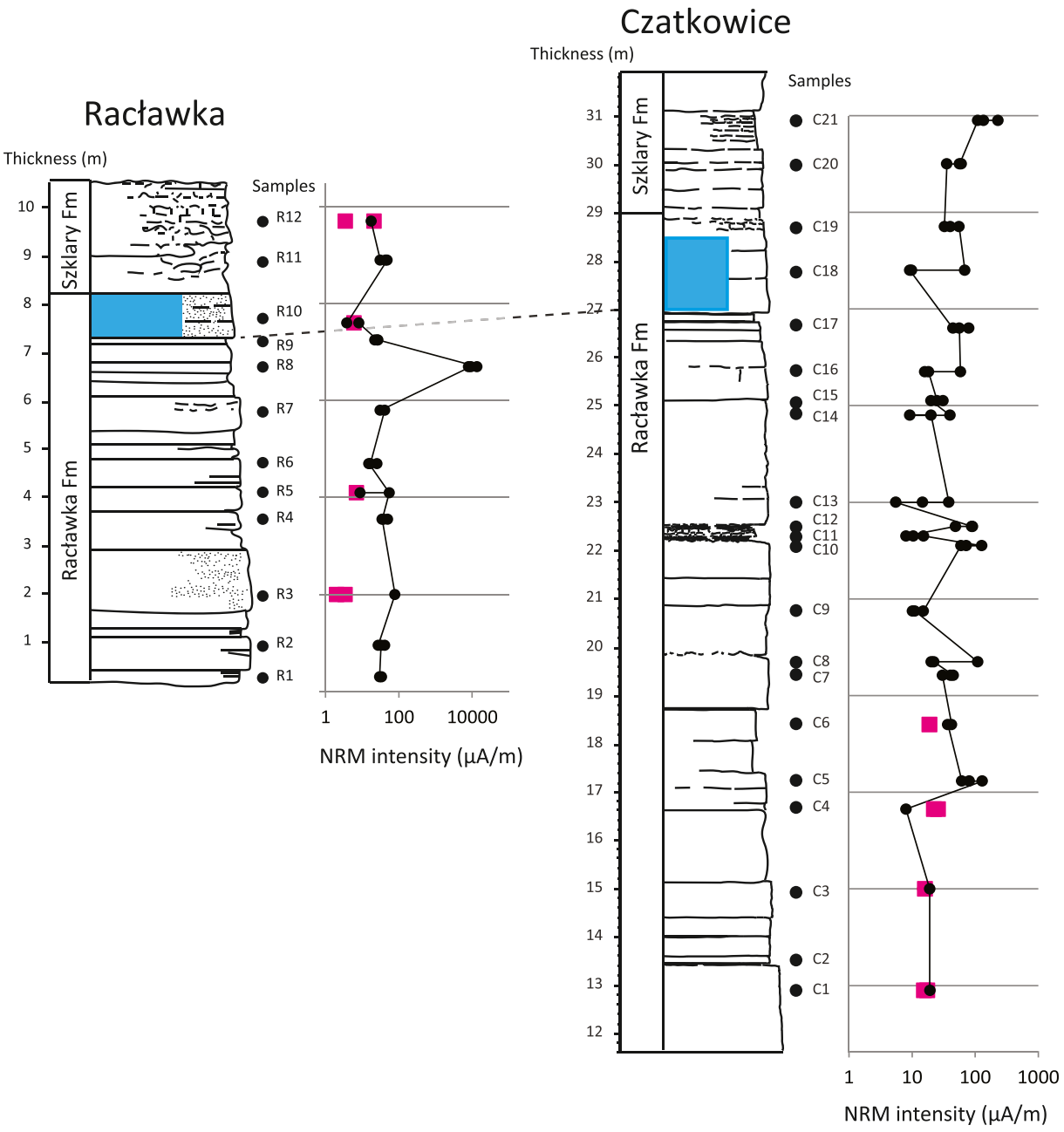

Fig. 4. Lithological logs and correlation of the Racławka and Czatkowice sections, sampled levels and NRM intensity (measurements in pink squares have uncertainties of >20%). Dashed line is the inferred position of the Devonian-Carboniferous boundary and correlation level between the Racławka and Czatkowice sections. Oolites are indicated in blue.

device), and a noise level of ca. $1x10^{-12}$ Am^2, which measures a singly positioned specimen with four measurements of each axis. As specimens were weak, we flipped the samples and measured four positions again after each step, so each specimen was measured eight times in total per step. Typical holder magnetisations were less than 10 µA/m.

For specimens from all locations, magnetisations were calculated using principal component analysis (Kirschvink, 1980) visualised on Zijderveld diagrams (Zijderveld, 1967), using the interpretation portal of http://Paleomagnetism.org (Koymans et al., 2016). The bedding dips of the Blankenheim section were near horizontal, so no tectonic correction was applied here. Mean directions were calculated using Fisher statistics (Fisher, 1953). We fitted great-circles when components with overlapping blocking temperatures or coercivity spectra were present. Lines and planes were inferred following an eigenvector approach (Kirschvink, 1980). We use the method of McFadden and McElhinny (1988) to determine specimen mean directions for the great-circle solutions.

Susceptibility versus temperature (up to 700 °C in air) runs were performed on representative specimens using an MFK-1 Kappabridge with CS4 furnace and a sensitivity of 10^{-7} SI. Multiple heating (6°/minute) and cooling runs (10°/minute) were performed. Room temperature susceptibility measurements were conducted using the same Kappabridge.

3.2. *Racławka and Czatkowice, Poland*

Oriented hand samples were taken from the Racławka section (R sample codes) and Czatkowice quarry (C sample codes), from which conventional paleomagnetic cores (25 mm Ø) were drilled in the paleomagnetic laboratory of the Polish Geological Institute. 24 hand

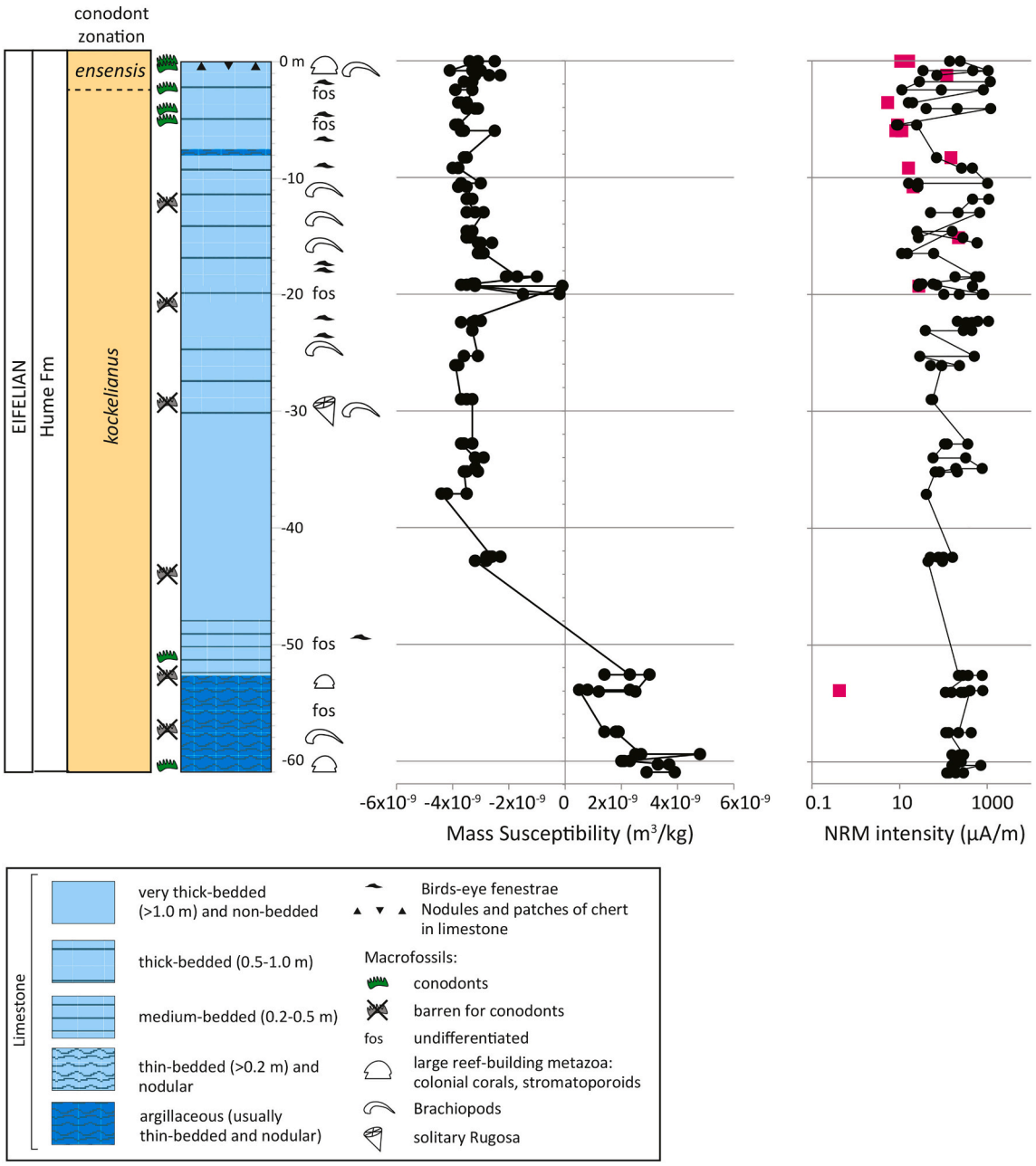

Fig. 5. Lithological log of the Hume Formation with sampled levels, bulk magnetic susceptibility and NRM intensity (measurements in pink have uncertainties of >20%). The log is modified after Kabanov et al. (2019).

samples from the Czatkowice quarry were taken, as well as 12 of the Racławka section. The sampled part for this study contains the uppermost part of the Racławka Formation, which encompasses the presumed Devonian-Carboniferous boundary, and the lower part of the Szklary Fm. A tentative correlation between the Racławka and Czatkowice sections was based on the levels of characteristic oolitic-layers assumed as the Devonian-Carboniferous boundary interval (Fig. 4). Samples were processed at the Paleomagnetic laboratory Fort Hoofddijk, of Utrecht University, the Netherlands. In total 98 specimens were subjected to thermal (66 specimens), as well as AF (98 specimens) demagnetisation. Thermal demagnetisation was performed in a magnetically shielded furnace to maximum temperatures of 340 °C, using temperature increments of 20–60 °C. Thermally demagnetised specimens were subsequently treated with AF demagnetisation to avoid alteration-induced magnetisations (cf. van Velzen and Zijderveld, 1995). AF demagnetisation was performed with steps of 4–10 mT using an in-house built robotized system (dynamic range 3×10^{-12} to 5×10^{-5} Am^2; Mullender et al., 2016). After each demagnetisation step, the natural remanent magnetisation (NRM) was measured eight times on a 2G Enterprise horizontal cryogenic magnetometer equipped with three DC-SQUIDS (noise level 3×10^{-12} Am^2). Typical holder magnetisations were less than 20 µA/m. Declination (D) and inclination (I) angles were calculated for pre-tilt (TC) and post-tilt (NOTC) signals.

Thermomagnetic runs were performed on powdered samples, using a modified horizontal translation balance with a cycling field, usually 150–300 mT (Mullender et al., 1993). Six cycles of heating and cooling were performed, up to a temperature of 700 °C. Isothermal remanent magnetisation (IRM) acquisition curves were obtained up to 700 mT (pulsed field) and measured using a robotized SQUID magnetometer (Mullender et al., 2016). Kappabridge measurements were performed at the geomagnetism laboratory of the University of Liverpool, using the AGICO MFK-1 with a furnace attachment. Six heating and cooling cycles

Table 1
Glossary of paleomagnetic terminology.

Acronym	Definition	What does this mean
AF	Alternating field (demagnetisation)	Application of an oscillating magnetic field to a paleomagnetic specimen, in order to progressively demagnetise the sample
AMS	Anisotropy of magnetic susceptibility	A technique that is used to show preferred orientations of magnetic minerals in a rock
APWP	Apparent polar wander path	Apparent motion of the Earth's spin axis (pole), used to describe plate motion for a tectonic plate
ChRM	Characteristic remanent magnetisation	A characteristic paleomagnetic direction obtained from a sample, usually the primary magnetisation component after the removal of overprints
CRM	Chemical remanent magnetisation	A magnetisation that is acquired due to chemical processes below the Curie temperature of magnetic minerals
DC	Direct current	An electric current that flows in one direction only
DRM	Detrital remanent magnetisation	A magnetisation that is acquired in sedimentary rocks from the alignment of magnetic moments of detrital grains with Earth's magnetic field before compaction
GAD	Geocentric axial dipole	Assumption that, when averaged over a sufficient amount of time (>10^5 years), Earth's magnetic field is a stable dipole at the Earth's centre and aligned with Earth's rotation axis
GAPWaP	Global apparent polar wander path	A collection of APWPs of different plates that are recalculated to a single reference plate, used to describe global plate motions
GPTS	Geomagnetic polarity time scale	The black and white barcode that shows time series of geomagnetic field polarity, with normal (in black) and reversed polarity (in white)
IGRF	International geomagnetic reference field	A mathematical description of the structure of the Earth's main magnetic field to describe the large-scale, time-varying portion from 1900 A.D. to now
IRM	Isothermal remanent magnetisation	The magnetisation acquired by application of a strong magnetic field to a sample over a short time period (usually seconds)
MD	Multi-domain	Property of large magnetic grains that contain several magnetic domains, tending to make them poor magnetic recorders
NRM	Natural remanent magnetisation	The total magnetisation of a rock which may have been acquired by a variety of mechanisms and is conserved in the rock in the absence of an external magnetic field
PDF	Present day field	The Earth's recent geomagnetic field
PDRM	Post-depositional detrital remanent magnetisation	A magnetisation that is acquired during post-depositional modification of sediments such as compaction and diagenesis
PSD	Pseudo-single domain	A transition state between SD and MD, where the magnetic domain(s) can be distorted (vortex) but still remains a faithful recorder of the magnetic field
PSV	Paleosecular variation of the geomagnetic field	The description of spatial and temporal geomagnetic variability in the geologic past
Q_{PI}	Quality index of paleointensity data	A set of qualitative reliability criteria for palaeointensity results at the site-mean level
SD	Single domain	Single domain grains are uniformly magnetised to their saturation magnetisation and represent the best magnetic recorders
SP	Superparamagnetic	Property of grains that become strongly magnetised upon application of an external magnetic field but whose magnetic remanence decays in seconds or less
SQUID	Superconducting quantum interference device	A ring of superconducting material interrupted by thin insulators used as high sensitivity magnetometer, to measure extremely weak magnetic fields in paleomagnetic samples
SV	Secular variation	Describes variations of Earth's magnetic field over periods of months to hundreds of thousands of years
TRM	Thermoremanent magnetisation	A magnetisation that is acquired from cooling magnetic minerals below their Curie temperature
TVRM	Thermoviscous remanent magnetisation	A magnetisation that is acquired by exposure to a magnetic field while rocks are at elevated temperature (but below Curie temperatures)
VADM	Virtual axial dipole moment	An estimate of the strength of Earth's magnetic field based on the assumption that the field consists only of a geocentric axial dipole
VDM	Virtual dipole moment	An estimate of the strength of Earth's magnetic field based on the assumption that the field consists only of a geocentric dipole
VGP	Virtual geomagnetic pole	The position of a geocentric dipole calculated from a single observation of the direction of Earth's magnetic field
VRM	Viscous remanent magnetisation	A magnetisation that can be acquired when ferromagnetic materials are exposed to a magnetic field for some time (this is generally an easily removed overprint)

were performed on powdered samples up to a temperature of 700°C. Samples were repeatedly heated and cooled, after which the susceptibility was measured. Bulk susceptibility measurements were conducted at room temperature using the same Kappabridge.

A total of 5 specimens from Czatkowice (sample code CQ) were studied for hysteresis and back-field analysis using a Magnetic Measurements Advanced Variable Field Translation Balance (MMAVFTB) at the University of Liverpool. All resulting loops were corrected for the paramagnetic component and analysed using RockMag Analyzer (Leonhardt, 2006).

These same specimens were subject to measurements of frequency dependent susceptibility using an Agico MFK1 Kappabridge operating at frequencies of 976 Hz, 3.9 kHz and 15.6 kHz. Measured susceptibilities were around noise/holder level in some cases, which was recognised as increases in the susceptibility of > 10% at one of the two higher frequencies. Two samples were rejected for giving too noisy susceptibility readings.

3.3. Prohibition Creek, Canada

115 samples were taken at 44 levels over 60 metres of section of the Hume Formation, as well as 6 samples from 3 levels of the Canol shale. Sampling methods and laboratory procedures were the same as described earlier for the samples from Germany. All measured orientations in the field were corrected for a local declination of 20° (IGRF). A total of 40 specimens were subjected to stepwise thermal demagnetisation, 12 were demagnetised using AF demagnetisation, and another 81 specimens were demagnetised using a combination of thermal and AF demagnetisation. Typical holder magnetisations were less than 20 μA/m.

Hysteresis and frequency-dependent susceptibility experiments followed those performed on the Poland samples and were based on 7

specimens taken from the Prohibition Creek locality. Three of these samples were rejected for giving too noisy susceptibility readings.

4. Results

4.1. Blankenheim, Germany

4.1.1. Rock magnetic results

Magnetic susceptibility was usually below 10 x 10^{-6} SI at the start of the experiment. Magnetic susceptibility then increases slightly upon heating, after which a drop follows at a temperature of ~580°C, the Curie temperature of magnetite (Fig. 6). All specimens show a peak just before 580°C, which could be a Hopkinson peak (e.g., Dunlop, 2014), which is indicative of single domain (SD)/pseudo-single domain (PSD, or vortex state; Roberts et al., 2017) magnetite. Alternatively, this peak could be related to silicate or pyrite alteration, which is often the case in sediments. Susceptibility generally is much higher after heating, showing irreversible behaviour from 300-400°C, indicating the formation of new magnetic minerals. This is also seen by the large susceptibility increase upon cooling below 600°C, all indicative of substantial thermal alteration.

Hysteresis data (Königshof et al., 2016; see Fig. 7) point to low values of saturation magnetisation and ferrimagnetic susceptibility, indicative of trace amounts of ferrimagnetic minerals. Compared to the ferrimagnetic susceptibility, high field susceptibility values are one order of magnitude larger, indicative of a very small contribution of ferrimagnetic minerals and probably little or no creation of new magnetic minerals through mineralisation. The remanence is still increasing above 300 mT, indicative of a proportion of high-coercivity minerals (such as hematite) and points to a mixture of both low and higher coercivity phases. The time-dependent decay of an IRM_{500mT} (isothermal remanent magnetisation at 500 mT) was measured over 100 s and the normalized

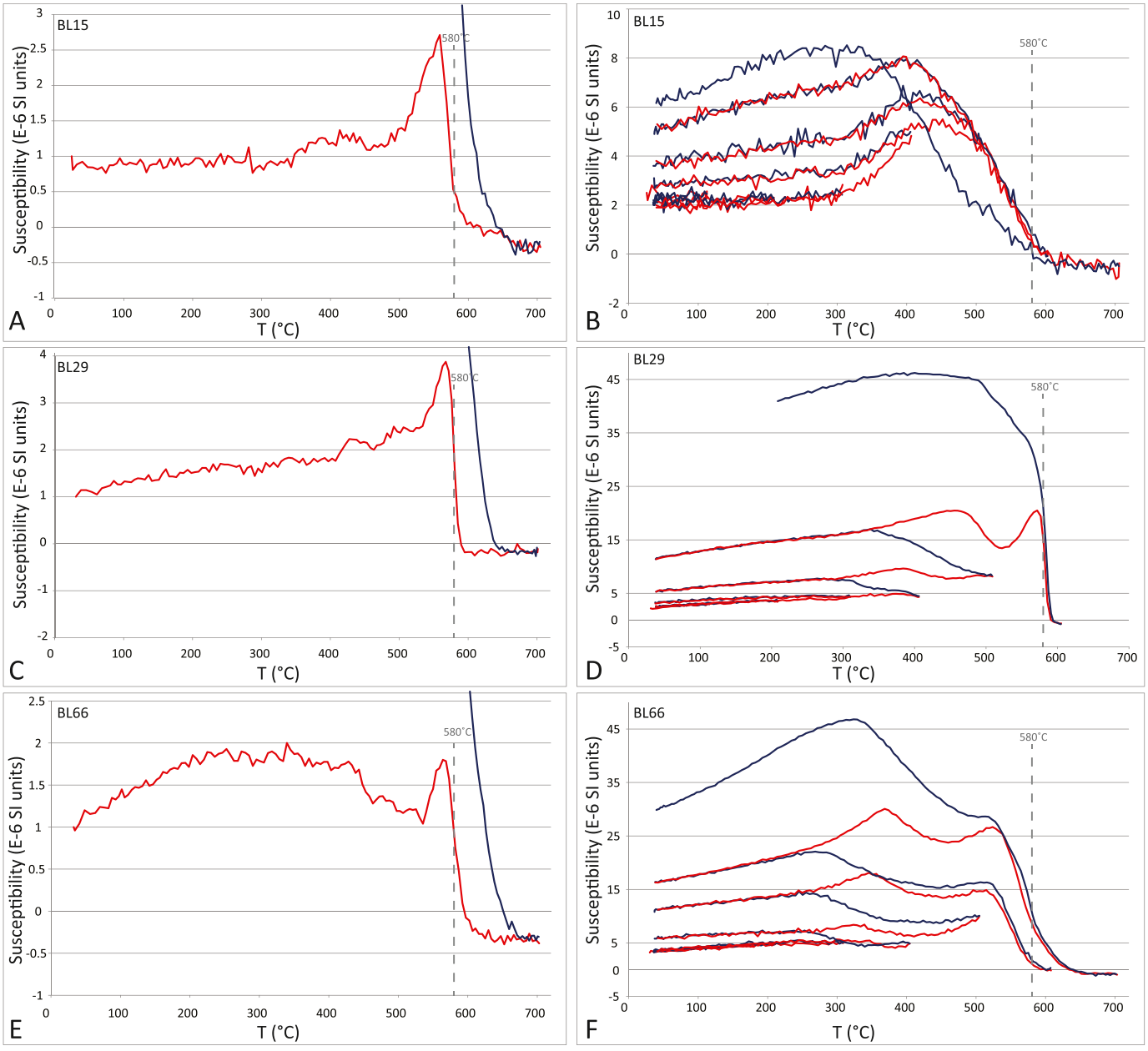

Fig. 6. Kappabridge magnetic susceptibility versus temperature runs of three samples of limestones from the Blankenheim section. On the left are single runs, on the right are multi-segment runs. Red lines indicate heating curves, blue lines are cooling curves. The Curie temperature of magnetite (580 °C) is indicated with a grey dashed line.

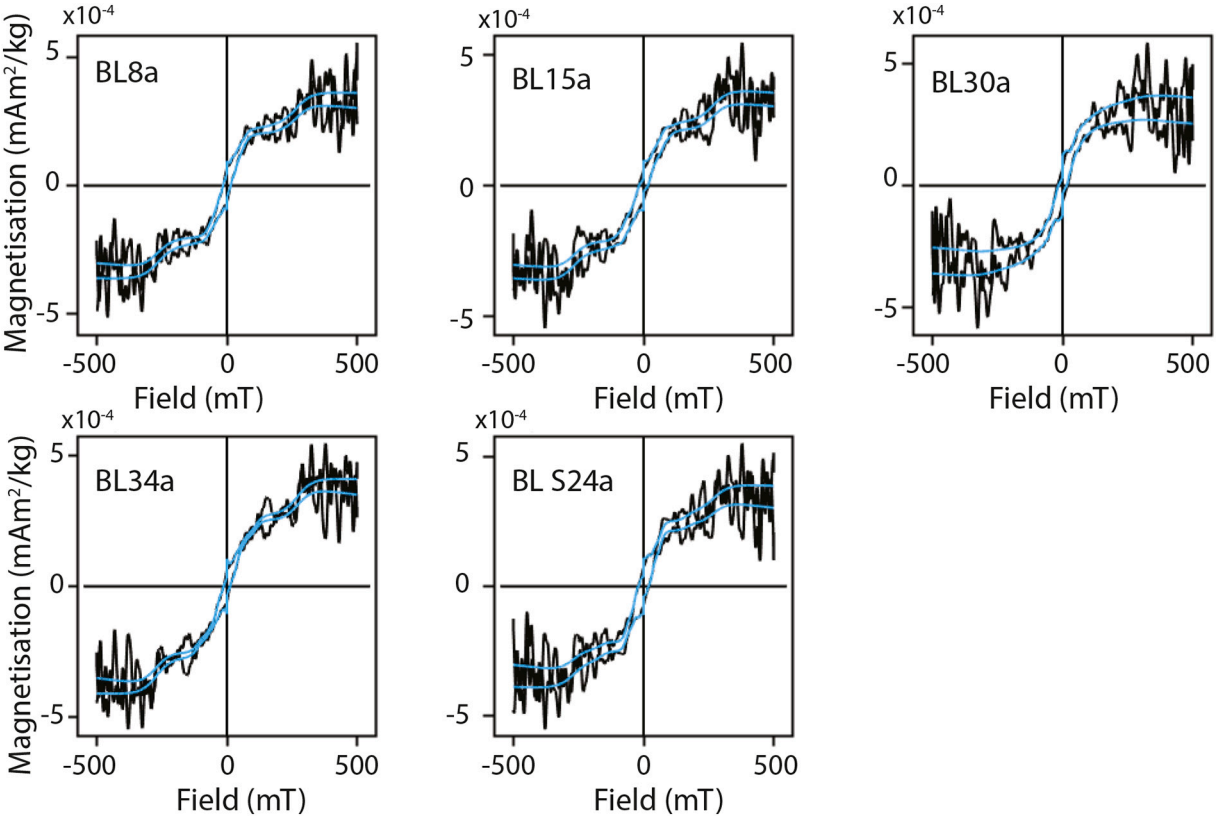

Fig. 7. Representative hysteresis loops of samples from the Blankenheim section, from the study of Königshof et al. (2016). Sample numbers roughly correspond to same stratigraphic height as bed numbers from this study (see Fig. 3). All samples are limestones except for sample BL S24, which is from a shale.

viscosity coefficient corresponds to the slope in the IRM_{500mT} decay versus Log10 of the time in seconds. The results obtained (Königshof et al., 2016) are indicative of a slow decay and relatively coarse grains in the range of SD. Accordingly, the hysteresis data in a Day plot (see Fig. 8) fall along the pseudo-single domain (PSD) and single domain + multi domain (SD + MD) mixing curve (Dunlop, 2002). These results point to the occurrence of trace amounts of ferrimagnetic grains, with a relatively coarse grain size, probably of detrital origin.

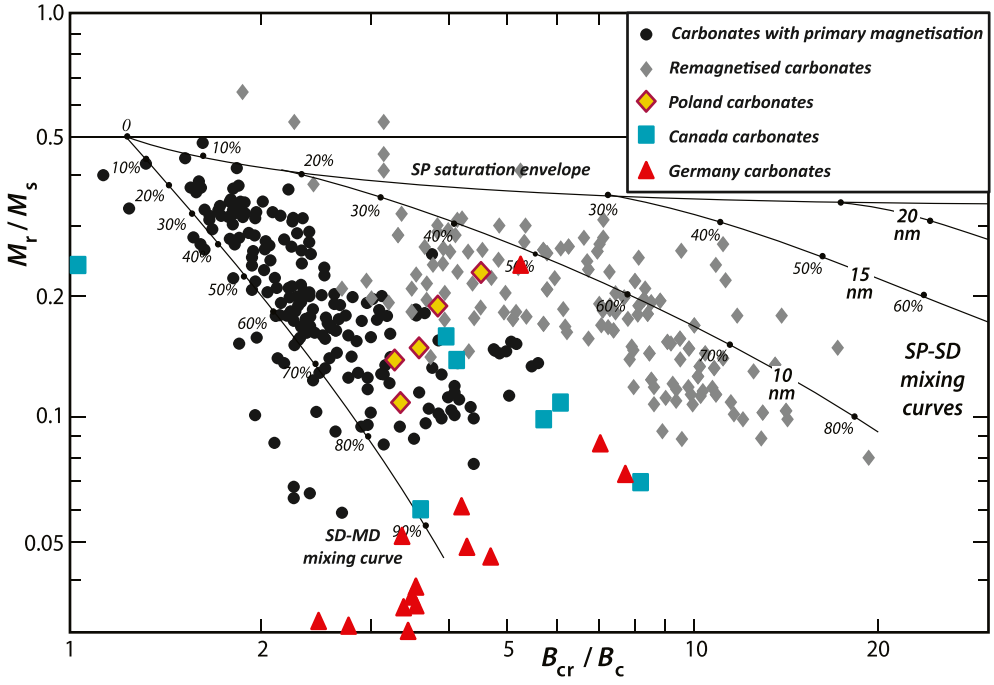

Fig. 8. Day plot (ratio of remanent coercivity (Bcr) to coercivity (Bc) against the ratio of saturation remanence (Mr) to saturation magnetisation (Ms)) with results of samples from Poland, Canada and Germany, with data from (un)remagnetised carbonates of Jackson and Swanson-Hysell (2012) in black and grey.

4.1.2. Directions

Samples from the Blankenheim section generally have NRM intensities of 10-100 μA/m and measurements on the RAPID magnetometer were challenging, as the RAPID would often give erratic measurements. To avoid these erratic measurements, we sometimes measured specimens several times, and excluded all measurements that have standard deviations larger than 20% of the magnetisation from interpretation. All demagnetisation data are provided in the supplementary information (files S1, S3 and S6).

Demagnetisation behaviour generally does not define only linear segments on Zijderveld plots, but many specimens exhibit incomplete component separation characterised by demagnetisation paths along great-circles. Nearly all samples contained a low temperature/low coercivity (LT) component in the direction of the modern field, in some cases; this could not be removed (see Fig. 9A). A large proportion of samples show a strong reversed (possibly Kiaman-age) overprint, which in many cases cannot be fully demagnetised (see Fig. 9B and 9C). Characteristic remanent magnetisation (ChRM) generally decreases towards the origin of the Zijderveld diagrams (see Fig. 9), although some specimens cluster (Fig. 9E and 9F) and in some cases, the paths seem to pass the origin (see Fig. 9G). The low temperature/coercivity (LT) component has a mean direction of dec= 11.9°, inc= 66.2°, α_{95} = 3.0° (Fig. 9A), generally agreeing with the expected inclination of the modern GAD (geocentric axial dipole) field (around 67.6°).

Around half of the samples show a strong southerly and negative inclination middle stability component (MT), which in most cases remains at the highest demagnetisation steps (see Fig. 9B and 9C). This component has a mean of dec= 204.9°, inc= -24.2°, α_{95} = 5.1° (see Fig. 10B). The APWP (apparent polar wander path) of Torsvik et al. (2012) predicts directions (converted to reverse polarity) for the Kiaman reverse superchron, (~320-260 Ma), of dec ≈ 205° ± 5° (320 Ma) to dec ≈ 202° ± 3° (260 Ma) and inc ≈ 12° ± 9° (320 Ma) to inc ≈ -34° ± 4° (260 Ma). The reverse directions that we observe in many samples agree well with Kiaman directions as expected for the location of Blankenheim between 320 Ma and 260 Ma. The mean MT component is closer to the predicted directions at 260 Ma, so we consider this component to have been acquired during the Permian. Ribbert (1983) determined peak orogenesis in the region to have occurred during the late Carboniferous, which could have resulted in overprinting. Zwing and Bachtadse (2000) report a Kiaman overprint in the Rhenish Massif with a direction of dec = 186.3°, inc = 8.0°, indicating that their direction could represent an older (late Carboniferous) overprint compared to our Blankenheim reverse polarity Kiaman directions (the α_{95} uncertainties do not overlap).

The ChRM generally decreases towards the origin of the Zijderveld diagrams (see Fig. 9), although in some samples the ChRM does not fully demagnetise (Fig. 9E and 9F), and in other cases misses the origin (Fig. 9G). The mean of the ChRM component is dec = 207.5°, inc = 33.8° and α_{95} = 8.5. Reported directions for the Late Devonian in igneous rocks from the Frankenstein igneous complex in the Rhenish Massif are around dec = 200°, inc = 40° for reverse polarity samples (see Fig. 10C; closed blue star), and dec = 10°, inc = -43° for normal polarity samples (see Fig. 10C; open blue star; Zwing and Bachtadse, 2000). The mean ChRM component (69 directions and 2 great-circle solutions) in the Blankenheim section overlaps with the Late Devonian reverse polarity direction of Zwing and Bachtadse (2000). We note, however, that this direction is also an intermediate direction between a present-day field and an inferred Kiaman overprint direction (calculated from the global apparent polar wander path-GAPWaP; Torsvik et al., 2012). In some cases, it seems likely that the Kiaman direction is not fully resolved (see for example Fig. 9D and 9I). Half the specimens (73), did not yield ChRM directions, and only showed LT or MT components, and no directions resembling a Devonian normal polarity were identified.

4.2. Racławka and Czatkowice, Poland

4.2.1. Rock magnetic results

Thermomagnetic runs using a Curie balance, as well as Variable Field Translation Balance (VFTB) measurements yielded no useful results because of the extremely weak magnetisations of the samples (tens to hundreds of μA/m). Kappabridge runs show an increase in susceptibility up to ~300°C, after which the susceptibility rises more sharply up to around 420°C (Fig. 11). Subsequently, susceptibility starts to decrease until around 550°C, likely indicating the presence of low Ti-titanomagnetite, with specimens generally showing reversible behaviour. IRM acquisition curves are divisible into two groups according to the presence of low and high (>300 mT) coercivity phases (see Fig. 12). The first group, which includes the majority of samples, is dominated by a low coercivity phase (e.g., Fig. 12A, 12B) and shows virtually no sign of a high coercivity phase between 100 and 400 mT. The second group shows a smaller contribution from a low coercivity phase (Fig. 12C), and does not reach saturation at the maximum applied field of 600 mT (Fig. 12D). In contrast to the range in IRM saturation, curves of susceptibility versus temperature are fully dominated by a single phase in both groups, suggesting the dominance of magnetic carriers with Curie temperature < 580°C (e.g., Fig. 12A vs Fig. 12C), which are presumed to be magnetite. Hysteresis loops measured for 5 specimens (Fig. 13) showed no evidence of wasp-waisting and saturated at 300-400 mT. On a Day plot (Day et al., 1977), they plot in the pseudo-single domain (PSD) region and intermediate between SD-MD and superparamagnetic-single domain (SP-SD) mixing curves of Dunlop (Dunlop, 2002) (Fig. 6). Frequency-dependent susceptibility was negligible (decreases < 3%), supporting the interpretation that only an insignificant proportion of SP grains might be associated with chemical remagnetisation (Jackson and Swanson-Hysell, 2012).

4.2.2. Directions

Three components of magnetisation are observed (Fig. 14), corresponding to LT, MT and high temperature/coercivity (HT) intervals. Thermal demagnetisation was generally successful up to 300°C; at higher temperatures, uncertainties on the measurements became very large (>20%). Samples show low NRM intensities, ca. 10-100 μA/m (see Fig. 4). Some samples (e.g., R3; see supplementary file S3) show intensities of <5 μA/m and uncertainties on measurements of these samples are often more than 100%. In some cases, samples show components that resemble a modern field (Fig. 14A), or a Kiaman field (as calculated from the GAPWaP of Torsvik et al., 2012; Fig. 14B). The most well-resolved specimens show three components (Fig. 14C-H), which we interpret to represent a recent field carried by soft magnetic carriers (LT), a Kiaman field overprint (MT), and a HT component, interpreted to record a primary Devonian field, respectively. Demagnetisation behaviour commonly consists of overlapping components, indicated by demagnetisation paths following great-circles (e.g., C21.2, Fig. 11F, C20.1, Fig. 14H). One sample (R8.3; supplementary file S3) shows a very strong magnetisation (~500 times stronger than other samples) and demagnetises in a straight line towards the origin of the Zijderveld diagram. We interpret this behaviour as remagnetisation, possibly due to a lightning strike.

The LT component is typically demagnetised after 175°C or 16 mT (Fig. 15A), and in some samples, this component is absent. At higher demagnetisation steps, 58 specimens show a southerly and up-directed MT component, interpreted as a Kiaman component (see Fig. 15B and 15C). In 68 specimens, no ChRM could be resolved. It remains unclear whether the Kiaman direction was acquired pre-tilting (TC) or post-tilting (NOTC). Kiaman directions (TC) are dec = 187.7°, inc = -27.2°, α95 = 5.3°, while Kiaman (NOTC) directions are dec = 199.5°, inc = -17.9°, α95 = 5.4°. Our Kiaman averages are close to early Permian results obtained from volcanic rocks in this region by Nawrocki et al. (2008). The APWP of Torsvik et al. (2012) predicts directions for the Kiaman of dec ≈ 216° ± 4° (320 Ma) to dec ≈ 208° ± 3° (260 Ma) and

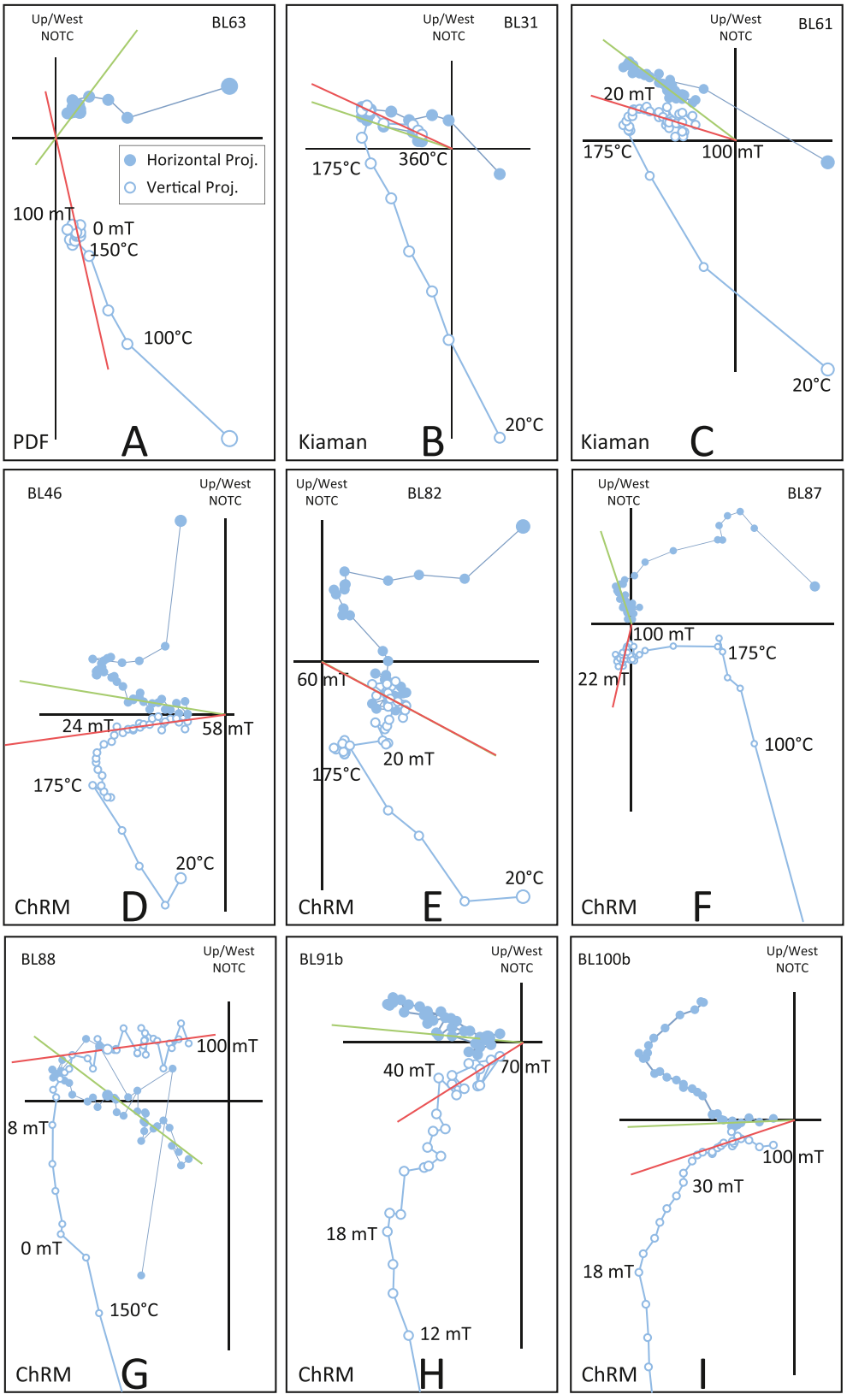

Fig. 9. Examples of representative Zijderveld diagrams of samples from the Blankenheim section with interpreted vectors (red and green lines). As bedding in the section is subhorizontal, tectonic corrections are not applicable.

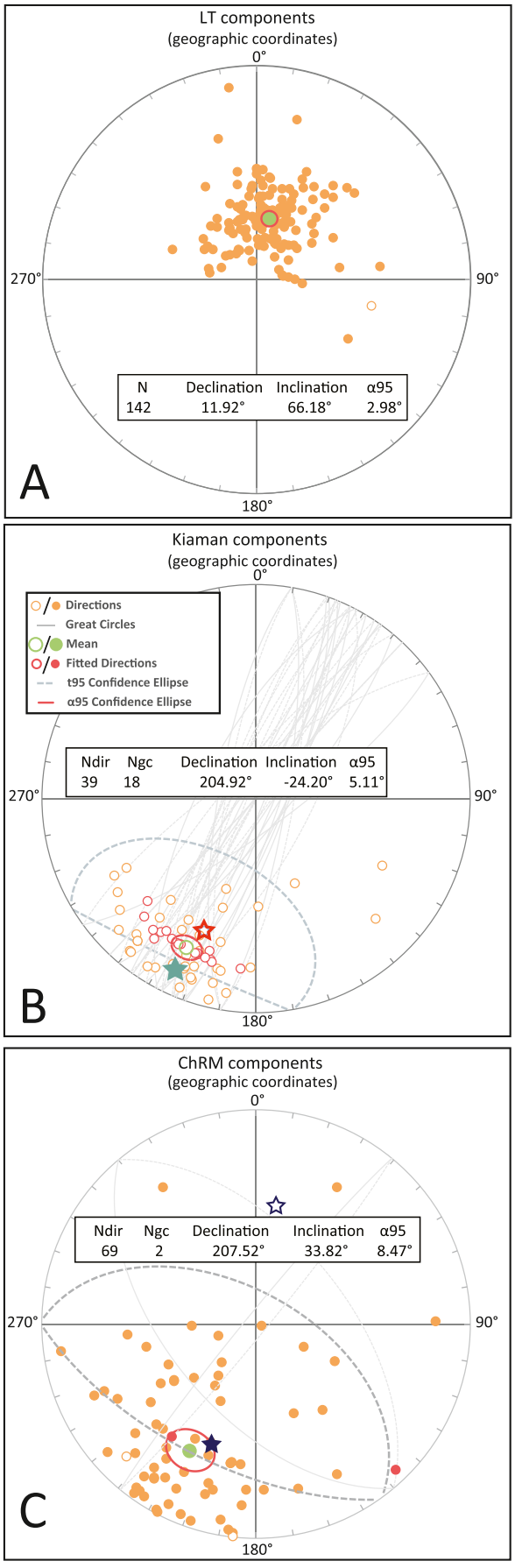

Fig. 10. Equal area plots of interpreted directions of the Blankenheim section. Closed (open) circles and stars represent positive (negative) inclinations. A. Interpreted low temperature/low coercivity components. B. Interpreted reverse polarity components with expected directions based on the Eurasian APWP of Torsvik et al. (2012). The red star represents the expected direction at 260 Ma (Permian), the turquoise star is the expected direction at 320 Ma (Carboniferous). Ndir is the number of directions, Ngc is the number of great-circle solutions, α95 represents cone of confidence around the mean which contains the true population mean direction with 95% probability. C. Interpreted characteristic remanent magnetisation (ChRM) components, with blue stars marking the directions from Zwing and Bachtadse (2000)

(caption on next column)

inc ≈4° ± 10° (320 Ma) to inc ≈ -39° ± 4° (260 Ma). Our directions fit with Kiaman inclinations, but declinations are more southerly than expected, which could be related to local rotation of the Moravia-Silesia block. Since this block is only expected to have moved poleward since the Permian, a post-Kiaman remagnetisation would not fit with the directions that we obtained.

A total of 26 specimens from the Polish sections show dual polarity ChRM components, interpreted as Devonian reverse (Fig. 14C-D) and normal (Fig. 14E-H) polarities. Directions representing the Devonian normal polarity are better resolved than Devonian reverse polarity directions. Many samples show clear great-circle paths towards normal Devonian polarities. This can be explained by partial component overlap between the normal ChRM and Kiaman component, which will give much longer great-circle paths than reverse ChRM + Kiaman overlap. Specimens that represent Devonian normal polarities average to dec = 41.2°, inc = -35.1°, α_{95} = 8.4°, while Devonian reverse polarities average to dec = 237.9°, inc = 49.9°, α_{95} = 17.0° (see Fig. 15D-E). These directions correspond to poles with lat = 11.5° and long = 160.3° (normal) and lat = -5.7°, long = 152.6° (Devonian reversed converted to normal polarity; Table 2). Although the mean normal (converted) and reversed directions overlap within error (see Fig. 16), a reversal test using a bootstrap common true mean direction (CTMD) test (Tauxe, 2010) in http://Paleomagnetism.org (Koymans et al., 2020) is negative.

4.2.3. *Polarity interpretation*

The lower part of both the Czatkowice and Racławka sections yielded mostly Kiaman overprints, but three samples indicate Devonian reverse polarity (Czatkowice; Fig. 17). Between 22-25 metres (Czatkowice), two samples show normal polarities. Above this, there is a reversed interval. The top of the section shows convincingly normal polarity ChRMs, and these samples display indistinguishable rock magnetic properties from the other samples. This part of the section typically shows demagnetisation along great-circle trends that end in a well-defined direction.

The Racławka section is correlated to the Czatkowice section based on biostratigraphy and lithostratigraphy. The tops of both sections also show a similarity in demagnetisation diagrams, with samples of both sections progressing along similar great-circles and ending in similar directions (see Fig. 14E-H and supplementary file S3). The uppermost normal magnetozone of the Czatkowice quarry thus corresponds to the upper part of the Racławka section. The available tie point for the Czatkowice quarry is the inferred position of the Devonian-Carboniferous boundary just above sample C17 (at 27 m), which correlates to the Racławka section between samples R9 and R10 at 7.3 m (thin dashed line in Fig. 17). This suggests that the inferred Devonian-Carboniferous boundary is near the base of a normal magnetozone.

4.3. *Prohibition Creek, Canada*

4.3.1. *Rock magnetic results*

Specimens show an increase of susceptibility up to ~400°C, after which susceptibility decreases (Fig. 18). Specimen NW16.2 (Fig. 18A) shows a decrease until 580°C, indicating the presence of magnetite. Unlike the samples from Germany, a clear Hopkinson/alteration peak is not observed. Specimen NW21.2 (Fig. 18B) shows a decrease until

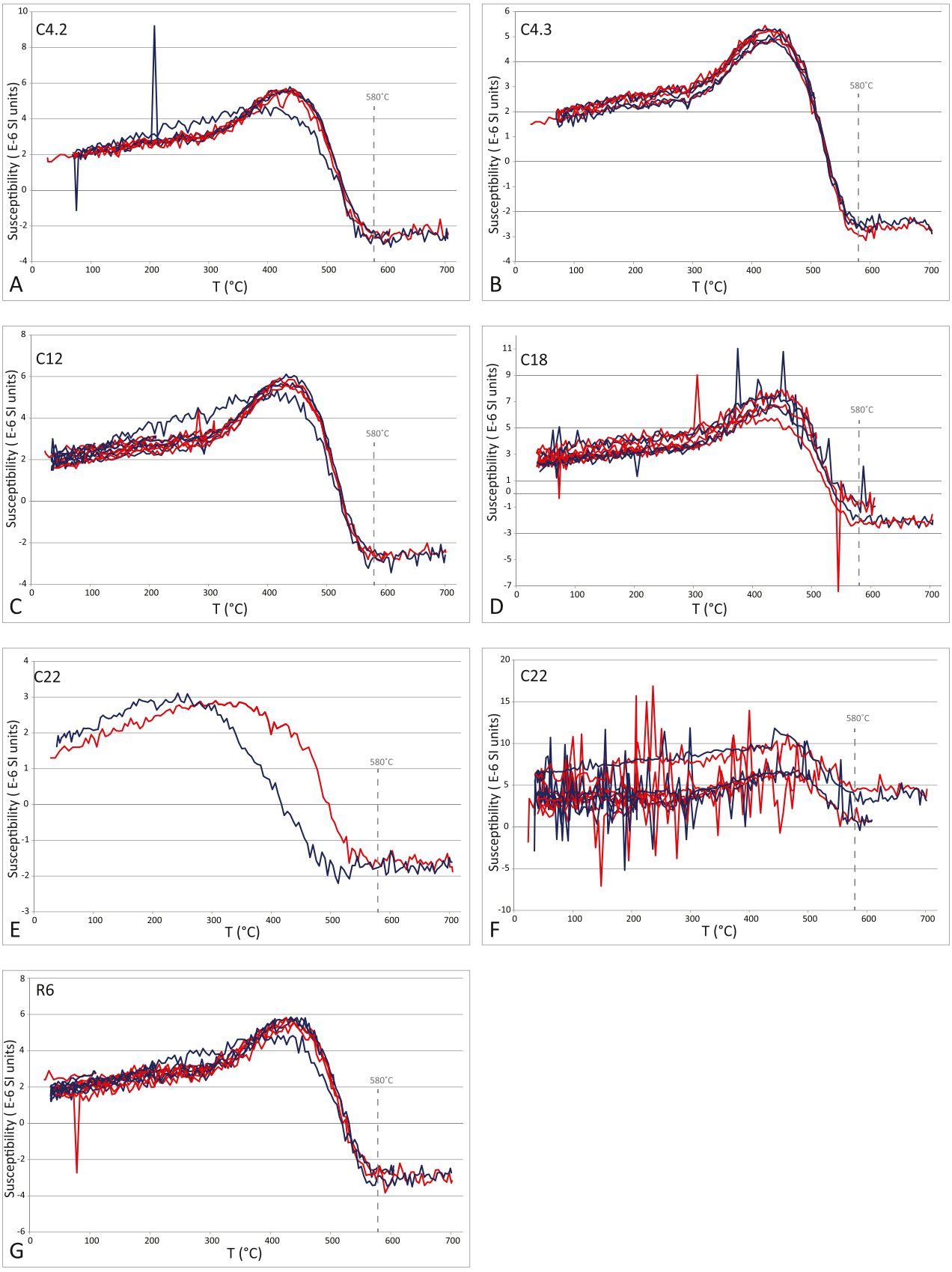

Fig. 11. Kappabridge susceptibility versus temperature runs of five samples of limestones from the Czatkowice quarry (A-F), and one from the Racławka section (G). All runs are multi-segment runs, with the exception of sample C22 (E). The Curie temperature of magnetite (580 °C) is indicated with a grey dashed line.

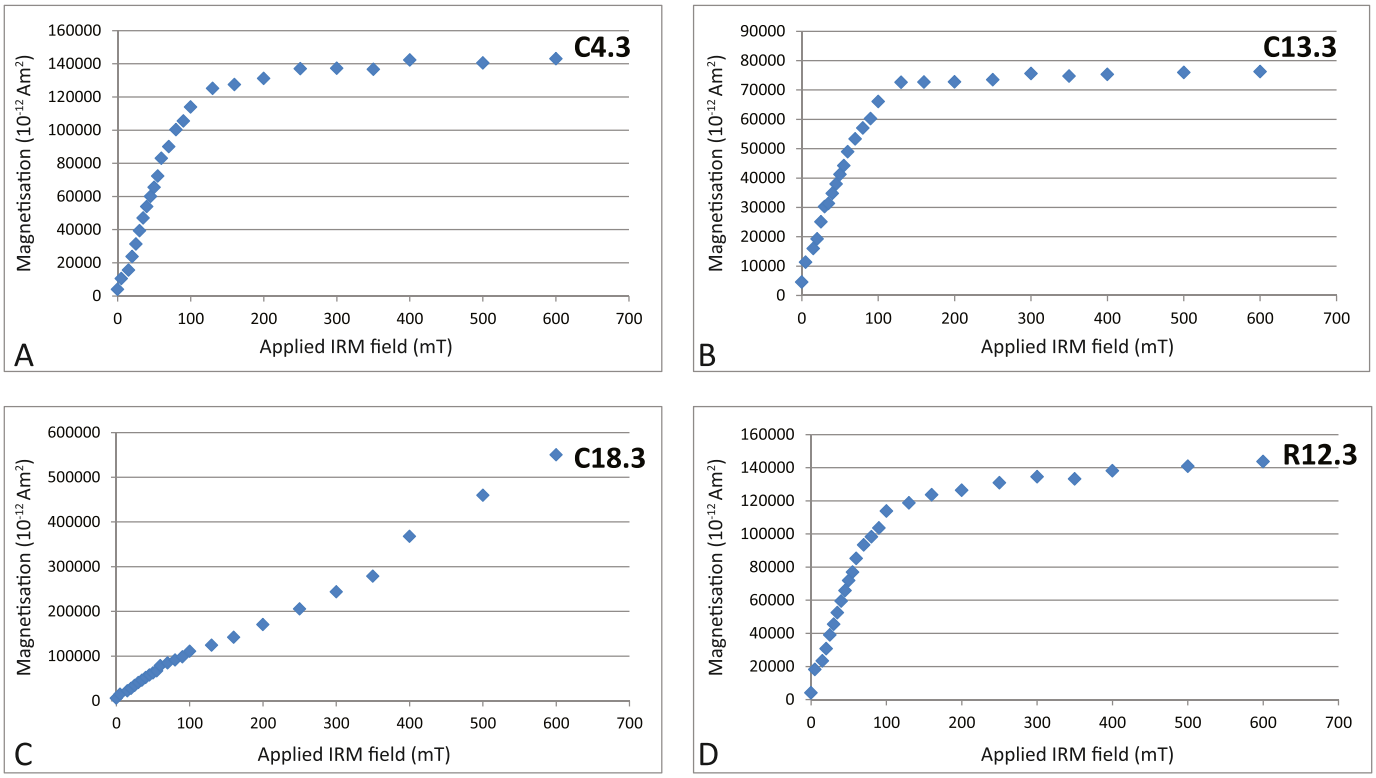

Fig. 12. Representative examples of isothermal remanent magnetisation runs of samples from Poland, three from the Czatkowice quarry (A-C) and one from the Racławka section (D).

around 600°C which could indicate minor hematite. At the end of the experiment, samples have roughly the same susceptibility as at the start and samples generally show reversible behaviour.

Hysteresis loops measured for 7 specimens (Fig. 19) showed little or no evidence of wasp-waisting and saturated mostly at 300-400 mT. On a Day plot (Day et al., 1977), samples plot in the PSD region, mostly intermediate between SD-MD and the SP-SD mixing curves of Dunlop (2002) (Fig. 8). Frequency-dependent susceptibility was minor (decreases < 8%) and comparable to the observed noise level. Like the Racławka and Czatkowice samples, there is no support for the presence of a significant proportion of SP grains that might be associated with chemical remagnetisation (Jackson and Swanson-Hysell, 2012).

4.3.2. Directions

Most specimens show NRM intensities on the order of 10-100 μA/m, but some show intensities up to 1200 μA/m, which are generally found in the top parts of the section where there is more variability in initial NRM intensity (see Fig. 5). Although specimens display a wide range of component removal steps, there seems to be no difference in thermal or alternating field demagnetisation behaviours. Sister specimens rarely behave the same. Most specimens show only a very small LT component, which is generally removed around 175°C or 10 mT (see Fig. 20A), but some specimens are dominated by this component (see Fig. 20B and 20C). The LT component resembles a modern field; with inclinations of around 80° (the expected inclination for a modern field is 77°). A large proportion of the samples (37 specimens) show an ESE, upward-directed (reverse polarity) magnetisation expected for a Carboniferous (~320 Ma) Kiaman magnetisation (using the North American APWP from Torsvik et al. (2012); Fig. 20D-F). HT components observed in the specimens do not cluster, but show a random scatter (see Fig. 20G-J). Equal area plots of all interpreted components are shown in Fig. 21. Clustering of directions is also poor in specimen coordinates (see Fig. 21E), indicating that these HT components are unlikely to reflect a measurement artefact.

5. Discussion of new results

5.1. Blankenheim, Germany

5.1.1. Age constraints

Although the base of the *Tortodus kockelianus* Zone is missing, and it is thus difficult to estimate how much time is represented in the section, an estimate of the maximum time interval represented can be inferred. Absolute durations of individual conodont zones in the Devonian are not rigorously constrained because of the lack of radiometric ages in the Middle Devonian. However, the *Tortodus kockelianus* Zone has an estimated duration of around 2 Myr (when the *Tortodus eiflius* zone is included; see Becker et al., 2020) and encompasses the whole Junkerberg Fm. The Blankenheim section, which represents only a portion of the Junkerberg Fm, likely corresponds to at most a few hundred kyr. De Vleeschouwer et al. (2018) describe a sedimentation rate of 3.2 cm/kyr for the Wetteldorf section, which contains the Emsian-Eifelian boundary and is located ~40 km from the Blankenheim section. While there are large lateral variations in facies in the Eifel Mountains, based on the similar lithology, we estimate that sedimentation rates in the Blankenheim section are of the same order, which would suggest that the Blankenheim section covers ca. 250 kyr.

5.1.2. Origin of the magnetic signal

Königshof et al. (2016) studied the Blankenheim section using magnetic susceptibility data as a proxy for paleoclimatic changes. To constrain the impact of diagenesis, they used hysteresis data, isothermal remanent magnetization and short-term remanence decay data (Königshof et al., 2016). Hysteresis measurements indicate the paramagnetic fraction as the main carrier of the magnetic susceptibility, since the high field susceptibility (χ_{hf}) is well correlated to the total magnetic susceptibility, while the ferrimagnetic susceptibility (χ_{ferri}) is weakly related. The ferrimagnetic minerals are composed of a mixture of low coercivity minerals (such as magnetite) and high coercivity minerals

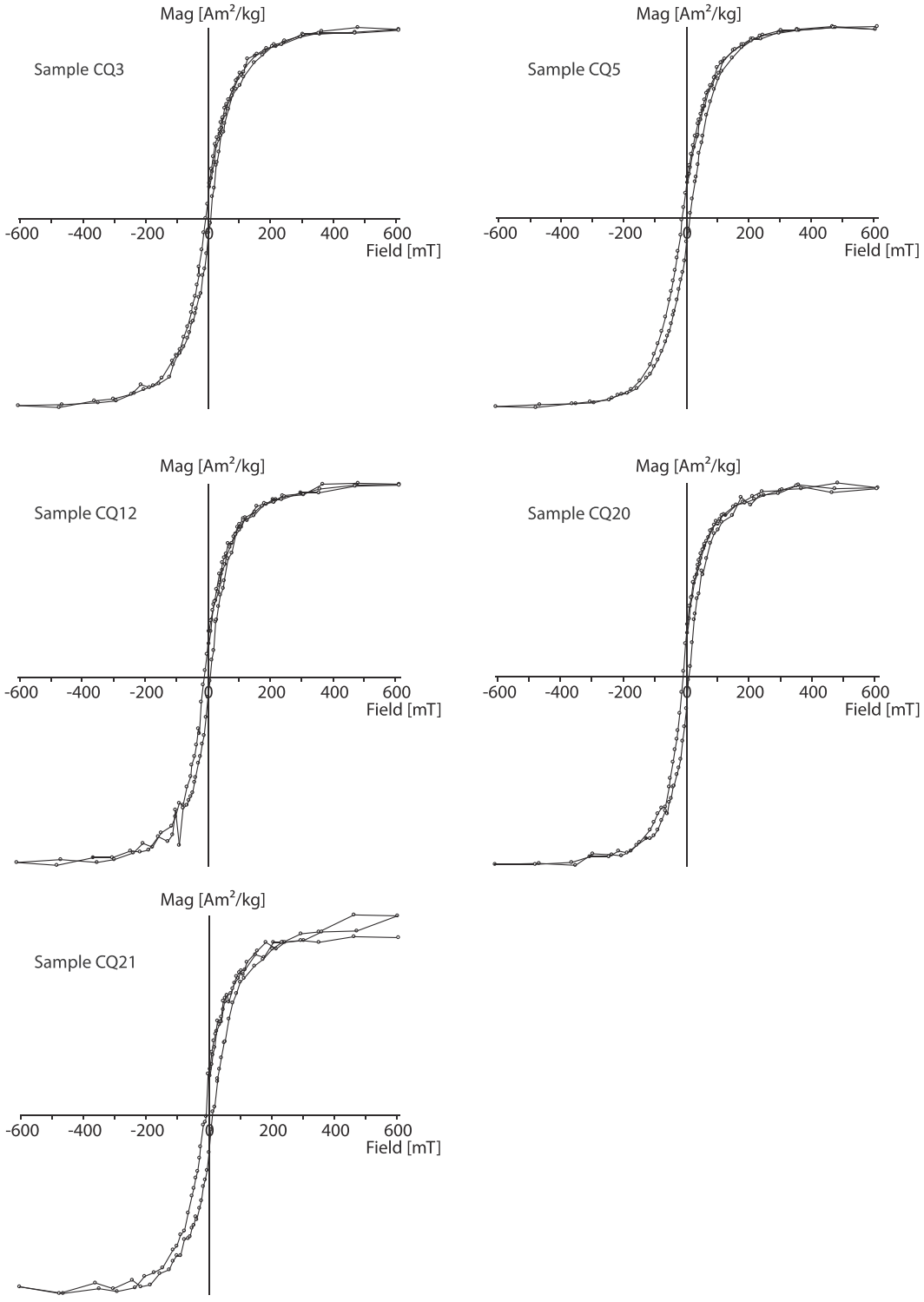

Fig. 13. Representative hysteresis loops of samples from the Czatkowice Quarry.

(such as hematite/goethite, evidenced by the lack of induced remanence saturation at 300 mT). Hysteresis and decay remanence with time both suggest relatively coarse ferrimagnetic grains, along an SD + MD mixing curve of the Day plot (Day et al., 1977). The Rhenohercynian fold and thrust belt, which includes the Blankenheim section, has experienced a large remagnetization event (e.g., Da Silva et al., 2012, 2013; Garza and Zijderveld, 1996; Zegers et al., 2003; Zwing et al., 2005). However, this remagnetization event created new magnetite grains with a SP grain size. In our study, the coarse grain size (SD + MD) as well as the low conodont alteration index (between 1.5 and 2.0), indicates maximum temperatures of remagnetisation of 55°C (Helsen and Königshof, 1994) that seem to have little to no impact in producing new ferrimagnetic phases. We therefore consider it likely that the NRM is dominantly carried by primary detrital phases, overprinted in many cases entirely by subsequent thermo-viscous remanent magnetisations associated with prolonged exposure to strong geomagnetic fields in the Kiaman superchron and Bruhnes chron. If there are small amounts of SP grains generated by remagnetisation events, these have had limited or no

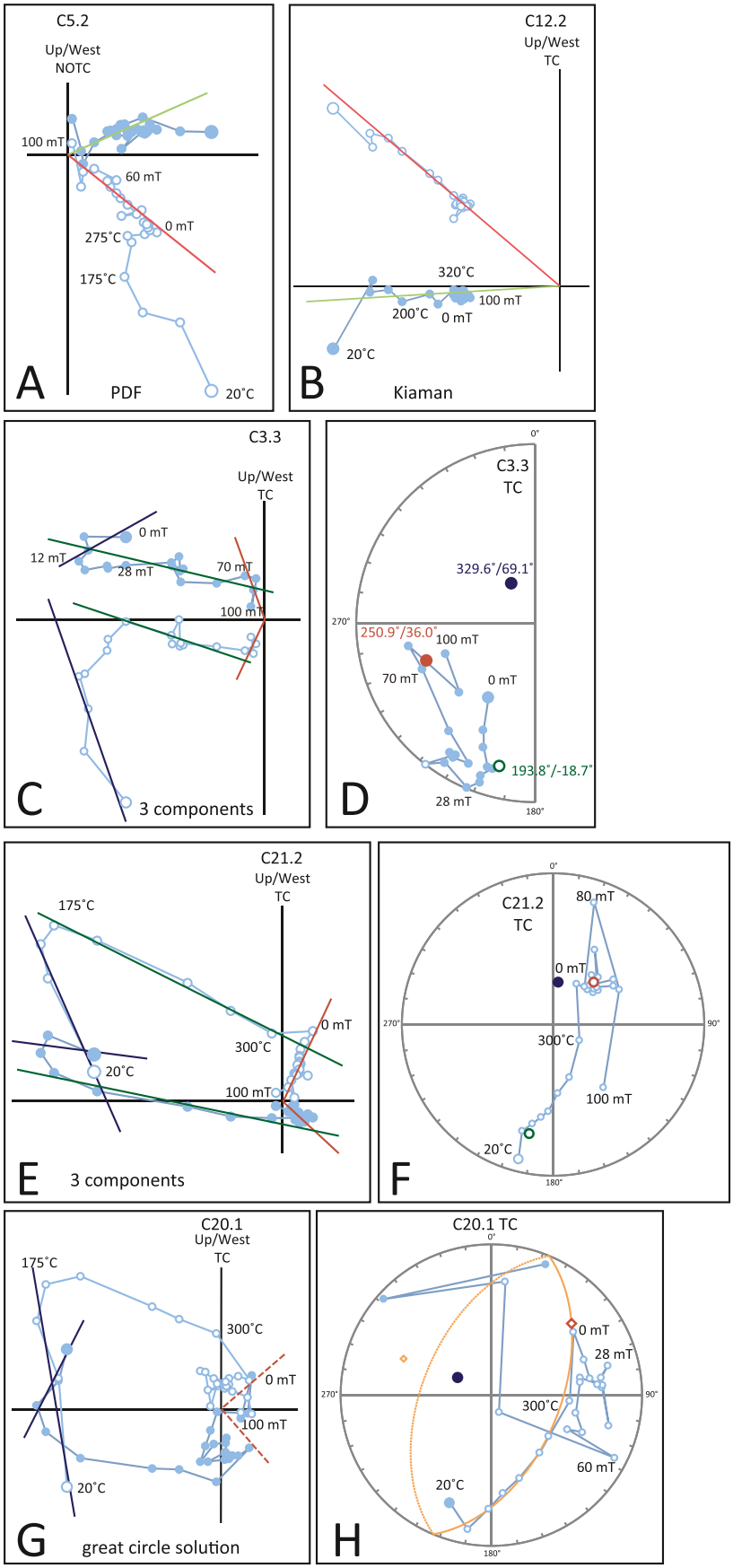

Fig. 14. Representative examples of Zijderveld diagrams and equal area projections of samples from the Polish sections. Legend is the same as Fig. 9. A. Sample showing a pervasive overprint that resembles the present-day field (PDF). B. Sample showing a pervasive overprint that resembles a Kiaman field. C. Sample C3.3 showing three components. D. Sample C3.3 with three interpreted components in an equal area plot. E. Sample C21.2 showing three components. F. Sample C21.2 with three interpreted components in an equal area plot. G. Zijderveld diagram of sample C20.1 showing demagnetisation along a great-circle path. H. Sample C20.1 and the interpreted great-circle and solution (red diamond).

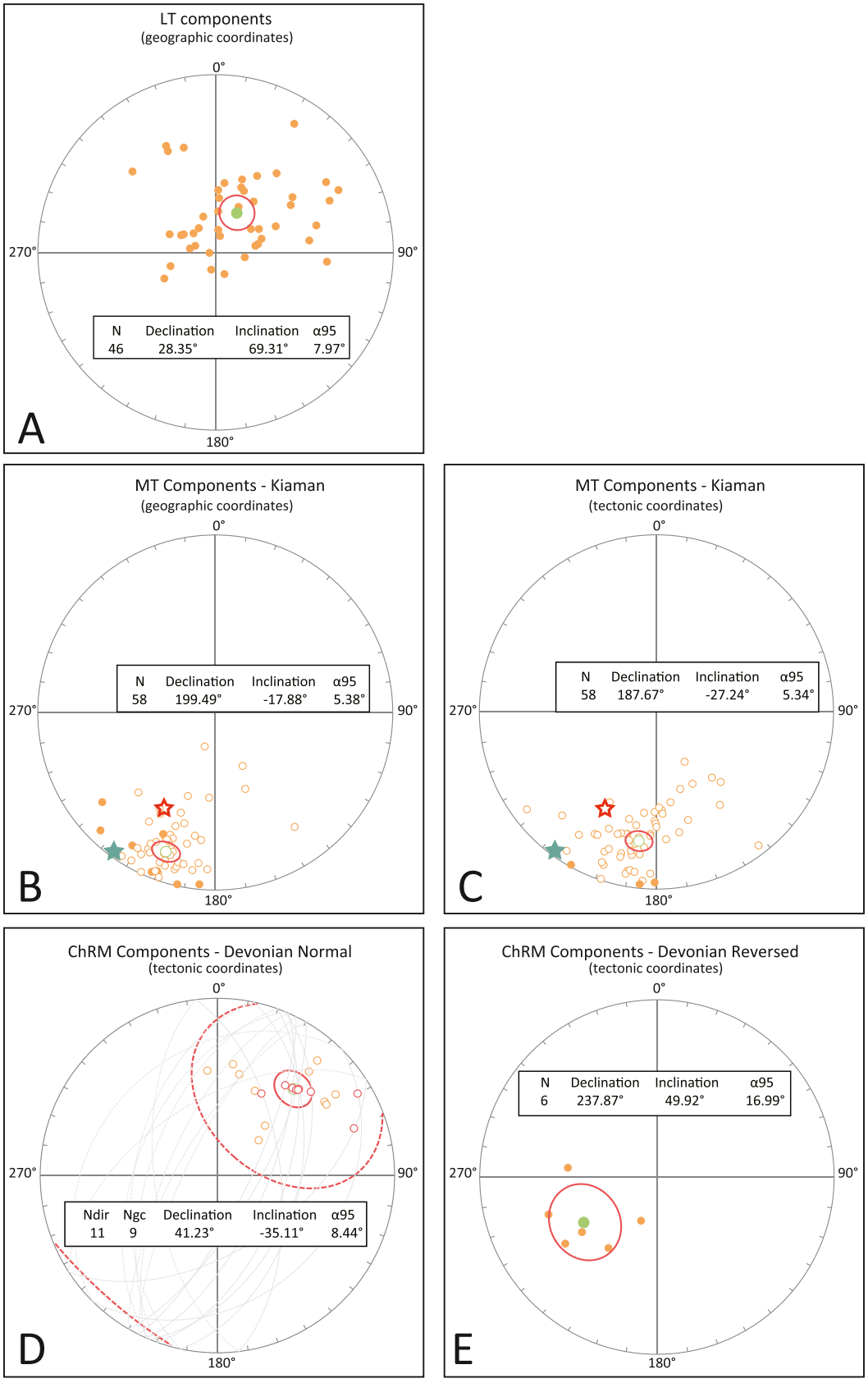

Fig. 15. Equal area plots of interpreted directions of Polish samples. Legend is the same as Fig. 10. A. LT components that resemble a modern field direction. B. Components interpreted to represent a direction acquired during the Kiaman superchron before tectonic correction. C. Components interpreted to represent a direction acquired during the Kiaman superchron after tectonic correction. The red stars represent the expected direction at 260 Ma (Permian); the turquoise stars the expected direction at 320 Ma (Carboniferous). D. ChRMs and great-circles that we interpreted as representative of Devonian normal polarity. E. ChRMs that we interpreted as likely representative of Devonian reverse polarity.

Table 2
Average directions and corresponding poles.

Site name	Lat	Long	Component	Dec	Inc	α95	to N dec	to N inc	VGPlat	VGPlong
Blankenheim, Germany	50.44 N	6.64 E	Kiaman notc	204.9	-24.2	5.1	24.9	24.2	47.1	149.5
			ChRM Drev?	207.5	33.8	8.5	27.5	-33.8	16.9	159.4
Racławka and Czatkowice, Poland	50.16 N	19.64 E	Kiaman notc	199.5	-17.9	5.4	19.5	17.9	45.9	171.4
			ChRM Dnor	41.2	-35.1	8.4	41.2	-35.1	11.5	160.3
			ChRM Drev	237.9	49.9	17.0	57.9	-49.9	-5.7	152.6
Prohibition Creek, Canada	65.18 N	126.22 W	Kiaman notc	115.7	-36.6	7.0	295.7	36.6	29.1	129.0

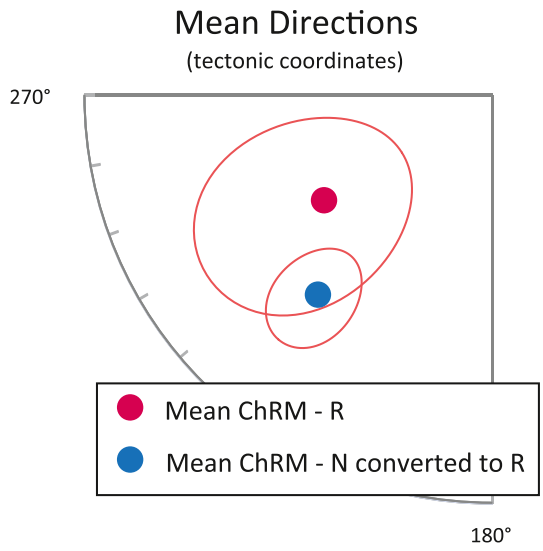

Fig. 16. Averaged normal (N) and reverse (R) polarity ChRM directions converted to the same hemisphere show overlap of directions, indicating that two populations of directions are largely antipodal.

overspill into the stable natural remanence.

5.1.3. Interpretation of the magnetostratigraphy

Becker et al. (2020) used polarity patterns as presented in previous versions of the timescale in their polarity timescale in the GTS2020, but it is unclear which studies these patterns are based on. The polarity is denoted as normal for the early Eifelian in GTS2020, and unknown for the late Eifelian. The Blankenheim section covers part of the late Eifelian. The ChRM directions that we observe could indicate a Devonian reverse polarity, similar to the Devonian direction reported by Zwing and Bachtadse, 2000. We find an average direction of dec = 207.6°, inc = 34.4°, α_{95} = 8.4° (direction reported by Zwing and Bachtadse (2000) is dec = 198°, inc = 40°, α_{95} = 4.9°). However, due to the absence of field tests, we refrain from interpreting our data as primary Devonian directions. Although we consider it unlikely, we cannot entirely exclude the possibility that this direction is somehow an unexplained combination of a Kiaman direction and a modern field direction.

5.2. Racławka and Czatkowice, Poland

5.2.1. Age constraints

Paszkowski (in Dvorák et al., 1995) originally assumed an early to middle Tournaisian age of the Dubie and Racławka Formations. According to Wolniewicz (2009), the assemblage of foraminifera found in the Góra Żarska Member of the Dubie Formation indicate the Famennian *Quasiendothyra communis*– *Quasiendothyra regularis* foraminiferal zone, which corresponds to the Upper *Palmatolepis marginifera* – Upper *Palmatolepis expansa* conodont zones (Wójcik, 2012). A similar assemblage of foraminifera, with *Quasiendothyra communis communis* and *Eoendothyra regularis* and no representatives of *Q. kobeitusana* and Carboniferous tournayellids have been found in the upper part of the Racławka Formation within the studied interval during fieldwork in 2016. The early Tournaisian age of the Szklary Formation is suggested based on the presence of a foraminiferal assemblage with *Earlandia elegans* and *Eochernyshinella crassitheca*, which corresponds to the Belgian MFZ2 Foraminiferal Zone and *Siphonodella belkai* conodont zone of the Ural region (Bąk et al., 2014; compare to Poty et al., 2007). A Carboniferous (Tournaisian) age was proven also for the Przy Granicy Formation based on conodonts (Appelt, 1998; compare to Gromczakiewicz-Łomnicka, 1974). A local hiatus at the Devonian-Carboniferous boundary due to the global Hangenberg regression cannot be completely ruled out, as there is no record of uppermost Famennian foraminifera.

The exact position of the Devonian-Carboniferous boundary in the Czatkowice Quarry, as well as in the Racławka Valley section is still uncertain. However, similar to the Kraków platform area, upper Famennian cyclic sequences with oolites and bahamite grainstones were described from Montagne Noire (La Serre section; e.g., Feist et al., 2000) and Aachen-Velbert area sections (Hance and Poty, 2006). These sections contain the same succession of characteristic lithofacies, calcretised and stylolitised subaerial exposure surfaces, transgressive lags and bentonite layers, which are covered by up to 2 m of oolitic-bahamitic grainstone bed (bed no 159 in the Anseremme section) corresponding to the Devonian-Carboniferous boundary (Hance and Poty, 2006). The Rhenish Slate Mountains also contain records of oolites above the Devonian-Carboniferous boundary (Becker et al., 2021). The precise lithostratigraphic correlation of the aforementioned sections, as well as identification of the basal Tournaisian boundary in the Czatkowice quarry need further investigation.

5.2.2. Origin of the magnetic signal

Further up in the Czatkowice section than our sampled interval, in the Przy Granicy Formation (late Tournaisian age), Appelt (1998) found Mississippian conodonts with very low CAI values of 1-1.5, similar to the values from the Blankenheim section. Both the Holy Cross Mountains and the Eifel Mountains were part of the Variscan fold belt, and low CAI values can be explained by the lack of deep burial of the Devonian sedimentary rocks. Grabowski and Nawrocki (1996) tentatively suggest that remagnetisation in this area is linked to late Variscan ore mineralisation, while Zwing (2003) mentions a complex remagnetisation history for the Holy Cross Mountains further north. It is unclear whether the ChRM represents a near-depositional magnetisation overprinted with viscous remanent magnetisations (VRMs), or a later chemical remagnetisation related to Variscan ore mineralisation. However, considering the dual polarity obtained from both sections, as well as the good correlation between the two sections based on magnetostratigraphy, we consider the latter unlikely. Regardless, any remagnetisation must have occurred without significantly elevating temperatures, as CAI values are low, and without generating significant quantities of SP/SD grains, because hysteresis loops are distinct from remagnetised carbonates. It is noteworthy that Ordovician carbonates from the Holy Cross Mountains that have similar CAI as our Devonian rocks are variably overprinted by Kiaman remagnetisations, and show well-resolved normal and reverse Ordovician polarities (Hounslow et al., 2021; Schätz et al., 2006).

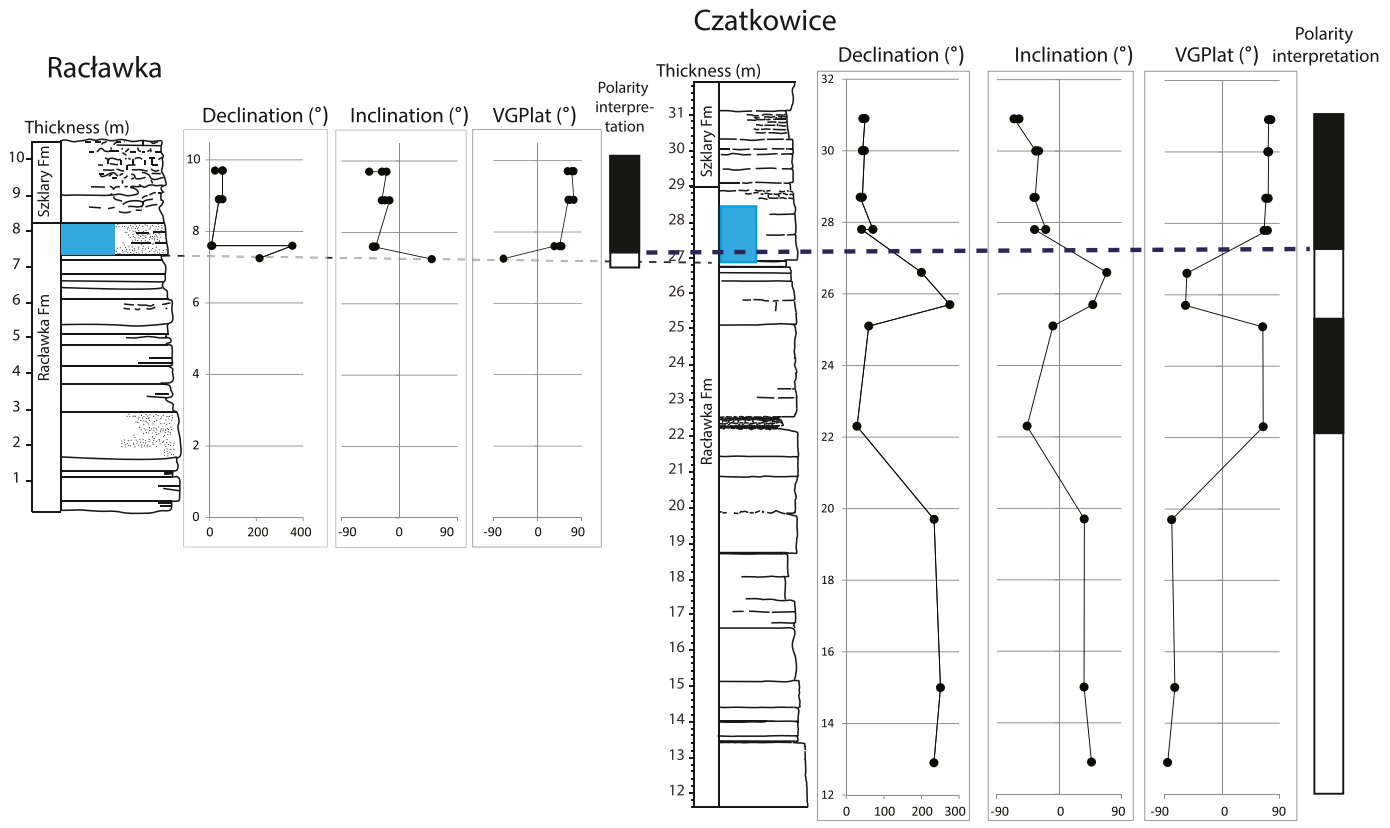

Fig. 17. Magnetostratigraphic interpretation alongside lithological logs of the Racławka and Czatkowice sections and correlation between the sections based on the magnetic polarity interpretation (thick dashed line) and lithostratigraphy (thin dashed line).

5.2.3. *Interpretation of the magnetostratigraphy*

Our limited sampling of the Upper Devonian in the Racławka and Czatkowice sections has not enabled a comparison with the polarity pattern of the study of Hansma et al. (2015), which covered the Frasnian-Famennian boundary (see Fig. 1). The directions we find in our Polish samples represent both polarities, and results are consistent between the two measured sections, which we can confidently correlate based on the magnetic polarity pattern (thick dashed line in Fig. 17) and biostratigraphy. Liu et al. (1991) find a reverse magnetozone with an overlying normal magnetozone just above the Devonian-Carboniferous boundary, and we find a similar relationship (but with different biostratigraphic control). Kolesov (2007) finds a similar Reversed-Normal magnetozone boundary in both the Kamenka section in NE Russia and the Kozhim section in the northern Urals, rather closer to the inferred Devonian-Carboniferous boundary like in our data. These differences are likely explained by imprecision in placement of the Devonian-Carboniferous boundary.

5.3. *Prohibition Creek, Canada*

We observe three components of magnetisation in the samples from Canada, one resembling a modern field, one resembling a Carboniferous reverse polarity, and one that is scattered and may have no geological significance (see Fig. 21). We thus cannot make an interpretation concerning Devonian directions or polarities from the Canadian samples.

5.3.1. *Age constraints*

The upper 61 m of the Hume Formation at Prohibition Creek mainly consist of bioclastic mudstone and wackestone with birds-eye fenestral structures and rare macrofossils, and wackestone/packstone in the uppermost 3 m and lowermost 10 m of the studied interval (Kabanov et al., 2019). Most archival and recent samples taken for conodont biostratigraphy in this part of the Hume Formation were barren, except for a few samples in the wackestone/packstone beds. Faunas are dominated by icriodid taxa in the lowermost beds and by polygnathid taxa in the uppermost beds. However, the index taxa for the upper Eifelian part of standard conodont zonation, *Tortodus kockelianus* and *Polygnathus ensensis,* are not present in the samples. Lithological correlation with the Hume type section, and several other sections representing the Hume Formation in the northern Mackenzie Mountain front (Gouwy, unpublished data; Gouwy and Uyeno, 2018), allows projection of the standard conodont zonation onto the Prohibition Creek section, based on the faunas identified in the different sections. For the *T. kockelianus* Zone, *Polygnathus curtigladius*, the local auxiliary taxon used to indicate the base of the zone (Uyeno et al., 2017), is projected onto the Prohibition Creek section at 90 m below the top of the Hume Formation. The *kockelianus* Zone in the studied interval covers thus roughly two thirds of the entire *kockelianus* Zone in the section. The index taxon *P. ensensis* has a delayed first appearance in the lowermost part of the Hare Indian Formation in the Mackenzie Mountains and Mackenzie Valley area. The base of the *P. ensensis* Zone is indicated by the appearance of the brachiopod *Eliorhynchus castanea*, index for the *castanea* brachiopod Zone (Pedder, 2017), whose base coincides with the base of the *P. ensensis* Zone, in the Hume type section, and is projected at 2.5 m below the top of the Hume Formation in the studied section. Based on the conodont zones identified in the section and the estimated 2 Myr duration of the *kockelianus* Zone (when the *eiflius* zone is included; Becker et al., 2020), the studied interval represents roughly 1.3 Myr.

5.3.2. *Origin of the magnetic signal*

The observed low temperature component is likely a VRM acquired during the Bruhnes chron. The reverse polarity component could represent either a thermoviscous remanent magnetisation (TVRM; e.g.,

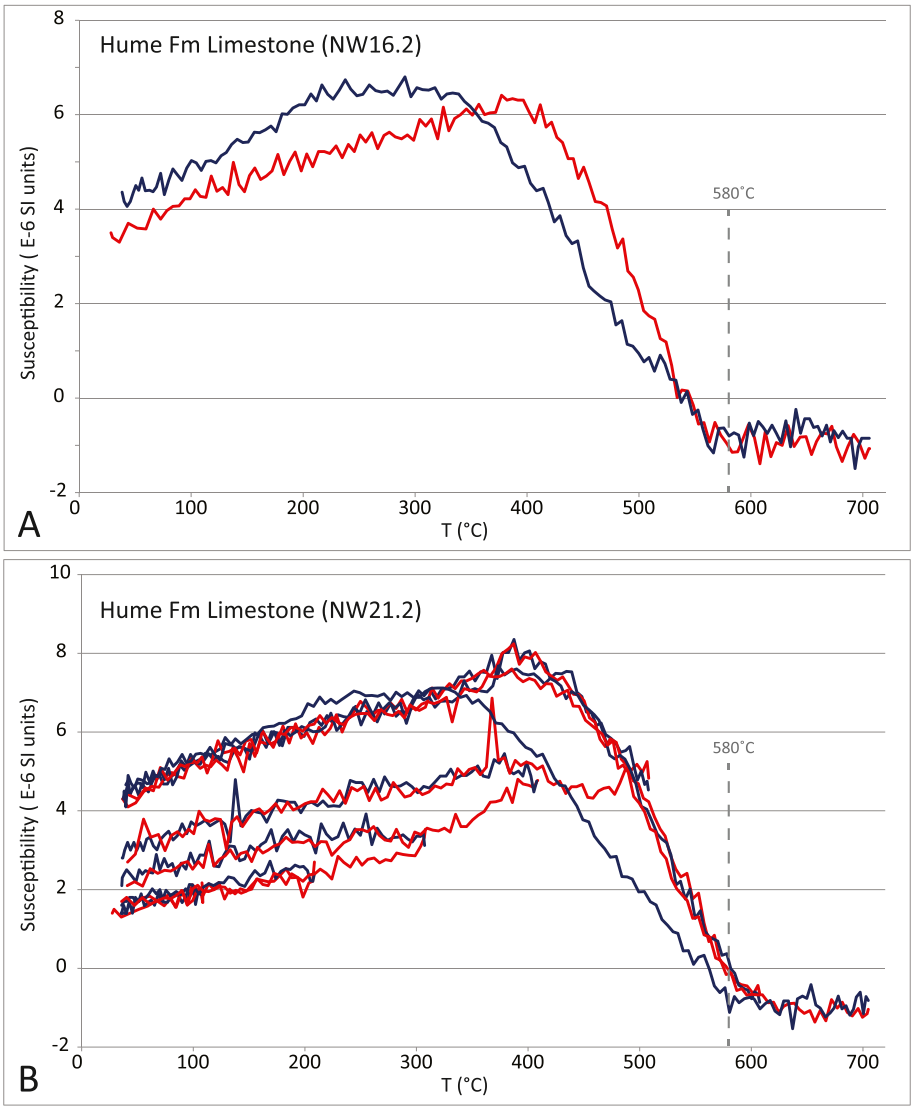

Fig. 18. Kappabridge susceptibility versus temperature runs of samples of the Hume Formation. The Curie temperature of magnetite (580 °C) is indicated with a grey dashed line.

Kent, 1985), or a chemical remanent magnetisation (CRM) acquired during the Kiaman superchron. Since this component does not converge towards the origin, and the rock magnetic results do not indicate introduction of new magnetic minerals, we tentatively conclude that this component represents a TVRM. We hypothesise that the remaining high-temperature component could represent a primary (post-) detrital remanent magnetisation reflecting a chaotic magnetic vector from the time of deposition, or could be meaningless, but we currently cannot conclusively choose between either of these two.

5.4. Summary of new results

Our new results are of varying quality. The results from the sections that we have measured in Germany and Canada yield problematic paleomagnetic results. The samples from the Blankenheim section show either only a Devonian reverse polarity (see Fig. 9), or represent a direction that is a mixture between the Kiaman field and a modern field, but we cannot presently distinguish between these two, due to the lack of field tests. Samples from Canada show three types of directions: components likely resembling a modern field direction, components resembling a Carboniferous Kiaman direction, and unknown components that show extremely large scatter (see Fig. 21). The Polish sections, however, seem to produce reliable directions in some specimens.

Results from the Polish sections can be compared to literature poles from Devonian sedimentary rocks from the Holy Cross Mountains. Grabowski and Nawrocki (2001) found seven groups of data, of which four are located on a great-circle (Fig. 22). The authors discuss in detail how their data might be explained, but do not provide an all-encompassing solution, and conclude that a definite tectonic interpretation is not possible. They discuss the necessity for some poles to be the result of remagnetisation, as they were derived from limestones with high CAI and/or show secondary dolomitisation. However, explaining all results would require large vertical-axis tectonic rotations that are not in agreement with structural observations in the area. Another hypothesis considered was strain modification of magnetic minerals, which however disagreed with their AMS (anisotropy of magnetic susceptibility) results. Our Devonian normal polarity average (dec = 41.2°, inc = -35.1°) falls between two of their directions (denoted DO and JO; Grabowski and Nawrocki, 2001) and lies along the great-circle that Grabowski and Nawrocki (2001) describe (see Fig. 22). Our Devonian reverse polarity average (dec = 237.9°, inc = 49.9°) does not compare to any of their results. Thus, while we conclude that the new paleomagnetic directions obtained from our Polish sections probably represent reliable Devonian field directions, rocks from this area collectively present a

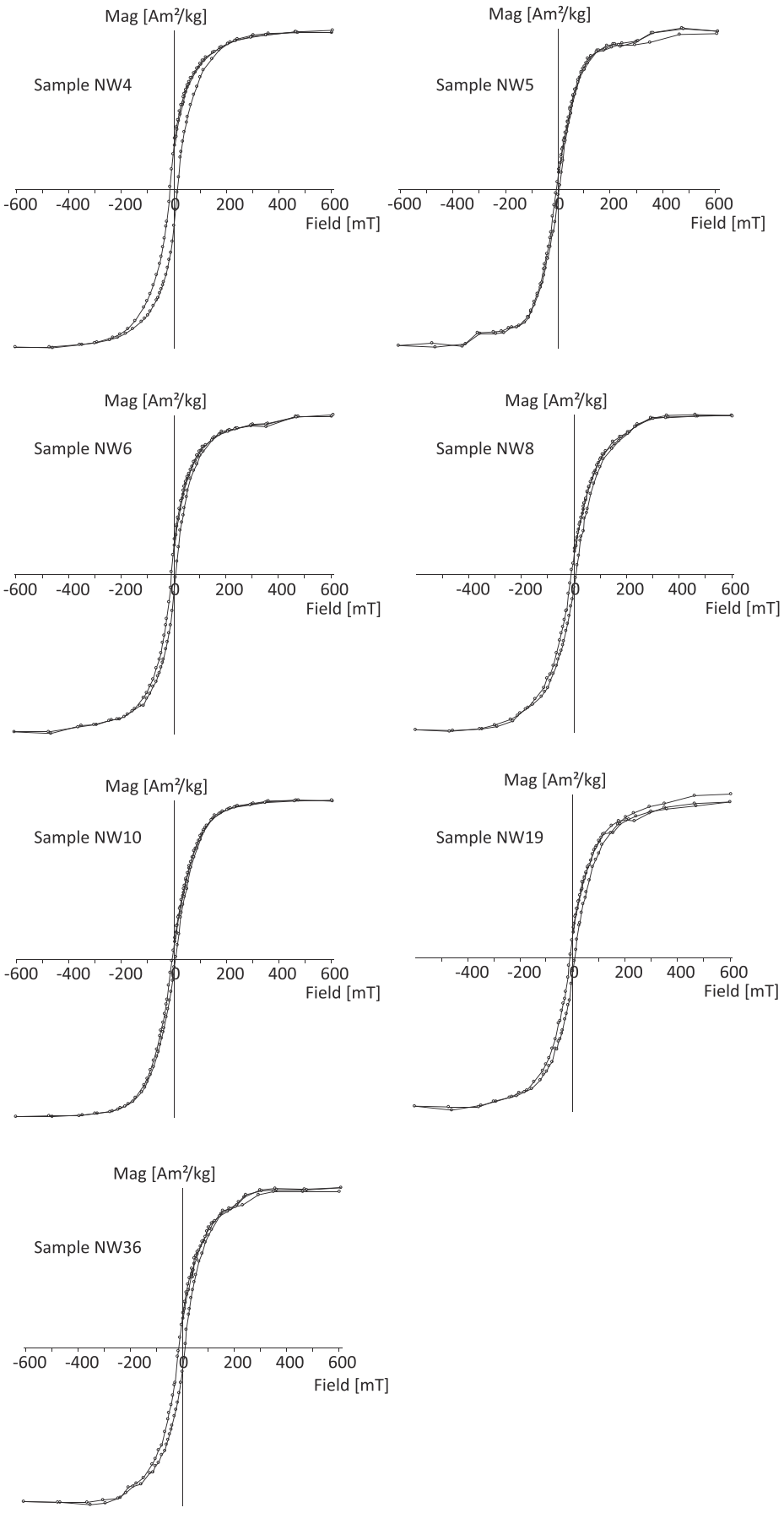

Fig. 19. Hysteresis loops of representative samples from the Prohibition Creek section.

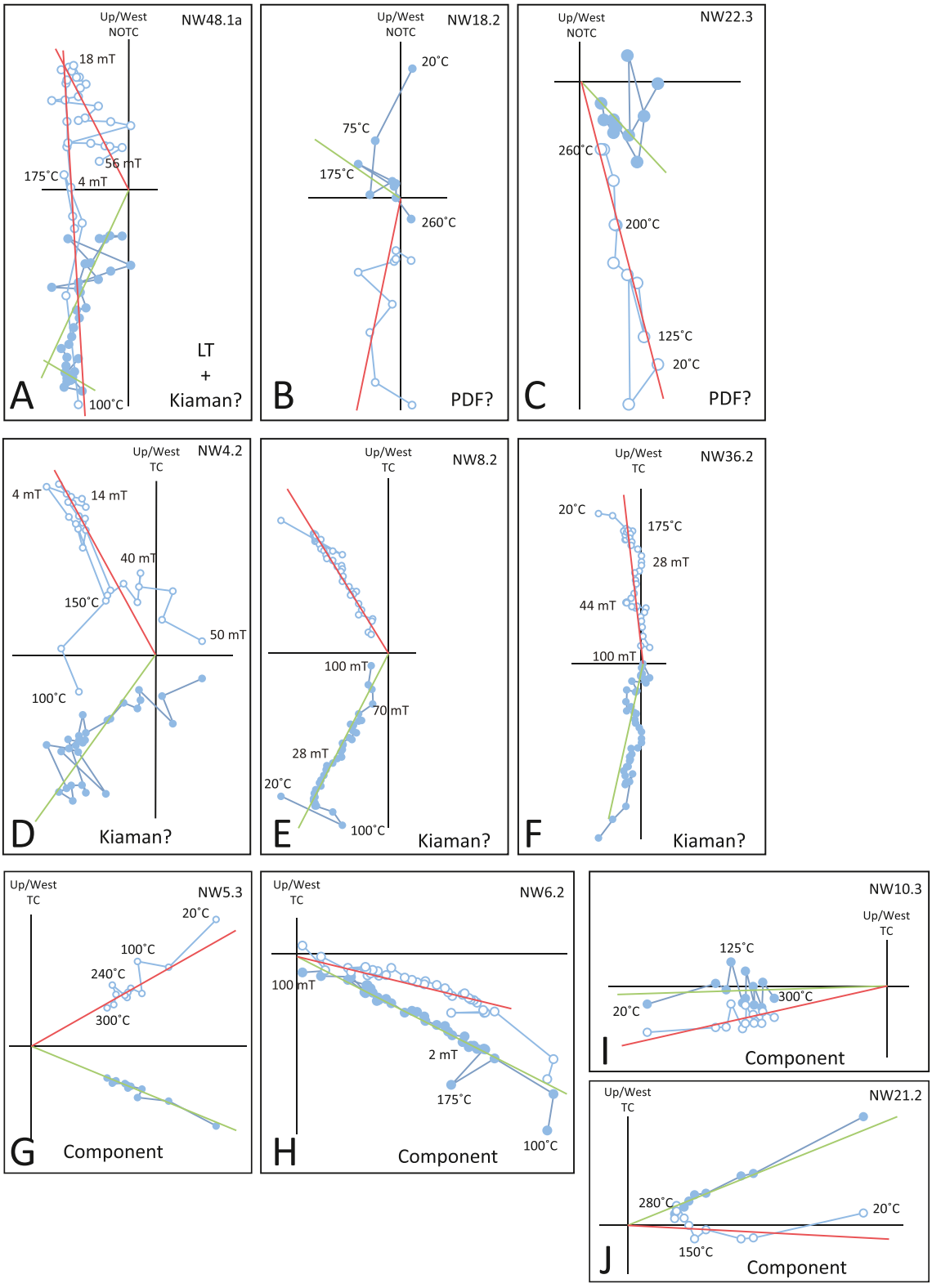

Fig. 20. Representative Zijderveld diagrams for samples from Canada. Legend is the same as Fig. 9. A. Sample shows a low temperature component (LT) and a component that we interpret to represent a Kiaman direction. B. and C. Samples showing a pervasive overprint that resembles a present day field (PDF). D-F. Samples showing a pervasive overprint that resembles a Kiaman direction. G-J. Samples showing clear demagnetisation towards the origin of the Zijderveld diagrams, but directions are extremely scattered.

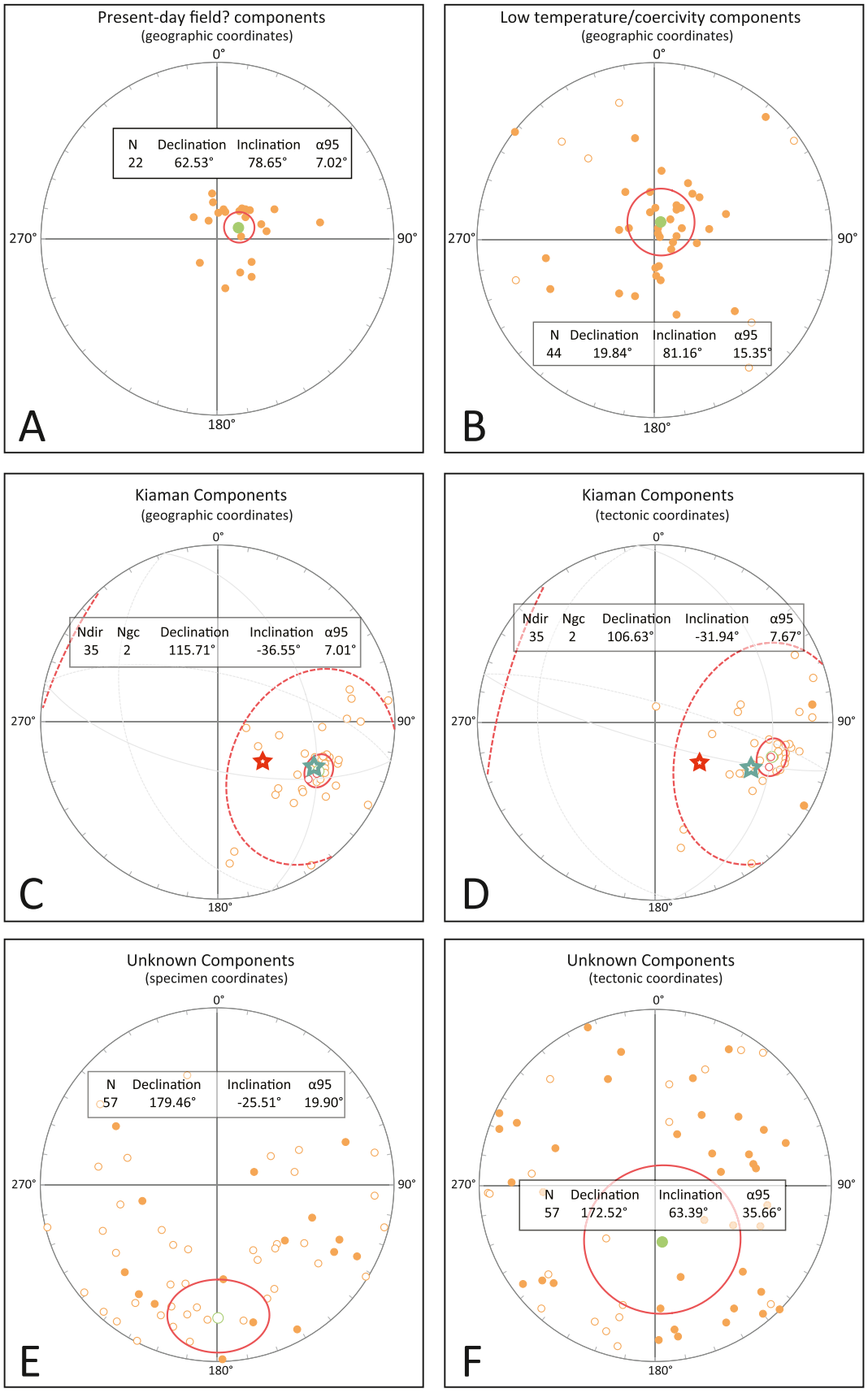

Fig. 21. Equal area plots of the interpreted directions of samples from Canada. Legend is the same as Fig. 10. A. Directions that (somewhat) resemble a modern field. B. LT components mostly resemble a modern field, albeit with large scatter. C. Components that resemble a Kiaman direction (before tectonic correction). D. Components that resemble a Kiaman direction (after tectonic correction). The red stars represent the expected direction at 260 Ma (Permian); the turquoise stars the expected direction at 320 Ma (Carboniferous). E. Unknown components plotted in specimen coordinates. F. Unknown components plotted after tectonic correction.

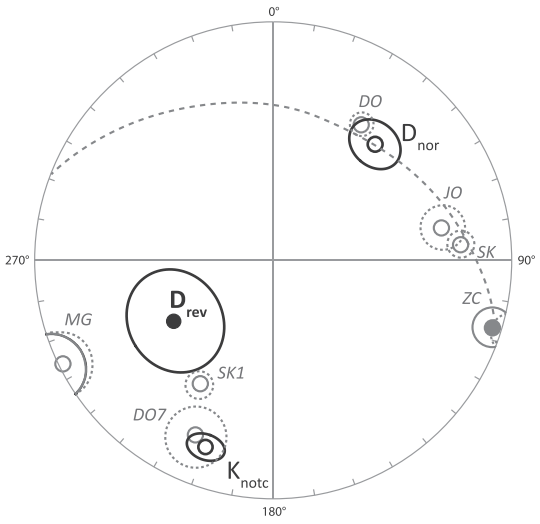

Fig. 22. Comparison of our newly acquired directions D_{nor} (Devonian normal polarity average) and D_{rev} (Devonian reverse polarity average) with paleomagnetic directions from Grabowski and Nawrocki (2001). K_{notc} is our Kiaman direction without bedding correction.

puzzling record of the magnetic field.

One of the common observations from Devonian paleomagnetic results is that the rocks have suffered from widespread remagnetisation, mostly during the Kiaman reverse superchron (e.g., North America: Irving and Strong, 1985, Irving and Strong, 1984; Mac Niocaill and Smethurst, 1994; McCabe and Elmore, 1989; Belgium: Garza and Zijderveld, 1996; Zegers et al., 2003; Ukraine: Jeleńska et al., 2015; Smethurst and Khramov, 1992; Poland: Kadziałko-Hofmokl et al., 1999; Nawrocki, 1993; Algeria: Aïfa, 1993; Mauritania: Kent et al., 1984; Germany: Zwing and Bachtadse, 2000; Australia: Schmidt et al., 1986; Ireland: Pastor-Galán et al., 2015; Urals: Iosifidi and Khramov, 2013). However, one important question remains unresolved: how can rocks record an overprint when the conditions for overprinting are barely met? Königshof et al. (2016) provide detailed rock magnetic studies on samples of the Blankenheim section, and indicate that thermally-related alteration appears to be very weak, based on thin-sections and preservation of fossils. Conodont alteration index values indicate that the succession in the Blankenheim section was subjected to maximum temperatures of around 55 °C, which are unlikely to cause significant thermal-overprinting (e.g., Pullaiah et al., 1975). Furthermore, Königshof et al. (2016) argue that superparamagnetic grains, which they expect in remagnetised samples, are not very common. The grain size of the magnetite grains in the Blankenheim section is in favour of a detrital origin (Königshof et al., 2016). So, while conditions for the probable preservation of a primary Devonian paleomagnetic signal have been met, our directional results show a pervasive partial Kiaman overprint. In order to gain a broader insight into the Devonian geomagnetic field we turn to reviewing the global dataset of published paleomagnetic measurements.

6. Review of Devonian paleomagnetic studies

6.1. Magnetostratigraphy of the Devonian

The geomagnetic polarity time scale (GPTS) is heavily reliant on marine magnetic anomalies which are preserved in oceanic crust until the Middle Jurassic. However, due to subduction of oceanic plates, a GPTS for the Early Jurassic and older must instead be derived from records obtained from outcrops or drill cores. For the Triassic, a lot of progress has been made in the last few years (e.g., Kent et al., 2019; Maron et al., 2019). The Early Permian and Pennsylvanian are dominated by predominantly reverse polarity of the Kiaman superchron (e.g., Hounslow and Balabanov, 2018), while the somewhat limited data for the Mississippian indicate mixed polarity (Hounslow, 2021). Constraining the GPTS and reversal frequency for the Devonian to Carboniferous is crucial for understanding the behaviour of Earth's magnetic field. The Earth's magnetic field is hypothesised to have a 'heartbeat', of varying average reversal frequency and intensity, with a periodicity of about 200 million years (e.g., Pavlov and Gallet, 2005). A strong magnetic field is generally associated with magnetic superchrons, such as the Cretaceous normal superchron (e.g., Tarduno et al., 2002). These are intervals of millions of years in which the magnetic field is extremely stable and there are no (or very few) reversals of the geomagnetic field. On the other hand, a weak field is commonly associated with frequent reversals, such as the middle-late Jurassic hyperactivity (e.g., Kulakov et al., 2019). Changes in the strength of the field and the reversal frequency are thought to be driven by changes in heat flow across the core-mantle boundary, which may in turn be linked to supercontinent cycles and subduction flux (Hounslow et al., 2018). This 200 Myr periodicity hypothesis relies on the behaviour of the magnetic field during the Devonian (420-360 Ma). The 'heartbeat' hypothesis predicts a weak field for this time, with a high reversal frequency.

Construction of a GPTS for the Paleozoic requires a careful inspection of Devonian magnetostratigraphy. In Fig. 1, we give an overview of the polarity patterns that were provided for the Devonian in the most recent versions of the geologic time scale (GTS; 2020, 2016, 2012 and 2004). In Becker et al. (2020), the polarity pattern in the Devonian is taken from the 2012 version (Becker et al., 2012), with an additional polarity pattern obtained from the Canning Basin in Australia by Hansma et al. (2015). A prior version of the timescale (Ogg et al., 2016a) shows conflicting polarity patterns around the Devonian-Carboniferous boundary. Ogg et al. (2016a), in their chapter on the Devonian, put the boundary in an interval of unknown polarity, while in the chapter on the Carboniferous, Ogg et al. (2016b) put the Devonian-Carboniferous in a reverse polarity interval. These inconsistencies are largely inherited from older versions of the timescale, as the patterns of Becker et al. (2012) differ from the patterns of Davydov et al. (2012). However, the most problematic issue with the Devonian polarity patterns as presented in the GPTS is that it is unclear what data they are based on. Clues to the origins of these polarity patterns are the Russian hyperchron names such as 'Sayan hyperchron', 'Donetzian mixed polarity hyperchron', which indicates that these geomagnetic polarity intervals largely have their origins in the Russian 'general stratigraphic scale' (Guzhikov, 2019; Khramov and Shkatova, 2000), first created by Khramov and Rodionov (1980), which is in part based on non-magnetostratigraphic data. In this 'general stratigraphic scale', it is unclear which datasets of have suffered from remagnetisation, and which data were included into the GPTS (see discussion in Guzhikov, 2019). The review of Carboniferous polarity by Hounslow et al. (2021) has largely dispensed with these older uncertain datasets. As Fig. 1 illustrates, the Russian Devonian timescales of Kolesov (2005) and Khramov and Shkatova (2000) are incompatible with the GPTS of 2004, 2012 and 2016.

The only well-documented studies of Devonian magnetostratigraphy are from Frasnian-Famennian (Late Devonian) carbonates in the Canning Basin in Australia (Green et al., 2021; Hansma et al., 2015). All other studies that provide magnetic polarity patterns (e.g., Kolesov, 2007; Kolesov, 2005; Kolesov, 1984) do not show the data on which they are based, preventing the quality of the magnetostratigraphic data to be assessed. Sampling strategies for constructing a magnetostratigraphy are very different from paleopole type studies. Studies aimed at reconstruction of poles generally collect ≥5 samples per site, and sites are typically not uniformly distributed through rock successions. In contrast, for magnetostratigraphic studies sampling ideally consists of closely-spaced, evenly distributed samples with respect to stratigraphic height. The large magnetostratigraphic study by Hansma et al. (2015) used almost 900 samples, and was performed on rocks which were challenging due to weak magnetisations. Hansma et al. compared their

data with previous studies on the same sections (Chen et al., 1995; Hurley and Van Der Voo, 1987), and reported that their new data clustered in the southwestern quadrant of the stereonet, in agreement with the poles of the previous studies. However, Hansma et al. applied a 45° cut-off centred on the mean of the prior poles, which eliminated nearly half of their data points (45% of Oscar range data and 40% of Horse spring data). Applying this process, Hansma et al. reported a field that is moderately rapidly reversing (reversal frequency is on the same order as during the Paleogene, ca. 2 reversals per Myr) even when omitting magnetozones based on a single sample. However, the correlation of the magnetozones between their two time-equivalent sections is rather ambiguous and their untreated data is near randomly distributed on a sphere (see Fig. 23). The more recent study of Green et al. (2021) on carbonates from a drill core in the Canning Basin shows very similar findings. The conglomerate test of Heslop and Roberts (2018) indicates strong support for a uniform distribution of these directions. Clearly, applying a 45° cut-off on a near-uniform distribution of directions that are randomly ordered with respect to stratigraphic height will produce a conclusion of a rapidly reversing field. The creation of a robust magnetostratigraphy from these results is therefore in doubt, unless it can be corroborated, and we suggest that inclusion of the inferred magnetozones in any GPTS is unwise.

6.2. *Tectonic paleomagnetic studies of the Devonian*

Since the early days of paleomagnetic study, it has been a struggle to reconstruct Devonian plate tectonics using paleopole datasets (e.g., Livermore et al., 1985). Plate reconstructions based on paleomagnetism have been shown to be challenging to match with climate belts and lithologic indicators of paleolatitude, notably with Russian gypsiferous sediments in the Late Devonian (Khramov, 1967; Witzke, 1990; Witzke and Heckel, 1988). Evans (2006) looked at the geographic distribution of evaporites and surmised that Devonian and Ediacaran evaporites show an anomalous distribution compared to Cenozoic-Carboniferous evaporites when using paleopoles to infer paleolatitudes. For many plates, reliable Devonian poles are lacking. We focus our review here on

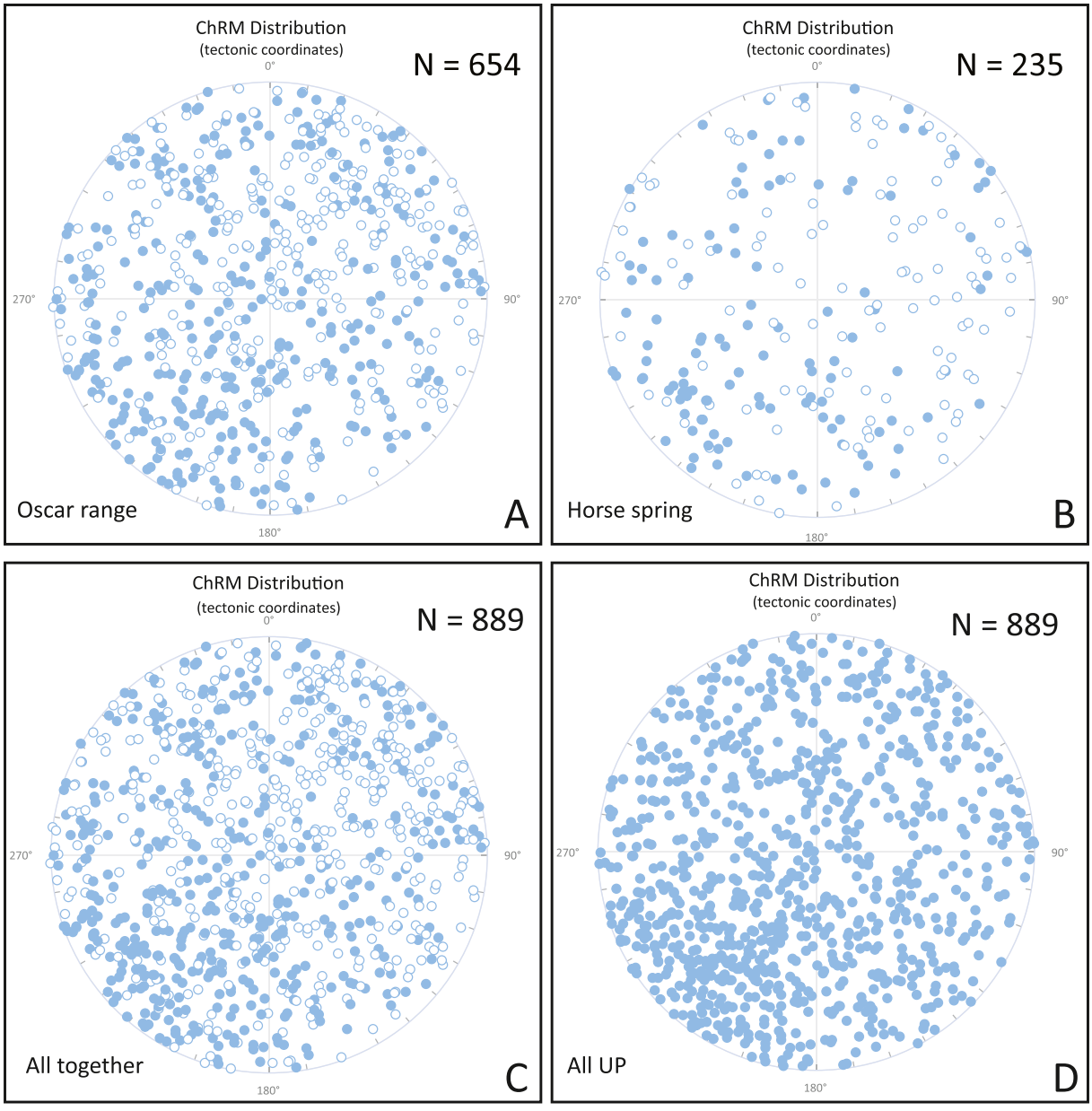

Fig. 23. All data from the study of Hansma et al. (2015) on the Canning basin in Australia. A. All data from the Oscar Range. B. All data from Horse spring. C. All data from Oscar Range and Horse spring together. D. All data together converted to the same hemisphere.

the poles that were used for construction of global apparent polar wander paths, which are constructed based on paleomagnetic poles from the large continents. The discussion below is incomplete with respect to poles from smaller plates and complex tectonic settings. We provide an overview of all the paleomagnetic studies on Devonian rocks studies that we assessed in an extended bibliography (supplementary file S8). More than 40 years ago, Morel and Irving (1978) suggested that reliable plate tectonic reconstructions can be made from the middle Carboniferous onwards, whereas for the Devonian, reconstructions are poorly constrained due to the scarcity of results (on average ~8 paleomagnetic results per 10 Myr, compared to an average of ~20 for Carboniferous and later times; Morel and Irving, 1978). Morel and Irving (1978) introduced two apparent polar wander paths, based on the inclusion or exclusion of paleomagnetic data obtained from Australia, based on a total number of 56 paleopoles. They show an X-path, which is relatively straight, and a Y-path, which has a large loop (see discussion in Vérard, 2004). The Y-path results in drift rates for plates that are 40-60 cm/yr. (Vérard, 2004), rates which are above the hypothesised maximum speed at which plates tend to move (Conrad and Hager, 1999; Meert et al., 1993; Zahirovic et al., 2015). We note here the similarity of Devonian paleomagnetic results to those of the Ediacaran, a time period for which complex paleomagnetic data would also result in anomalously high plate speeds (e.g., Abrajevitch and Van der Voo, 2010).

Cocks and Torsvik (2002) provide a review of paleopole data and fauna from 500-400 Ma and conclude that the reliability of paleopole data decreases into the Devonian. Also Torsvik et al. (2012) note that data is truly scarce from the Middle Devonian to the Mississippian. Fig. 24 shows the number of poles in the APWP of Torsvik et al. (2012), which highlights that there has been little progress in improving the scarcity of Devonian paleopole data since 1978. Cocks and Torsvik (2007) highlighted that between the Llandovery (early Silurian) and latest Permian, there are only two reliable poles for the reconstruction of Siberia and Baltica. One has an age of around 360 Ma, close to the Devonian-Carboniferous boundary, and the other one an age of 275 Ma, (late early Permian). Bachtadse and Briden (1990) indicate that the Devonian is the most problematic segment of the Gondwana APWP and Torsvik et al. (2012) show that data coverage is especially poor for Laurentia between 400-340 Ma and that paleopoles for 260-350 Ma and 390-380 Ma are instead interpolated. This interpolation results in the so-called 'Siluro-Devonian cusp' (Torsvik et al., 2012), which has been interpreted as an episode of extreme true polar wander (e.g., Piper, 2006; van der Voo, 1994). In short, there is an agreement that plate tectonic reconstructions in the Devonian suffer from a severe scarcity of high-quality paleopole data.

In assessing the quality of paleopoles, a common approach is to classify the poles based on the reliability criteria of Van der Voo (1990), a widely accepted approach to filter-out older studies based on inadequate demagnetisation techniques. The Van der Voo criteria are used to quantitatively assess the quality of paleomagnetic poles and for each of the 7 Q-criteria, the palaeopole gets 1 point. Commonly only poles that have a minimum value of Q=3 are taken into account for construction of apparent polar wander paths. The minimum criteria (Q=3) state that the rocks must (1) have a well-determined age and presumption that the magnetisation is of the same age, (2) give results that are based on a sufficient number of samples and (3) be from rocks that were adequately demagnetised. Reliability can be further increased by field tests that constrain the age of magnetisation, structural controls are provided, reversals are observed, and there is no resemblance to paleopoles of a younger age. Algeo (1996) used 35 poles obtained from Devonian rocks to assess polarity bias in the Devonian, with each of these passing a number of quality criteria of Van der Voo (1990). Similarly, Mac Niocaill and Smethurst (1994) use 11 poles for the reconstruction of the APWP of Laurentia. Torsvik et al. (2012) used 18 Devonian paleopoles for the construction of the GAPWaP (see Fig. 24), with many having a high Q-index, up to the maximum of 7 using the Van der Voo (1990) criteria. As discussed below, however, problems still remain with Devonian paleopoles even if they have a high Q-index, indicating that scarcity of paleomagnetic data for the Devonian has not yet been solved by using modern techniques.

For the Australian part of East Gondwana, for example, Torsvik et al.

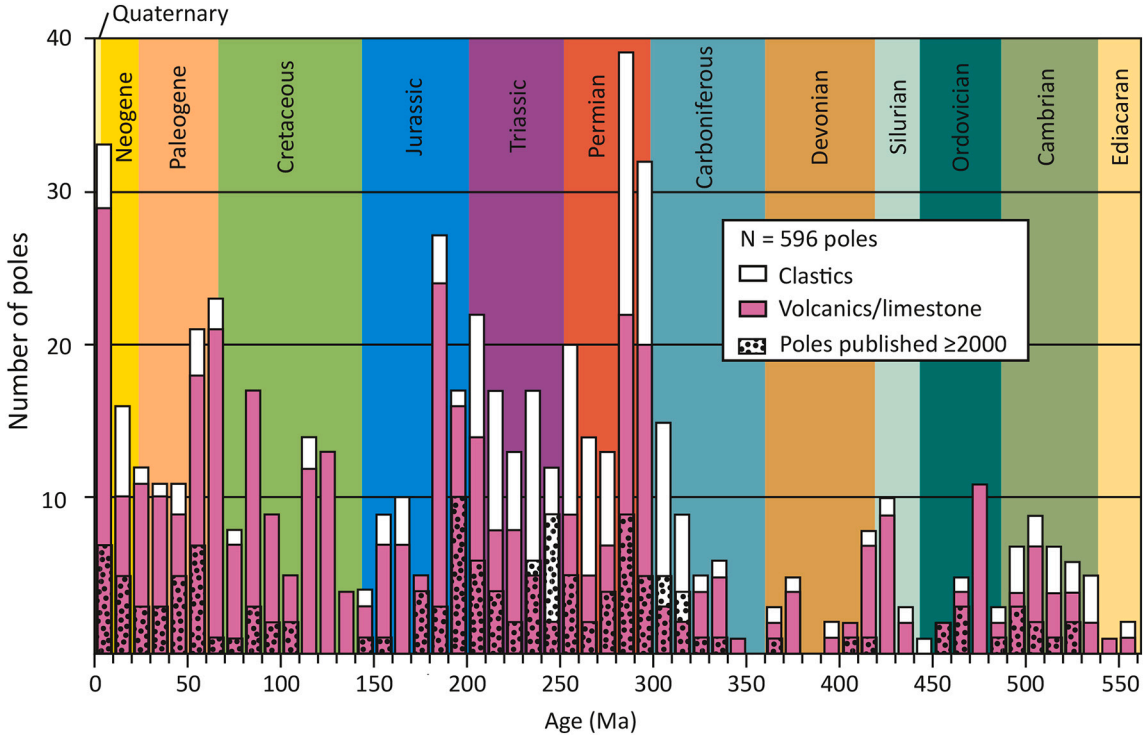

Fig. 24. Number of poles in 10 Myr bins in the GAPWaP of Torsvik et al. (2012) (modified after Torsvik et al., 2012), plotted on the Geologic Time Scale 2020 (Gradstein et al., 2020). Dotted are the poles that were included in the GAPWaP which were published after the year 2000.

(2012) include four poles. Three of these poles are from the Canning Basin and are obtained from the same, or time-equivalent formations (Chen et al., 1995; Hurley and Van Der Voo, 1987). The 4th pole is cited as 'E. Tohver, pers. comm. (2012)', which we assume was subsequently published as Hansma et al. (2015). Arguably, these three poles all form just one pole, as they were obtained from the same rocks. That is, if these data should be taken into account at all, as we discussed previously the problems with the Hansma et al. (2015) data. The Chen et al. (1993) paleopole for the Australian APWP cannot be reconciled with the data from Africa by Bachtadse and Briden (1991), while both of these studies are included in the GAPWaP. The only pole taken into account for the western Gondwana APWP is from the Bokkeveld Group in South Africa from the study of Bachtadse et al. (1987). However, Bachtadse and Briden (1990) do not consider data from Bokkeveld Group as meeting the requirements for a key pole due to 'complicated rock-magnetic behaviour'. We do not seek to discredit the Devonian portions of APWPs, but highlight these issues to show that upon closer inspection nearly all Devonian paleomagnetic data are problematic. It is noteworthy that the problematic pole from the Canning basin (E. Tohver, pers. comm., 2012) is the only study in the Devonian part of the GAPWaP of Torsvik et al. (2012) that was published in the last 25 years. This brings to light an important challenge in paleomagnetism; namely that there are few robust studies using modern methods that aim to construct paleopoles from the large stable continents, while the global apparent polar wander path for the last 500 million years is by no means complete.

For the Devonian, a perverse impression arises; the smaller a dataset is, the more likely it is to provide acceptable results. Larger datasets often show results that are problematic, as they may show groups of directions that either cannot be explained, or have resulted in competing explanations involving large tectonic rotations, extreme plate speeds, or episodes of true polar wander (e.g., Lewandowski, 1995; Nawrocki, 1995). When sample size is increased, the risk of obtaining (groups of) complicated directions that cannot be reconciled with other data increases. This can be seen for example in the study of Bazhenov et al. (2013) who extended the sampling of Levashova et al. (2007). Levashova et al. (2007) report a succession of lava flows exhibiting secular variation (which describes the changes in the magnetic field on timescales of typically several tens of thousands of years or less) consistent with the predominantly GAD field during most of the Cenozoic. However, the extended sampling of Bazhenov et al. (2013) reveals lava flows where the magnitude of secular variation is substantially greater than previously reported. Bazhenov et al. (2013) find that the directions from part of their lava succession shows secular variation that is several times greater than in another part. Other examples include Hawkins et al. (2019), who used the directions of Kravchinsky et al. (2002), but also show additional directions that were not published in the original study. A similar situation is observed for the Cheviot Hills lavas in the north of England, where Hawkins (2018) shows more directional groups than the original study of Thorning (1974), which is included in the APWP of Torsvik et al. (2012). Grabowski and Nawrocki (2001) find several directional groups in middle to upper Devonian sediments from Poland, which cannot all simultaneously be explained (see also Fig. 22). Sallomy and Piper (1973) describe a distribution of directions that is not simply antipodal. They find two groups that they interpret as normal and reverse polarity, then sites classed as groups A and B, and then nine further 'unclassified' sites. The directions from the Sallomy and Piper (1973) study were reanalysed by Shatsillo and Pavlov (2019), who interpret them as due to non-dipolar behaviour of the field during the Devonian.

Directional groups are common in volcanic successions (e.g., Knight et al., 2004; Van Der Boon et al., 2017), as volcanic rocks are formed rapidly, and may not average out secular variation. If directional groups are also observed in sedimentary rocks, as the study of Grabowski and Nawrocki (2001) seems to suggest, this likely indicates that the field stayed in a stable configuration for a long time while detrital remanence magnetisation was locked in. Martin (1975) hypothesised that the interval in their study on Middle Devonian limestone sampled a normal polarity interval, a reverse polarity interval, and a transitional interval in which the field reverses polarity, and secular variation might not be averaged out. Considering the relatively slow sedimentation rates for limestones, this is an unusual conclusion. The normal and reverse polarities of Martin (1975) are furthermore not antipodal. Directional groups and extreme scatter that are seen in these studies are difficult to explain by remagnetisation (e.g., Løvlie et al., 1984), which would have likely led to more consistent directions since the presumed remagnetising conditions would have occurred simultaneously across all sites.

In summary, the APWPs for continental plates in the Devonian rely on sparse data, for which palaeopole quality is hard to assess due to the absence of supplementary data. The number of paleopoles that are considered reliable has decreased since the 1970's (e.g., Mac Niocaill and Smethurst, 1994; Morel and Irving, 1978; Torsvik et al., 2012). The general characteristics that arise from Devonian data are that studies have often found several groups of directions that cannot all be simultaneously explained, or the scatter in directions is extremely large, so directional averaging is unwarranted. Due to the positive-outcome bias that exists in most fields of science (e.g., Fanelli, 2012), one wonders whether this data scarcity from Devonian paleomagnetic studies is due to many more non-positive results. As there have clearly been many studies done on Devonian paleomagnetism, we do not consider it likely that scarce results are due to a lack of study of Devonian paleomagnetism. Furthermore, extensive rock magnetic studies may be required by reviewers to supplement datasets (e.g., this study, Bazhenov et al., 2013), or the results are too complex to interpret and authors might refrain from publishing their Devonian datasets (e.g., Powerman et al., 2013).

6.3. Studies of geomagnetic field behaviour

Absolute paleointensity studies typically provide snapshots of the strength of the magnetic field, so obtaining a comprehensive paleointensity record throughout the Devonian requires many studies. Paleointensity data spanning the interval 200-500 Ma have recently been reassessed using the Quality of Paleointensity (Q_{PI}) framework (Biggin and Paterson, 2014) by Hawkins et al. (2021) and Bono et al. (2022). Since Sallomy and Piper (1973), the Devonian field has been suggested to have a strength that was an order of magnitude lower than the modern field. Subsequent paleointensity studies from Devonian volcanic rocks have supported this conclusion, revealing a weak to very weak field (e.g., Briden, 1966; Didenko and Pechersky, 1989). Until recently, many measurements of Palaeozoic paleointensity were acquired using techniques that are not considered to meet modern standards of reliability. Several recent studies (Hawkins et al., 2021; Hawkins et al., 2019; Shcherbakova et al., 2021; Shcherbakova et al., 2017) have, however, confirmed the central observation - the field in the Devonian and early Carboniferous was unusually weak compared to any subsequent period. Hawkins et al. (2021) found that paleointensities show an extremely weak magnetic field in the Devonian, with some outliers during the Early Devonian (around 400 Ma), a time interval for which there are both weak and strong paleointensity results. It is possible that the field dropped in strength from weak in the Early Devonian to extremely weak in the Middle and Late Devonian, but many more paleointensity data are needed to verify this.

Bono et al. (2022) use the PINT v8.0.0 database to determine a long-term median dipole moment of 48 ZAm^2, averaging the past 4 billion years. The modern field is stronger, around 80 ZAm^2 (Thébault et al., 2015). The field in the Devonian is thus much weaker (Hawkins et al., 2019; Shcherbakova et al., 2017), with a median value of 17 ZAm^2 (Hawkins et al., 2021). Hawkins et al. (2021) suggest this low field interval extended for at least 80 Myr, from the Early Devonian into the early Carboniferous and named it the Mid-Palaeozoic Dipole Low.

Here we investigate whether the time-averaged strength of the

magnetic field changed during the Devonian. Robust estimates of the paleofield are challenging to obtain for rocks of any age due to the ubiquitous presence of non-ideal magnetic recorders which are prone to laboratory-induced alteration. Typical paleointensity studies have a success rate of ~20%; this effect is further complicated by two additional factors (Tauxe and Yamazaki, 2007). Firstly, early paleomagnetic techniques had variable capability for recognizing spurious magnetizations, but community standards on data reporting have since evolved to include metrics on data quality. Thus, early studies require careful inspection and/or removal from analyses if unsuitable measurements are recognized (Biggin and Paterson, 2014). Secondly, large (i.e., multidomain) magnetic grains can represent a substantial fraction of the remanence magnetization in some rocks. Multidomain grains have geologically short magnetic relaxation times (<<100 Myr; Dunlop and Özdemir, 1997), and while these rocks may be suitable for paleodirection/magnetostratigraphic studies, such samples can yield unreliable paleointensities in older geologic materials. For these reasons, careful selection criteria must be balanced with the desire to maximize the quantity of data included in a description of long-term field behaviour. Hawkins et al. (2021) and Bono et al. (2022) compiled and analysed a dataset of field strength estimates for the Devonian and assessed the reliability of paleointensity data using the Q_{PI} (Biggin and Paterson, 2014) approach. Using a combination of the PINT database (Bono et al., 2022), with Shcherbakova et al. (2021) and paleointensity data from Hawkins et al. (2021), we selected sites which met the following criteria for our analysis: 1) directions were not identified as transitional in polarity by authors of the study, 2) there are at least three intensity determinations per site, and 3) site data are of reasonable quality (total $Q_{PI} \geq 3$). Virtual dipole moments were determined using published inclination and paleointensity data; if inclination data were not available (14/120 sites), a virtual axial dipole moment was determined assuming a site latitude of 30.6° (which yields a dipole moment halfway between an equatorial and polar site latitude). Here, paleointensity sites are from volcanic cooling units recording "instantaneous" snapshots of the field. Selected data were grouped into 1 Myr bins to produce time-averaged estimates; only bins which contained more than one site were considered for characterizing the trend (see Fig. 25). Different selection criteria were explored (either a stricter one requiring Q_{PI} criteria AGE+MD+ALT+DIR to have passed, number of intensity determinations ≥ 3, and number of sites per bin ≥ 3, or a more relaxed one accepting any non-transitional paleointensity sites with at least 3 determinations and bins with only one site). These alternate selection criteria do not substantially change the broad interpretation of a very weak field during the Middle to Late Devonian. However, the stricter selection criteria may address a potential suspicion of a low-field bias (Smirnov et al., 2017) by only selecting sites where magnetizations carried by non-ideal multidomain carriers are removed prior to the paleointensity experiment.

Organizing the data in this fashion suggests a geomagnetic field that was somewhat weaker than the Phanerozoic average during the Early

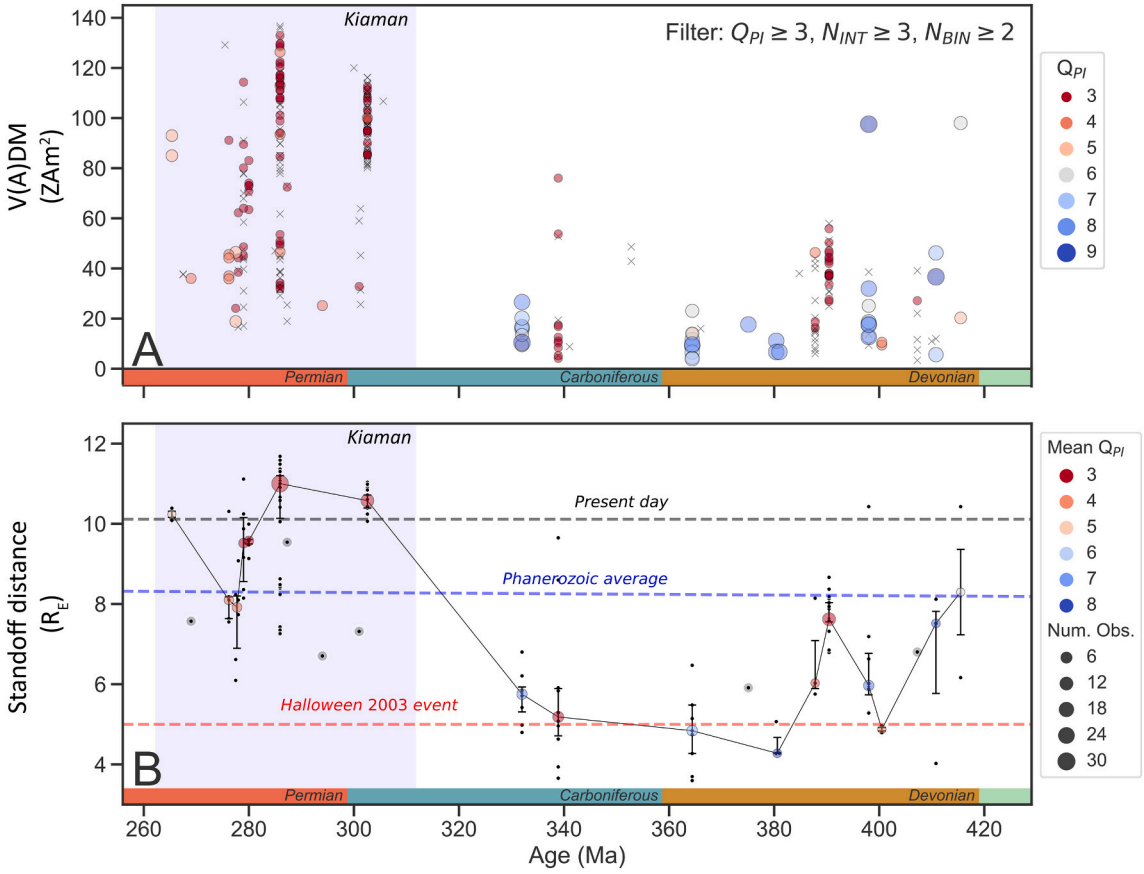

Fig. 25. A. Virtual (axial) dipole moments during the Devonian; studies included in the dataset are listed in Supplementary file S11. Symbol size and colour show Q_{PI} score; symbols marked with an "x" were not included in the standoff distance analysis. B. Median magnetopause standoff distance in Earth radii. Symbol size shows the number of sites within a 1 Myr bin; symbol colour shows the mean Q_{PI} score for that bin. Uncertainty bars show the interquartile range for each bin. Small dots show individual site standoff estimates; grey circles show age bins containing a single site. Ages for the Silurian-Devonian and Devonian-Carboniferous boundaries from Becker et al. (2020) and Carboniferous-Permian boundary from Henderson et al. (2020). Shaded region labelled "Kiaman" defines the Kiaman Reverse Superchron with associated high magnetic field strengths. Dashed lines show standoff distance for present day (black), long term average assuming median dipole moment of 48 ZAm^2 (Phanerozoic, Bono et al., 2022; in blue), and standoff distance during an extreme space weather event (Halloween 2003 event, Rosenqvist et al., 2005; in red).

Devonian and steadily weakened during the Middle Devonian, reaching a minimum by 380 Ma (Late Devonian). This interval of extremely weak field appears to have lasted for ~40−80 Myr, although constraining the duration is hampered by the lack of sufficiently high quality paleointensity data for the 340-360 Ma interval. By the onset of the Kiaman Superchron (see Fig. 25) at ca. 315 Ma, the field strength had recovered to reach or exceed the Phanerozoic mean field.

Two other aspects of long-term field behaviour that can be assessed using paleomagnetic records are average polarity reversal frequency (e.g., Biggin et al., 2012) and paleosecular variation (e.g., Doubrovine et al., 2019). Hansma et al. (2015) claimed to observe a minimum 44 reversals during the late Devonian (a ~24 Myr interval) translating to a reversal frequency of ~2 Myr^{-1}. However, the unusual treatment of data applied to a uniformly distributed dataset (see Section 6.1) raises serious questions over the validity of this reversal record. Bazhenov et al. (2013) also reported unusual paleosecular variation behaviour in a study of lavas in Kazakhstan (see Section 6.2). As noted, secular variation appears to have been enhanced for at least part of the Late Devonian. High scatter of directions caused by secular variation, if confirmed, would suggest a reduced role of the axial dipole in the morphology of the Late Devonian field (Biggin et al., 2020).

7. Explanations for suboptimal paleomagnetic results from Devonian rocks

A wide-ranging review of Devonian paleomagnetism has highlighted that there is a global paucity of published paleomagnetic studies in this period. Most paleomagnetic studies on Devonian rocks are decades old and may not contain the data detail and scientific rigour that is typically expected of contemporary studies. Where recent studies have been published (e.g., Green et al., 2021; Hansma et al., 2015; Hawkins, 2018; Hawkins et al., 2019; Shatsillo and Pavlov, 2019), the data tend to represent paleomagnetic directions that are more scattered than usual, in some cases to an extreme extent. We consider below different reasons for why the Devonian paleomagnetic results may be odd.

7.1. Weak magnetisations

The lack of reliable paleomagnetic data for the Devonian has long been implicitly assumed as a possible indicator for a weak magnetic field, and this has been confirmed by modern studies of paleointensity. A weak magnetic field (Hawkins et al., 2021, Hawkins et al., 2019; Shcherbakova et al., 2021, Shcherbakova et al., 2017) will have led to weakly magnetised rocks, which enhance the risk of remagnetisation after the Devonian, in times when the field was stronger. Weak magnetisations also increase the difficulty of obtaining primary paleomagnetic data from sediments due to magnetometer sensitivity limits. Indeed, Devonian rocks classically have extremely weak magnetisations, which often makes exhaustive quantitative analysis challenging. The Devonian has partly acquired a bad reputation for paleomagnetic studies due to studies from the 1960's when equipment was much less sensitive than today. However, even now with very sensitive magnetometers, measuring Devonian carbonates is still a big challenge, as we have found. Jeleńska et al. (2015) also reported very weak NRM intensities which hampered measurements and interpretation. NRM intensities for Devonian rocks are generally in the range of 10^{-3} A/m or below. Although sediments in general have weaker magnetisations than igneous rocks, with values down to 10^{-6} A/m (e.g., Claesson, 1979; Kadziałko-Hofmokl et al., 1999; Kent, 1979), there are studies that report very weak NRM intensities for Devonian igneous rocks, with values in the range of 10^{-4}-10^{-5} A/m (e.g., Hargraves et al., 1987; Jeleńska et al., 1995; Sallomy and Piper, 1973). Normally, NRM intensities of igneous rocks are much higher, in the range of 0.1-10 A/m (e.g. Dunlop and Özdemir, 1997). Considering the linear relationship between the field and magnetisation (e.g., Dunlop, 2011), and the field in the Devonian likely being at most around 10 times weaker than the modern field, a weak field is likely not the sole explanation for weakly magnetised basalts, and other hypotheses may need to be developed to fully explain weak magnetisations in Devonian volcanic rocks.

7.2. Remagnetisation

In Devonian rocks, remagnetisations acquired during recent times and during the Kiaman Superchron are common. Therefore, remagnetisations certainly contribute to the difficulty in obtaining good paleomagnetic data. There was of course ample time and opportunity for remagnetisation after the Devonian. Geodynamo models suggest that during superchrons, the field is strong (e.g., Driscoll and Olson, 2011) and most estimates (but not all; Garcia et al., 2006) from the Kiaman support this (Hawkins et al., 2021). Mountain building in the late Carboniferous-early Permian provided excellent remagnetisation conditions, and many consider that recovering primary Devonian magnetisations is troubling due to remagnetisation during the Kiaman superchron (McCabe and Elmore, 1989; Perrin and Prévot, 1988; Shatsillo and Pavlov, 2019; Thominski et al., 1993; Zwing, 2003). While there is an abundance of studies that explored remagnetisation issues of Devonian rocks, understanding of the mechanisms and imaging of the grains responsible for the remagnetisation remains limited (for extensive reviews of remagnetisation mechanisms of (Devonian) rocks, we refer to Elmore et al. (2012) and Van der Voo and Torsvik (2012)). Zwing (2003) suggests that almost 90% of overprints in late Paleozoic rocks have a reverse polarity, and two thirds are remagnetised between 350 and 250 Ma, which corresponds well with the Kiaman overprints in our samples. Remagnetisation has been linked to four possible origins, 1) heating and associated enhanced thermal remanent and thermoviscous remanent magnetisations (TRMs and TVRMs; Middleton and Schmidt, 1982); 2) smectite-illite transformation during burial (Katz et al., 1998); 3) fluid-related mineralisation in permeable units, 4) diagenetic-related production of new magnetic Fe-phases (Roberts, 2015), or a combination of these (e.g., Minguez et al., 2016). Thermally controlled overprints (causes # 1 and 2) are relatively easy to assess (e.g., Middleton and Schmidt, 1982), because estimates for maximum temperatures can be determined using conodont alteration indices (CAI) and vitrinite reflectance (R_{max}) data. When CAI values show that rocks have not been significantly heated, it is commonly inferred that Kiaman remagnetisations must thus have occurred through chemical-mineralogical remagnetisation processes (CRMs, causes # 3 and 4). CRMs are often inferred to be related to processes that drive fluids going through rocks. These hypotheses of chemical remagnetisation of Devonian rocks are often inferred based on the lack of evidence for thermally controlled overprints. In light of common problems of chemical remagnetisation, it is remarkable that Devonian rocks are considered suitable for cyclostratigraphy based on rock magnetic data or magnetic susceptibility (Crick et al., 2001; Crick et al., 1997; Da Silva et al., 2016; De Vleeschouwer et al., 2017; De Vleeschouwer et al., 2015; Ellwood et al., 1999; García-Alcalde et al., 2012), while yielding no primary paleomagnetic directions because of inferred chemical remagnetisation (Courtillot et al., 1986; Weil and Van der Voo, 2002; Zegers et al., 2003; Zwing, 2003). The so-called 'squeegee model' (Oliver, 1992) has been invoked to explain widespread remagnetisations of Devonian rocks in North America that have only been heated to low temperatures (< 150°C). The squeegee model infers the existence of cold orogenic fluids at distances very far away from the mountain building front in the Appalachians. However, some studies have had difficulty tying remagnetisation to orogenic fluids. For example Elmore et al. (2001) show two remagnetised formations in a single section, one formation consisting of sandstones, the other formation consisting of limestones. While they found evidence for fluid flow through the sandstones, there was no evidence for fluid-flow related alteration related in the limestones, with obtained Sr isotope ratios in the limestones corresponding to Devonian seawater values. Elmore et al. (2001) concluded that a connection between driven-fluid mineralisation and pervasive overprints is

circumstantial. For the Rhenish Massif, Zwing (2003) discarded the possibility that Devonian rocks were remagnetised by regional migration of orogenic fluids. Zwing (2003) observed remagnetisation related to pyrite alteration to magnetite, which they hypothesised to be related to pore fluids or movement of fluids along fractures and faults. In the Middle Devonian of the Rhenish Massif, Zwing concluded that a different mechanism must be responsible for remagnetisation, perhaps related to pressure solution. Shatsillo and Pavlov (2019) further outline problems with overprinting in detail, and our new data also shows that, even when rocks are not expected to have been overprint by the usual processes (significant heating/burial or remineralisation), Devonian rocks do not show straightforward paleomagnetic directions. Furthermore, the concern of remagnetisation also holds true for older time periods. Prior to the Devonian, however, many paleomagnetic data exist that are considered reliable, even for regions where the Devonian rocks show only remagnetised directions (e.g., Montagne Noire; Nysæther et al., 2002, Bohemian Massif; Zwing, 2003) and periods where the field was reportedly hyperreversing, such as the Middle Cambrian (e.g., Gallet et al., 2019), or the Ediacaran (Bazhenov et al., 2016; Kodama, 2021). It is striking that there are more accepted paleomagnetic data from the Ediacaran, as the field in the Ediacaran was likely as weak as, or weaker than in the Devonian (Bono et al., 2019; Shcherbakova et al., 2020; Thallner et al., 2021). This poses the question: was the field in the Devonian of a different character than the field in the Ediacaran?

7.3. A non-GAD field

The approach of Hansma et al. (2015) to define magnetic polarity, using a 45° cut-off on VGP latitude, implicitly assumes that the field is a dipole, approximately aligned with Earth's rotation axis (GAD field). Any fixed cut-off approach assumes that the field is a relatively stable dipole and spends little time in transitional directions, since these are eliminated by the cut-off (e.g., Cromwell et al., 2018). As nearly half of the data are excluded based on the 45° cut-off in the study of Hansma et al. (2015), if their data truly represent the Devonian magnetic field, the stable GAD hypothesis is not suitable to describe the Devonian magnetic field. Shatsillo and Pavlov (2019) have argued for a significant contribution of an equatorial dipole to the Devonian magnetic field. The assumption that the time-averaged field coincides with a stable GAD underpins all plate tectonic reconstructions. Thus, if the field in the Devonian is indeed different from, this may explain paleopole studies that have resulted in conflicting X- and Y-paths (Morel and Irving, 1978).

7.4. Summary

The high Q-scores for Devonian paleomagnetic data in the GAPWaP indicate that the scarcity of reliable Devonian data is not purely a problem of widespread remagnetisation. As our newly obtained data show, rocks that are well qualified to have reliably recorded the magnetic field at time of formation often give ambiguous results, and obtaining accurate paleomagnetic data even from 'good' rocks is challenging. We interpret this to be an indication of a non-uniformitarian nature of the geomagnetic field during the Devonian, and not solely an intrinsic problem of the rocks' history of overprinting. It is striking that few studies show unambiguous Devonian paleomagnetic results, although we note that it is often difficult to judge the quality of the data, as many of the studies are some 25-60 years old, and supplementary data is generally absent.

Several studies have suggested that the field during the Devonian was different from the modern geomagnetic field (e.g., Hawkins et al., 2019; Shatsillo and Pavlov, 2019; Shcherbakova et al., 2021; Shcherbakova et al., 2017). These datasets were all obtained from volcanic rocks, which have TRMs, that are normally stronger than the detrital and post-depositional remanent magnetisations (DRMs and PDRMs) in sedimentary rocks that magnetostratigraphy relies on. Shatsillo and Pavlov (2019) argue that mean directions in the Early and Middle Devonian are not bimodal and antipodal, as expected from a GAD field, but show different clusters. Sedimentary rocks tend to average out paleosecular variation, while rapidly cooled volcanic rocks do not. Thus, the effect in sedimentary rocks (as well as in slow-cooling intrusive rocks) might be that several directional sets are contained within a single sample, and the directions compare poorly to those obtained from volcanic rocks. Shatsillo and Pavlov (2019) argue that the results of Piper (2007) from intrusive rocks were not caused by true polar wander, as argued for by Piper, but rather due to multiple composite directions caused by slow cooling.

If the Devonian geomagnetic field was truly weak or non-uniformitarian, the paleomagnetic community needs to reconsider which results are 'negative'. We emphasise the need for more studies and encourage scientists to publish their Devonian paleomagnetic results even if they are complex or appear unreliable. We also stress the risk associated with over-interpreting results and invoking peculiar regional tectonics or significant episodes of true polar wander, as it can be complicated afterwards to assess the data underlying these explanations. We argue that the conventional view on the Devonian as 'all overprint' is unlikely to provide a sole explanation for the scarcity of good Devonian paleomagnetic results, as intense overprinting cannot explain the presence of directional groups or large directional scatter.

8. Did Earth's magnetic field have an impact on life in the Devonian?

The remarkable evolutionary dynamics of the Middle-Late Devonian, with multiple extinctions of marine faunas, are summarised in Fig. 26. Following Becker et al. (2016, 2020), biotic events are ranked from most severe 1st order mass extinctions, to progressively less severe 2nd, 3rd and 4th order events. As highlighted above, there has been much debate on the causes of the Late Devonian mass extinctions, with a variety of suggested triggers, including explosive volcanism, global warming and cooling, or multi-causal processes. The fact that the events themselves consist of multiple steps reflects the complexity of extinction-radiation pathways (e.g., Aretz, 2021; Boyer et al., 2021; Fields et al., 2020; Kaiho et al., 2021; Marshall, 2021; McGhee and Racki, 2021; Paschall et al., 2019).

Marshall et al. (2020) have linked the terrestrial phase of the Hangenberg Crisis at the Devonian-Carboniferous boundary to an increase in ultraviolet (specifically, UV-B) radiation, which they hypothesize is caused by an increase in convective transport of chlorine monoxide through global warming. Fields et al. (2020) disputed this and have instead suggested that increased UV-B radiation during the Hangenberg Crisis was caused by supernovae. Another proposed mechanism for partial destruction of the ozone layer is by explosive volcanism (e.g., Kutterolf et al., 2013; Self, 2015). Volcanism has been often invoked to be a main factor in end Devonian biotic crises, but there has been considerable discussion on which volcanic province was responsible (e.g., Racki, 2020). There are several candidates, such as the large igneous province of the Viluy traps in Siberia, the Kola traps in Russia and the Pripyat-Dnieper-Donets province (Kravchinsky, 2012) (see also Fig. 26). Sudden increases in UV-B radiation reaching the surface of the Earth have been linked to a weak shielding of the Earth's atmosphere by the magnetic field in other geologic periods (e.g., Meert et al., 2016). Earth's magnetic field protects the atmosphere by deflecting charged particles coming from the sun (solar wind). When Earth's magnetic field is weak, the solar wind is not deflected to the same extent, and can reach the upper atmosphere, where charged particles interact with the ozone layer. These charged particles dissociate N_2 and O_2, which contributes to the formation of NO_x and HO_x in the middle atmosphere, which in turn are key in the depletion of stratospheric ozone (e.g., Meert et al., 2016; Vogt et al., 2007). The depletion of the ozone layer increases UV-B radiation reaching Earth's surface.

Understanding the strength and shape of the Devonian

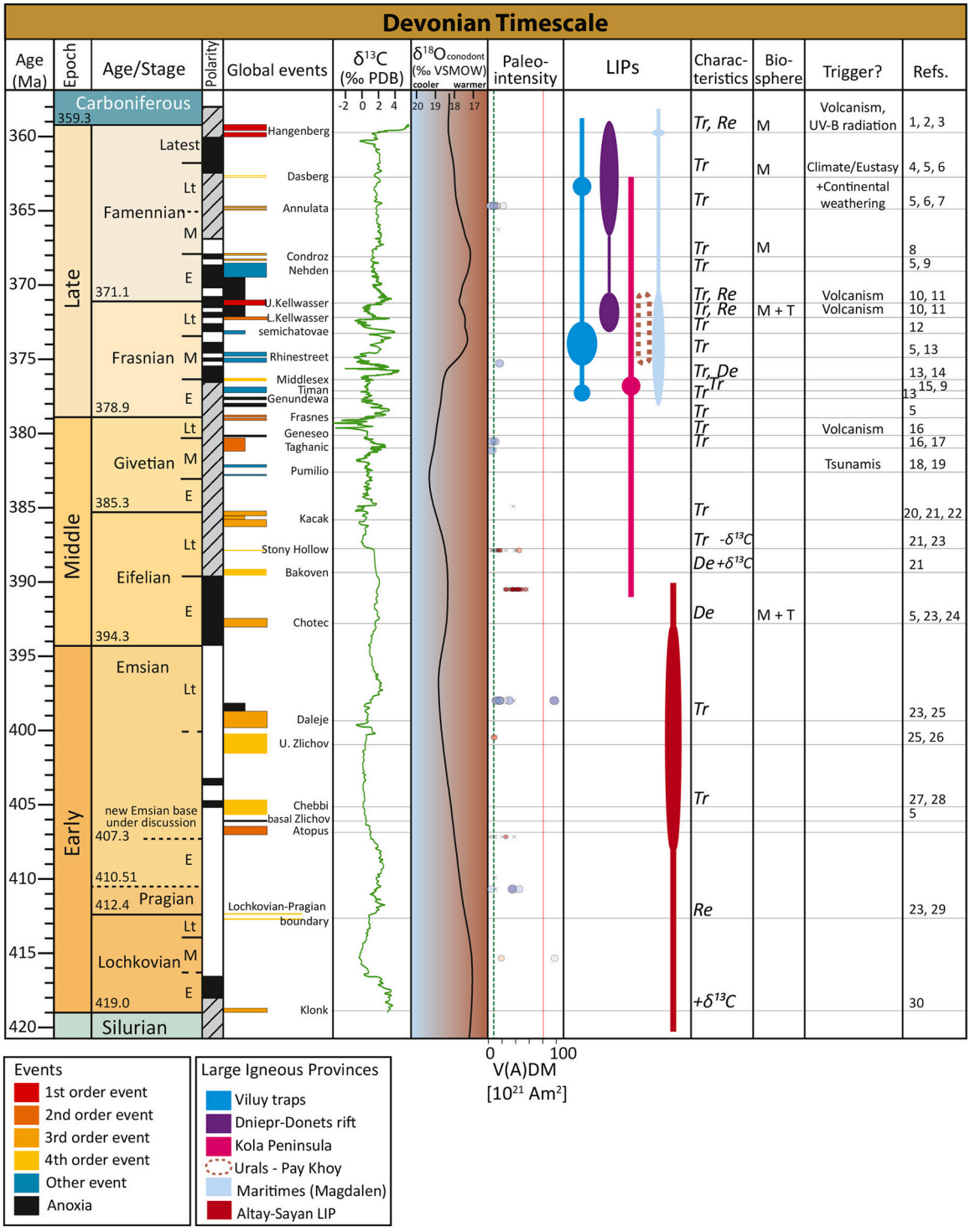

Fig. 26. Overview of biotic events and crises in the Devonian. Timescale from GTS2020 (Becker et al., 2020), magnetic polarity in black (white) is normal (reversed), grey is unknown. Global events from Becker et al. (2020, 2016), $\delta^{13}C$ is in reference to the Pee Dee Belemnite (PDB), $\delta^{18}O$ is in reference to the Vienna Mean Standard Ocean Water (VSMOW). Paleointensities from the PINT database (Bono et al., 2022) and Shcherbakova et al. (2021), green (red) line is the field strength in the Ediacaran (present day), large igneous provinces (LIPs) are after Racki (2020) and Ernst et al. (2021, 2020). Characteristics: Tr = transgression, Re = regression, De = deepening event, -$\delta^{13}C$ = negative $\delta^{13}C$ excursion, +$\delta^{13}C$ = positive $\delta^{13}C$ excursion. Part of biosphere affected: M = marine, T = terrestrial. To scale the volcanic pulses to the timescale of Becker et al. (2020), we used the Devonian-Carboniferous boundary, Frasnian-Famennian and Givetian-Frasnian boundaries in the fig. of Racki (2020). References : 1 - Kaiser et al. (2016), 2 - Pisarzowska et al. (2020), 3 - Marshall et al. (2020), 4 - Hartenfels and Becker (2009), 5 - House (2002), 6 - Hartenfels and Becker (2016), 7 - Percival et al. (2019), 8 - Becker et al. (2016), 9 - Becker and House (1997), 10 - Racki et al. (2018), 11 - Carmichael et al. (2019), 12 - Ziegler and Sandberg (1997), 13 - House and Kirchgasser (1993), 14 - Sandberg et al. (2002), 15 - Racki et al. (2004), 16 - Brett et al. (2011), 17 - Aboussalam and Becker (2011), 18 - Lottmann (1990), 19 - Becker and Aboussalam (2004), 20 - Königshof et al. (2016), 21 - DeSantis and Brett (2011), 22 - Suttner et al. (2021), 23 - Walliser (1996), 24 - Brocke et al. (2016), 25 - Tonarová et al. (2017), 26 - García-Alcalde (1997), 27 - Becker et al. (2020), 28 - Becker and Aboussalam (2011), 29 - Chlupác and Kukal (1988), 30 - Małkowski and Racki (2009).

magnetosphere and its concomitant magnetic shielding is critical for assessing increased penetration of charged solar particles into the atmosphere (relative to the present day or Phanerozoic average). A first-order approximation of the degree of magnetospheric shielding by the geomagnetic field is to quantify the distance to the magnetopause (the point at which solar wind pressure is balanced by Earth's magnetic field). We use the assumptions that virtual dipole moments represent a strictly dipole field, and that non-dipole contributions to field (both instantaneous and secular variation) resemble the present day field. These are conservative assumptions, which are expected to maximize the estimated magnetic shielding during the Devonian (following the approach of Tarduno et al., 2010). The estimated magnetopause standoff distances are presented in Fig. 25b.

The present day magnetopause is observed to be at a distance of ~10 Earth radii (R_E); under normal conditions, a value that fluctuates on annual time scales by $\leq$ 1 R_E due to changes in the location of the magnetic pole relative to the spin axis. The estimated magnetic standoff distance for the Early Devonian is consistent with that of the long-term Phanerozoic average (~8 R_E). During the Late Devonian nadir in field strength, the standoff distance was reduced to ~4–5 R_E. This distance is comparable to, or less than, the standoff distance minima observed during the Halloween 2003 event, a solar storm event which resulted in sufficient penetration of charged particles to generate auroras at low latitudes and disrupt the electrical grid in Sweden (Rosenqvist et al., 2005). However, unlike the Halloween 2003 event, which lasted on the order of days and can be seen as an ephemeral reduction in shielding, the standoff distance estimated for the Late Devonian represents the average standoff distance for millions to tens of millions of years. This reduction in shielding could be further exacerbated by magnetic storms and coronal mass ejections during the Devonian. Typical space weather can reduce the present-day magnetopause by ~1–2 R_E (Voigt, 1995), with greater reduction during more extreme events (e.g., Halloween 2003 event). If the paleomagnetosphere during the Devonian was substantially weaker and potentially less dipolar, as suggested by the paleomagnetic data, then shielding reductions during space weather events could be greater.

An additional property of the paleomagnetosphere is the magnetic polar cap: the region defined by open dipole field lines, inside which charged solar ions are funnelled towards Earth's surface. A second-order consequence of the polar cap is the occurrence of polar auroras at the lower latitudinal boundary of the polar cap. If the time-averaged paleomagnetic field is assumed to be fairly GAD-like during the Late Devonian, the lower bound of the polar cap (λ_P) and its surface area, can be estimated (following the approach of Siscoe and Chen (1975); see Supplementary file S9). During the Early Devonian, the median λ_P is estimated to be 68.9° (with an interquartile range spanning 66.2° to 69.5°; see Fig. 27a) which is somewhat lower than the present day latitude (71.9°; Siscoe and Chen, 1975) and suggests an increase in the relative surface area of the polar cap of ~1.5 times the present day shielding (Fig. 27b). When the geomagnetic field intensity was reduced during the Late Devonian, the polar cap could extend further southward to 63.7° (with an interquartile range spanning 61.8° to 65.0°; see Fig. 27c). This represents an increase in the surface area (relative to today) of a factor of ~2 (Fig. 27d), broadening the region where Earth's atmospheric ozone could be eroded due to dissociation of N_2 and O_2.

If the time-averaged field was substantially different from GAD, it is probable that the standoff distance could be further reduced and the validity of the polar cap description (with associated λ_P) could diminish.

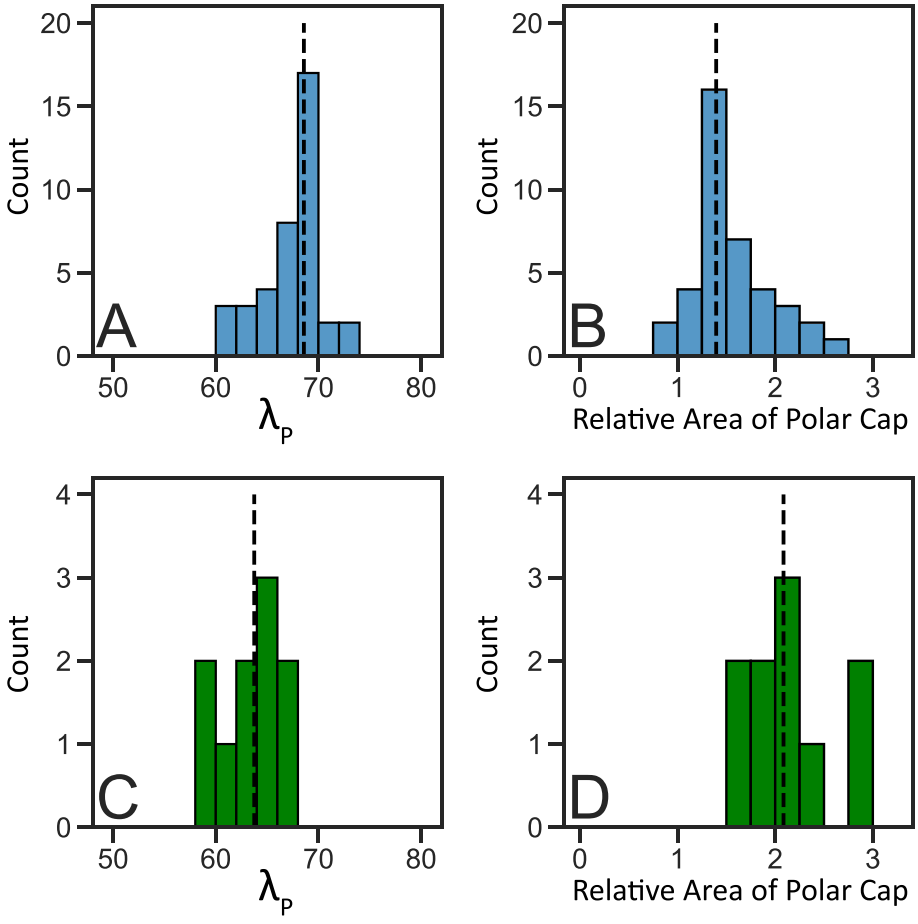

Fig. 27. Polar cap angle λ_P (left) and area relative to present day polar cap (right) estimated for each site V(A)DM. Dashed vertical lines mark median value. A and B: early Devonian (380-420 Ma); C and D: late Devonian (340-380 Ma).

As the contribution of a quadrupolar field increases relative to the dipole moment (a scenario representing the longest wavelength description of the non-dipole field), it is expected that λ_P could migrate up to ~10° towards the equator (Vogt et al., 2007). In a more extreme departure from a GAD field, models of the paleomagnetosphere during a simulated geomagnetic reversal (Stadelmann, 2004) suggest all latitudes could be susceptible to large fluxes of charged particles during extended periods of a weak, non-dipolar field.

We hypothesise that the magnetic field during the Devonian was in such a weak and unstable state that it constituted a substantial additional hazard for life. However, with our current knowledge, it is hard to estimate the contribution a weak magnetic field had in biotic crises in the Devonian. The weak magnetic field could have triggered specific biotic crises associated with its long-term secular variation (i.e. on the 10^5-10^6 year timescale), or its longer-term state (i.e. on the 10^7-10^8 year timescale) could have been a constant factor that enabled other triggers to have a bigger impact on the biosphere. Based on paleointensity evidence, we infer that Earth's magnetic field was extremely weak during the Devonian, and possibly periodically had a non-axial dipole configuration. Life during the Devonian thus might have been continuously 'on the edge' because of the weak protection of the atmosphere by the magnetic field, which meant that other triggers such as volcanism could have more easily enabled biological crises. The weak magnetic field could thus be one of the influencing factors in the multi-causal model that is favoured for the Late Devonian biotic crises (Racki, 2020). However, it is also possible that the field during the Devonian directly enabled biological crises through depletion of the ozone layer, which allowed more UV-B radiation to reach Earth's surface. In this case, however, it would be expected that malformed spores would be more widespread, and associated with other parts of the Devonian, instead of in distinctive intervals as the study of Marshall et al. (2020) suggests.

Future studies might provide perspectives on the causes for ozone depletion by looking at the duration of increased UV-B radiation, and assessing if there is evidence for enhanced UV-B radiation in the Early and Middle Devonian. The timescales on which UV-B radiation interacts with life on Earth, and the latitudes for which this effect is greatest are different for different causes of ozone layer depletion. For explosive volcanism, Self (2015) mentions that the increase in UV-B radiation reaches high and mid-latitudes and the effect lasts for a few years after the explosive eruption. Fields et al. (2020) discuss the scenario presented by Marshall et al. (2020), and note that the effect of the proposed mechanism would last only a few weeks. While the timescales associated with the Earth's magnetic field are highly variable (hours to millions of years), we think it is most plausible that the field was extremely weak for several tens of millions of years, as suggested by (Hawkins et al., 2021), and thus acted as a continuous stressor.

9. Outstanding questions pertaining to paleomagnetism of the Devonian

Despite the substantial amount of effort being expended, the body of knowledge concerned with most aspects of paleomagnetism in the Devonian remains small with respect to other geologic periods. Negative results are seldom published so it is likely that there may have been many more attempts at obtaining magnetostratigraphic records and other paleomagnetic data from Devonian rocks than the ones cited in our review. The timing and rate of polarity changes during the Devonian remains uncertain, and paleopole constraints on Devonian paleogeography are fragile and prone to controversial interpretations. A Devonian GPTS would fill in a major gap in the Paleozoic timescale, and would have great utility in high resolution global correlation since the Devonian was a time of many global crises including one of the 'big five' mass extinctions. For the study of the Earth's magnetic field, polarity records from the Devonian would allow assessment of the reversal frequency for an interval of some 60 million years duration. Reversal frequencies for other periods in geological history are a key constraint on the operation and evolution of the geodynamo with strong implications for mantle-forcing potentially linked to surface processes (e.g., Amit and Olson, 2015; Hounslow et al., 2018). Obtaining reliable Devonian paleopoles would be of huge benefit to precisely constrain paleolatitudes of the continents, and could significantly improve paleogeographic reconstructions.

Presently, the creation of a GPTS for the Devonian appears to be a task that will take several more decades of study to resolve, if at all possible. If the field in the Devonian was indeed multipolar in certain intervals, creating a global GPTS may be impossible, as creation of the GPTS is reliant on a dipolar field. To further understand the enigmatic field in the Devonian, we need more paleomagnetic data tightly linked to detailed stratigraphic-based studies both on sediments and volcanic rocks. Our overview of Devonian paleomagnetism raises rather more questions than it answers, and we hope that this study will promote new paleomagnetic studies on Devonian rocks. Furthermore, if studies can demonstrate (as we have attempted here), that the lack of conventional utility of a paleomagnetic dataset cannot readily be ascribed to the recording medium, then this serves as a direct test of the central hypothesis outlined here. In any case, we urge authors to supply their full data with their publications. Currently, many of the old data is difficult to assess, as they lack supplementary information.

Studies on (malformed) spores could also aid in assessing burial temperatures, and thus are a useful tool in assessing the likelihood of overprinting of the paleomagnetic signal. Marshall et al. (2020) mentioned that the thermal maturity of the spores in their studied section indicates a burial temperature of 107°C, a temperature at which it is likely that the paleomagnetic signal could be preserved. Future studies could focus on determining when the weak field period ended and the magnetic field recovered. It is likely that this is sometime during the Carboniferous, as many Devonian data seem to have late Carboniferous overprints. Data from the Kiaman superchron generally seem robust, indicating that the field must have recovered by the onset of the Kiaman superchron. For the beginning of the weak field period, we should look at the latest times prior to the Devonian for which paleomagnetic data show good results.

If the field was indeed extremely weak and the reduction in magnetic shielding had an influence on life on Earth, there might be more indications for increased UV-B radiation found in the biological record of the Devonian (e.g., Marshall et al., 2020). We suggest that this could be an interesting target for future studies. If there is no evidence for increased UV-B radiation elsewhere in the Devonian, this could imply that either the field was weaker or different in the Late Devonian compared to the Early and Middle Devonian, or the field was not a determining factor in the increase in UV-B radiation observed at the Devonian-Carboniferous boundary. Another intriguing question is whether the field could have had an impact on oceanic anoxia, perhaps through a link with partial destruction of the ozone layer, which would have been accompanied by a depletion of oxygen in the atmosphere (e.g., Meert et al., 2016; Vogt et al., 2007). The reverse has already been suggested for the Mesozoic, in which ocean anoxia ended through enrichment of atmospheric oxygen (e.g., Baker et al., 2017; Tsandev and Slomp, 2009).

Another major avenue of future work will be to investigate the mechanism behind the weak field period in the Paleozoic. Studies that modelled the geodynamo have suggested that the formation of the inner core would have caused the field to increase in strength (Driscoll, 2016). A recent estimate for inner core nucleation placed it at 565 Ma (Bono et al., 2019) but the actual timing remains highly contested (Biggin et al., 2015; Kodama et al., 2019; Lloyd et al., 2021; Smirnov et al., 2016; Sprain et al., 2018; Zhang et al., 2020). Furthermore, the theoretically plausible range is extremely broad (~400-1800 Ma) and encompasses the Devonian (Davies et al., 2015). While it is therefore not implausible that a weak field existed in the Devonian because of marginal thermal convection ahead of inner core nucleation (in a scenario similar to that suggested by e.g., Bono et al., 2019, but ~150 Myr later), other

explanations exist. In the last 200 Myr, the paleomagnetic field is observed to have undergone a long-term cyclic change, plunging into a hyper-reversing weak-field state in the Middle Jurassic, followed by a sharp recovery into the strong and stable Cretaceous Normal Superchron and subsequently monotonically destabilising over the last ca. 100 Myr (Biggin et al., 2012). Such an evolution is very likely linked to changes in conditions at the base of the mantle, influencing heat flow across the core-mantle boundary that is ultimately responsible for driving the geodynamo (McFadden and Merrill, 1984). Since ~200 Myr may be an emergent timescale of mantle convection (Coltice et al., 2013), it is tempting to view the Devonian as analogous to the Middle Jurassic weak-field hyper-reversing state (but probably more extreme and longer lasting) in a similar ca. 200 Myr cycle occurring previous to the most recent one. In such a scenario, paleomagnetic behaviour again recovered sharply from this weak, unstable state and evolved quickly into a stable, strong superchron (in this case, the Kiaman).

There have been several recent attempts to explain cyclic variations in paleomagnetic behaviour under the assumption that mantle forcing of the geodynamo is the causative mechanism (Amit and Olson, 2015; Biggin et al., 2012; Hounslow et al., 2018). These have all assumed that weak-field, hyper-reversing behaviour, such as that invoked for the Devonian, occurs as a result of core-mantle heat flow being elevated, globally or equatorially, and/or being more heterogeneous in comparison to more stable intervals. Such distinct core-mantle conditions could be related to prior reductions in subduction flux (Hounslow et al., 2018), superplume growth (Amit and Olson, 2015), and/or episodes of true polar wander (Biggin et al., 2012). Biggin et al. (2012) originally assessed the possible effect of true polar wander on the geodynamo in the interval 0-300 Ma using the record of Torsvik et al. (2012). They inferred that in the geodynamo's frame of reference, and assuming lowermost mantle heterogeneity similar to that observed today by seismology, core-mantle heat flow was elevated in the equatorial region at the time of the mid-Jurassic reversal hyperactivity. Their proxy for equatorial core-mantle boundary heat flow potentially provided an explanation for magnetic reversal behaviour at this time and during the subsequent transition to a non-reversing state in the mid-Cretaceous. Here, we extend this analysis back in time using a 0-450 Ma record of true polar wander (Torsvik et al., 2014).

Remarkably, the extended analysis (Fig. 28) describes a distinct minimum in the equatorial heat flow proxy in the middle part of the Kiaman superchron as would be expected if true polar wander played a significant role in controlling reversal frequency in the late Palaeozoic. More pertinently, it also describes a strong peak spanning the Devonian and early Carboniferous, predicting a maximum in reversal frequency at this time. This analysis does not support that true polar wander can account for the entirety of observed changes in paleomagnetic behaviour for the interval 0-450 Ma. Nevertheless, we consider the hypothesis, supported by this analysis, that true polar wander played a role in producing extreme paleomagnetic field behaviour in the Devonian to be worthy of further testing with new datasets and simulations.

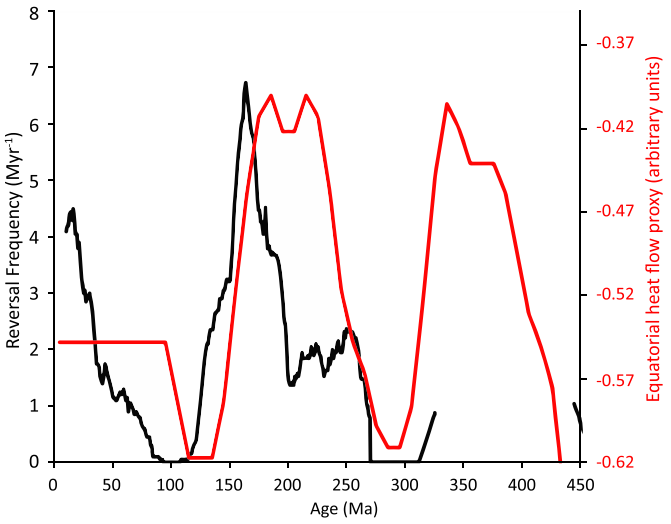

Fig. 28. Time series since 450 Ma of average geomagnetic polarity reversal frequency (black line) and a proxy for average core-mantle heat flux in an equatorial band (red line). This analysis is identical to that reported in Biggin et al. (2012) but extended from 300 to 450 Ma using the true polar wander model of Torsvik et al. (2014). The proxy for equatorial heat flow is obtained from integrating seismic velocity anomalies (taken from Becker and Boschi, 2002) within a ±10° latitude band in the palaeomagnetic reference frame after performing rotations in the mantle reference frame to account for true polar wander. For full details of this analysis, the reader is directed to Biggin et al. (2012).

10. Conclusions

We have presented new paleomagnetic data from four sections, as well as a detailed review of literature surrounding Devonian paleomagnetism. This synthesis has yielded the primary conclusion that the geomagnetic field in the Devonian field was probably substantially different to that of most of the subsequent Phanerozoic. We have explored the implications of a weak and potentially less dipole-dominated magnetic field during this interval of geologic history and attempted to outline a clear direction for future research in this area.

Our newly acquired paleomagnetic data from four Devonian sections provide challenging results to interpret. The data are not straightforward and strong overprints, both by Kiaman (Permo-Carboniferous reverse superchron) and recent fields, are evident. The remaining paleomagnetic signals are of varying quality, due partly to strong component overlap. The Blankenheim section in Germany shows Devonian-like directions of reverse polarity, which agrees with results from previous studies. However, as there are no field tests available, we cannot exclude the possibility that the obtained directions somehow result from a mixture of a recent field and Kiaman overprint. Polish carbonates show results characteristic for a Devonian field of normal polarity, with several samples likely representing reverse polarity. Again, due to the absence of field tests, we cannot completely rule out that the reverse polarity is a mixture between a recent field and Kiaman overprint. The characteristic directions from the Hume Formation in Canada show extremely large scatter in addition to recent and Kiaman overprints, and we cannot interpret these in a meaningful way. The large scatter is reminiscent of other studies on the Frasnian-Famennian from the Canning Basin.

We have reviewed a significant part of the available paleomagnetic data in the Devonian, which shows that most data are problematic. Data show directional groups or extreme scatter in many cases. We urge caution in using Devonian paleopoles for plate tectonic reconstructions and argue for a revision of the geomagnetic polarity timescale presented for the Devonian, as the reversal history is essentially unknown throughout the Devonian. More Devonian paleomagnetic studies are urgently needed to resolve these issues. While there are still many uncertainties regarding the field in the Devonian, it is plausible that the geomagnetic field was extremely weak and perhaps had a non-dipolar configuration. We consider it unlikely that any of the classically invoked reasons, such as pervasive overprinting or unsuitable lithologies, are the prime cause for the absence of high quality, unambiguous paleomagnetic data during this time period. Here we pose the question whether the weak field poorly shielded life on Earth during the Devonian, and if it was a contributing factor to the many biotic crises in this period.

We strongly emphasise the need for more paleomagnetic data from the Devonian, in particular in the Early and Middle Devonian. There is a general lack of data in all paleomagnetic disciplines; paleopoles, magnetostratigraphy and paleointensity. The lack of paleopoles hampers accurate plate tectonic reconstructions through the Devonian, leading to

uncertainty on climatic belts and paleogeographic reconstructions. Due to the lack of magnetostratigraphic data for the Devonian, we cannot assess reversal frequencies, which impacts the understanding of the evolution of the Earth's core and geodynamo. Construction of magnetostratigraphic records is dependent on the assumption of a geocentric axial dipole time-averaged field. If the Devonian geomagnetic field was indeed non-dipolar, as has been suggested, construction of a polarity record for (parts of) the Devonian would be impossible. Increasing the record of paleointensity data in the Devonian will allow assessment of the hypothesised relationship between the magnetic field, biotic crises and true polar wander.

Author contributions

Samples from Poland were collected on several field trips by A. van der Boon, A. Biggin, M. W. Hounslow, J. Nawrocki, K. Wójcik and M. Paszkowski. Samples from Germany were collected by A. van der Boon, P. Königshof and T. de Backer. Samples from Canada were collected by A. van der Boon, D. Thallner, P. Kabanov, S. Gouwy and R. VandenBerg. Paleomagnetic data collection and interpretation was done by A. van der Boon, A. Biggin, D. Thallner and M. W. Hounslow. A-C. Da Silva provided hysteresis measurements of the Blankenheim section. Paleointensity synthesis and magnetic standoff estimates were done by R. Bono. Biostratigraphy data collection and interpretation was done by J. Nawrocki, K. Wójcik, M. Paszkowski, P. Königshof, T. de Backer, P. Kabanov, S. Gouwy and R. VandenBerg. All authors contributed to scientific discussions and writing of the manuscript.

Declaration of Competing Interest

The authors declare that they have no known competing financial interests or personal relationships that could have appeared to influence the work reported in this paper.

Acknowledgements

This project was funded by Leverhulme Research Leadership award RL-2016-080 (to A. Biggin), and partly by an EPOS-IP (N. 676564) Multi-scale laboratories Trans-national Access pilot grant (to A. van der Boon), which is partly financed by NWO project number ALWIN.010. We thank Dennis Jackson for field assistance in Canada, as well as pilots Dennis Rusch, Thierry Breuls de Tiecken, Leslie MacFarlan, and Ruby McDonald of Norman Wells Renewable Research Council. We thank Jamie Dickson, Paul Warburton, Dawn Abel and Mila Mateeva for their help in measuring paleomagnetic samples. R. Bono was supported by the Leverhulme Trust Early Career Fellowship (ECF-2020-617). Participation of Kabanov, Gouwy, and VandenBerg is supported by GEM-GeoNorth Program of NRCan. This is NRCan contribution no. 20210159. This research benefited from a travel grant (to A. van der Boon) and in many other ways from UNESCO project IGCP-652 "Reading geologic time in Paleozoic sedimentary rocks: the need for an integrated stratigraphy". We are grateful to Ken Kodama and an anonymous reviewer for their constructive and insightful reviews that have improved this manuscript.

Appendix A. Supplementary data

All paleomagnetic directional data is supplied as .col files that can be opened in the interpretation portal of http://www.paleomagnetism.org. Please note that for the Canada and Blankenheim samples, AF steps are in Gauss (10 Gauss = 1 mT).

References

Aboussalam, Z.S., Becker, R.T., 2011. The global Taghanic Biocrisis (Givetian) in the eastern Anti-Atlas. Morocco. Palaeogeogr. Palaeoclimatol. Palaeoecol. 304, 136–164. https://doi.org/10.1016/j.palaeo.2010.10.015.

Abrajevitch, A., Van der Voo, R., 2010. Incompatible Ediacaran paleomagnetic directions suggest an equatorial geomagnetic dipole hypothesis. Earth Planet. Sci. Lett. 293, 164–170. https://doi.org/10.1016/j.epsl.2010.02.038.

Abrajevitch, A., Van der Voo, R., Levashova, N.M., Bazhenov, M.L., 2007. Paleomagnetic constraints on the paleogeography and oroclinal bending of the Devonian volcanic arc in Kazakhstan. Tectonophysics 441, 67–84. https://doi.org/10.1016/j.tecto.2007.04.008.

Aïfa, T., 1993. Different styles of remagnetization in Devonian sediments from the northwestern Sahara (Algeria). Geophys. J. Int. 115, 529–537. https://doi.org/10.1111/j.1365-246X.1993.tb01204.x.

Aïfa, T., Feinberg, H., Pozzi, J.P., 1990. Devonian-carboniferous paleopoles for Africa: consequences for Hercynian geodynamics. Tectonophysics 179, 287–304. https://doi.org/10.1016/0040-1951(90)90295-J.

Algeo, T.J., 1996. Geomagnetic polarity bias patterns through the phanerozoic. J. Geophys. Res. B Solid Earth 101, 2785–2814. https://doi.org/10.1029/95jb02814.

Amit, H., Olson, P., 2015. Lower mantle superplume growth excites geomagnetic reversals. Earth Planet. Sci. Lett. 414, 68–76. https://doi.org/10.1016/j.epsl.2015.01.013.

Appelt, J., 1998. Tournaisian conodonts from the basinal carbonates of the Krzeszowice area, southern Poland. Acta Geol. Pol. 48, 135–140.

Aretz, M., 2021. Late Devonian extinctions. In: Encyclopedia of Geology, 2nd ed. Elsevier Ltd.

Bachtadse, V., Briden, J.C., 1989. Palaeomagnetism of the Early to Mid-Ordovician Salala igneous ring complex, Red Sea Hills, Sudan. Geophys. J. Int. 99, 677–685. https://doi.org/10.1111/j.1365-246X.1989.tb02050.x.

Bachtadse, V., Briden, J.C., 1990. Palaeomagnetic constraints on the position of Gondwana during Ordovician to Devonian times. Geol. Soc. Mem. 12, 43–48. https://doi.org/10.1144/GSL.MEM.1990.012.01.03.

Bachtadse, V., Briden, J.C., 1991. Palaeomagnetism of Devonian ring complexes from the Bayuda Desert, Sudan—new constraints on the apparent polar wander path for Gondwanaland. Geophys. J. Int. 104, 635–646. https://doi.org/10.1111/j.1365-246X.1991.tb05707.x.

Bachtadse, V., Van der Voo, R., Hälbich, I.W., 1987. Paleomagnetism of the western Cape Fold belt, South Africa, and its bearing on the Paleozoic apparent polar wander path for Gondwana. Earth Planet. Sci. Lett. 84, 487–499. https://doi.org/10.1016/0012-821X(87)90013-6.

Bąk, M., Dulemba, P., Bąk, K., 2014. Early Carboniferous trilobite remains from limestones of the Dębnik Anticline, southern Poland. Geol. Geophys. Environ. 40, 27–32. https://doi.org/10.7494/geol.2014.40.1.27.

Baker, S.J., Hesselbo, S.P., Lenton, T.M., Duarte, L.V., Belcher, C.M., 2017. Charcoal evidence that rising atmospheric oxygen terminated Early Jurassic ocean anoxia. Nat. Commun. 8, 1–7. https://doi.org/10.1038/ncomms15018.

Bambach, R.K., Knoll, A.H., Sepkoski, J.J., 2002. Anatomical and ecological constraints on Phanerozoic animal diversity in the marine realm. Proc. Natl. Acad. Sci. U. S. A. 99, 6854–6859. https://doi.org/10.1073/pnas.092150999.

Bazhenov, M.L., Van der Voo, R., Levashova, N.M., Dominguez, A.R., 2013. Late Devonian palaeomagnetism of the North Tien Shan, Kyrgyzstan: Can secular variation vary on a short timescale? Geophys. J. Int. 193, 635–649. https://doi.org/10.1093/gji/ggt011.

Bazhenov, M.L., Levashova, N.M., Meert, J.G., Golovanova, I.V., Danukalov, K.N., Fedorova, N.M., 2016. Late Ediacaran magnetostratigraphy of Baltica: Evidence for Magnetic Field Hyperactivity? Earth Planet. Sci. Lett. 435, 124–135. https://doi.org/10.1016/j.epsl.2015.12.015.

Becker, R.T., Aboussalam, Z.S., 2004. The Frasne event - a phased 2nd order global crisis and extinction period. In: Abstracts of the SDS Annual Meeting - Rabat, Morocco, pp. 8–9.

Becker, R.T., Aboussalam, Z.S., 2011. Emsian chronostratigraphy - preliminary new data and a review of the Tafilalt (SE Morocco). SDS Newsl. 26, 33–43.

Becker, T.W., Boschi, L., 2002. A comparison of tomographic and geodynamic mantle models. Geochem. Geophys. Geosyst. 3, 1–48. https://doi.org/10.1029/2001GC000168.

Becker, R.T., House, M.R., 1997. Sea-level changes in the Upper Devonian of the Canning Basin, Western Australia. Cour. Forschungsinstitut Senckenb. 129–146.

Becker, R.T., Gradstein, F.M., Hammer, Ø., 2012. The Devonian period. In: The Geologic Time Scale. Elsevier, pp. 559–601. https://doi.org/10.1017/CBO9780511536045.015.

Becker, R.T., Königshof, P., Brett, C.E., 2016. Devonian climate, sea level and evolutionary events: An introduction. Geol. Soc. Spec. Publ. 423, 1–10. https://doi.org/10.1144/SP423.15.

Becker, R.T., Marshall, J.E.A., Da Silva, A.-C., 2020. The Devonian Period, Geologic Time Scale 2020. Elsevier. https://doi.org/10.1016/B978-0-12-824360-2.00022-X.

Becker, R.T., Hartenfels, S., Kaiser, S.I., Kaiser, S.I., 2021. Review of Devonian-Carboniferous Boundary sections in the Rhenish Slate Mountains (Germany), pp. 357–420.

Belka, Z., 1993. Thermal and burial history of the Cracow-Silesia region (southern Poland) assessed by conodont CAI analysis. Tectonophysics 227, 161–190.

Belka, Z., Skompski, S., Sobon-Podgorska, J., 1996. Reconstruction of a lost carbonate platform on the shelf of Fennosarmatia: Evidence from Viséan polymictic debrites, Holy Cross Mountains. Poland. Geol. Soc. Spec. Publ. 107, 315–329. https://doi.org/10.1144/GSL.SP.1996.107.01.22.

Biggin, A.J., Paterson, G.A., 2014. A new set of qualitative reliability criteria to aid inferences on palaeomagnetic dipole moment variations through geological time. Front. Earth Sci. 2, 1–9. https://doi.org/10.3389/feart.2014.00024.
Biggin, A.J., Steinberger, B., Aubert, J., Suttie, N., Holme, R., Torsvik, T.H., Van Der Meer, D.G., Van Hinsbergen, D.J.J., 2012. Possible links between long-term geomagnetic variations and whole-mantle convection processes. Nat. Geosci. 5, 526–533. https://doi.org/10.1038/ngeo1521.
Biggin, A.J., Piispa, E.J., Pesonen, L.J., Holme, R., Paterson, G.A., Veikkolainen, T., Tauxe, L., 2015. Palaeomagnetic field intensity variations suggest Mesoproterozoic inner-core nucleation. Nature 526, 245–248. https://doi.org/10.1038/nature15523.
Biggin, A.J., Bono, R.K., Meduri, D.G., Sprain, C.J., Davies, C.J., Holme, R., Doubrovine, P.V., 2020. Quantitative estimates of average geomagnetic axial dipole dominance in deep geological time. Nat. Commun. 11, 1–9. https://doi.org/10.1038/s41467-020-19794-7.
Bono, R.K., Tarduno, J.A., Nimmo, F., Cottrell, R.D., 2019. Young inner core inferred from Ediacaran ultra-low geomagnetic field intensity. Nat. Geosci. 12, 143–147. https://doi.org/10.1038/s41561-018-0288-0.
Bono, R.K., Paterson, G.A., van der Boon, A., Engbers, Y.A., Grappone, J.M., Handford, B., Hawkins, L.M.A., Lloyd, S.J., Sprain, C.J., Thallner, D., Biggin, A.J., 2022. The PINT database: A definitive compilation of absolute palaeomagnetic intensity determinations since 4 billion years ago. Geophys. J. Int. 229, 522–545. https://doi.org/10.1093/GJI/GGAB490.
Boyer, D.L., Martinez, A.M., Evans, S.D., Cohen, P.A., Haddad, E.E., Pippenger, K.H., Love, G.D., Droser, M.L., 2021. Living on the edge: The impact of protracted oxygen stress on life in the Late Devonian. Palaeogeogr. Palaeoclimatol. Palaeoecol. 566 https://doi.org/10.1016/j.palaeo.2021.110226.
Brett, C.E., Baird, G.C., Bartholomew, A.J., DeSantis, M.K., Ver Straeten, C.A., 2011. Sequence stratigraphy and a revised sea-level curve for the Middle Devonian of eastern North America. Palaeogeogr. Palaeoclimatol. Palaeoecol. 304, 21–53. https://doi.org/10.1016/j.palaeo.2010.10.009.
Briden, J.C., 1966. Variation of intensity of the palaeomagnetic field through geological time. Nature 212, 246–247. https://doi.org/10.1038/212246a0.
Briden, J.C., Turnell, H.B., Watts, D.R., 1984. British paleomagnetism, Iapetus Ocean, and the Great Glen fault. Geology 12, 428–431. https://doi.org/10.1130/0091-7613(1984)12<428:BPIOAT>2.0.CO;2.
Brocke, R., Fatka, O., Lindemann, R.H., Schindler, E., Ver Straeten, C.A., 2016. Palynology, dacryoconarids and the lower Eifelian (Middle Devonian) Basal Choteč Event: Case studies from the Prague and Appalachian basins. Geol. Soc. Spec. Publ. 123–169. https://doi.org/10.1144/SP423.8.
Carmichael, S.K., Waters, J.A., Königshof, P., Suttner, T.J., Kido, E., 2019. Paleogeography and paleoenvironments of the Late Devonian Kellwasser event: A review of its sedimentological and geochemical expression. Glob. Planet. Chang. 183 https://doi.org/10.1016/j.gloplacha.2019.102984.
Chen, Z., Li, Z.X., Powell, C.M.A., Balme, B.E., 1993. Palaeomagnetism of the Brewer Conglomerate in central Australia, and fast movement of Gondwanaland during the Late Devonian. Geophys. J. Int. 115, 564–574. https://doi.org/10.1111/j.1365-246X.1993.tb01207.x.
Chen, Z., Li, Z.X., Powell, C.M.A., 1995. Paleomagnetism of the Upper Devonian reef complexes, Canning Basin, Western Australia. Tectonics 14, 154–167. https://doi.org/10.1029/94TC01622.
Chlupác, I., Kukal, Z., 1988. Possible global events and the stratigraphy of the Palaeozoic of the Barrandian (Cambrian-Middle Devonian, Czechoslovakia). Sborník Geol. vèd. Geol. 43, 83–146.
Claesson, C., 1979. Early Palaeozoic geomagnetism of Gotland. GFF 101, 149–155. https://doi.org/10.1080/11035897909452573.
Cocks, L.R.M., Torsvik, T.H., 2002. Earth geography from 500 to 400 million years ago: A faunal and palaeomagnetic review. J. Geol. Soc. Lond. 159, 631–644. https://doi.org/10.1144/0016-764901-118.
Cocks, L.R.M., Torsvik, T.H., 2007. Siberia, the wandering northern terrane, and its changing geography through the Palaeozoic. Earth-Science Rev. 82, 29–74. https://doi.org/10.1016/j.earscirev.2007.02.001.
Coltice, N., Seton, M., Rolf, T., Müller, R.D., Tackley, P.J., 2013. Convergence of tectonic reconstructions and mantle convection models for significant fluctuations in seafloor spreading. Earth Planet. Sci. Lett. 383, 92–100. https://doi.org/10.1016/j.epsl.2013.09.032.
Conrad, C.P., Hager, B.H., 1999. Effects of plate bending and fault strength at subduction zones on plate dynamics. J. Geophys. Res. Solid Earth 104, 17551–17571. https://doi.org/10.1029/1999jb900149.
Courtillot, V., Chambon, P., Brun, J.P., Rochette, P., Matte, P., 1986. A magnetotectonic study of the Hercynian Montagne Noire (France). Tectonics 5, 733–751. https://doi.org/10.1029/TC005i005p00733.
Crick, R.E., Ellwood, B.B., El Hassani, A., Feist, R., Hladil, Jindrich, 1997. MagnetoSusceptibility Event and Cyclostratigraphy (MSEC) of the Eifelian-Givetian GSSP and associated boundary sequences in north Africa and Europe. Episodes 20, 167–175.
Crick, R.E., Ellwood, B.B., Hladil, J., El Hassani, A., Hrouda, F., Chlupác, I., 2001. Magnetostratigraphy susceptibility of the Přídolian-Lochkovian (Silurian-Devonian) GSSP (Klonk, Czech Republic) and a coeval sequence in anti-atlas Morocco. Palaeogeogr. Palaeoclimatol. Palaeoecol. 167, 73–100. https://doi.org/10.1016/S0031-0182(00)00233-9.
Cromwell, G., Johnson, C.L., Tauxe, L., Constable, C.G., Jarboe, N.A., 2018. PSV10: A Global Data Set for 0–10 Ma time-averaged field and paleosecular variation studies. Geochem. Geophys. Geosyst. 19, 1533–1558. https://doi.org/10.1002/2017GC007318.
Da Silva, A.-C., Dekkers, M.J., Mabille, C., Boulvain, F., 2012. Magnetic susceptibility and its relationship with paleoenvironments, diagenesis and remagnetization: examples from the Devonian carbonates of Belgium. Stud. Geophys. Geod. 56, 677–704. https://doi.org/10.1007/s11200-011-9005-9.
Da Silva, A.C., De Vleeschouwer, D., Boulvain, F., Claeys, P., Fagel, N., Humblet, M., Mabille, C., Michel, J., Sardar Abadi, M., Pas, D., Dekkers, M.J., 2013. Magnetic susceptibility as a high-resolution correlation tool and as a climatic proxy in Paleozoic rocks - Merits and pitfalls: Examples from the Devonian in Belgium. Mar. Pet. Geol. https://doi.org/10.1016/j.marpetgeo.2013.06.012.
Da Silva, A.C., Hladil, J., Chadimová, L., Slavík, L., Hilgen, F.J., Bábek, O., Dekkers, M.J., 2016. Refining the Early Devonian time scale using Milankovitch cyclicity in Lochkovian–Pragian sediments (Prague Synform, Czech Republic). Earth Planet. Sci. Lett. 455, 125–139. https://doi.org/10.1016/j.epsl.2016.09.009.
Davies, C., Pozzo, M., Gubbins, D., Alfè, D., 2015. Constraints from material properties on the dynamics and evolution of Earth's core. Nat. Geosci. 8, 678–685. https://doi.org/10.1038/ngeo2492.
Davydov, V.I., Korn, D.K., Schmitz, M.D., Gradstein, F.M., Hammer, Ø., 2012. The Carboniferous Period, The Geologic Time Scale 2012. Elsevier. https://doi.org/10.1016/B978-0-444-59425-9.00023-8.
Day, R., Fuller, M., Schmidt, V.A., 1977. Hysteresis properties of titanomagnetites: grain-size and compositional dependence. Phys. Earth Planet. Inter. 13, 260–267.
De Vleeschouwer, D., Boulvain, F., Da Silva, A.C., Pas, D., Labaye, C., Claeys, P., 2015. The astronomical calibration of the Givetian (Middle Devonian) timescale (Dinant Synclinorium, Belgium). Geol. Soc. Spec. Publ. 414, 245–256. https://doi.org/10.1144/SP414.3.
De Vleeschouwer, D., Da Silva, A.C., Sinnesael, M., Chen, D., Day, J.E., Whalen, M.T., Guo, Z., Claeys, P., 2017. Timing and pacing of the Late Devonian mass extinction event regulated by eccentricity and obliquity. Nat. Commun. 8, 1–11. https://doi.org/10.1038/s41467-017-02407-1.
De Vleeschouwer, D., Königshof, P., Claeys, P., 2018. Reading time and paleoenvironmental change in the Emsian-Eifelian boundary GSSP section (Wetteldorf, Germany): A combination of cyclostratigraphy and facies analysis. Newsl. Stratigr. 51, 209–226. https://doi.org/10.1127/nos/2017/0397.
DeSantis, M.K., Brett, C.E., 2011. Late Eifelian (Middle Devonian) biocrises: Timing and signature of the pre-Kačák Bakoven and Stony Hollow Events in eastern North America. Palaeogeogr. Palaeoclimatol. Palaeoecol. 304, 113–135. https://doi.org/10.1016/j.palaeo.2010.10.013.
Didenko, A.N., Pechersky, D.M., 1989. Direction and intensity of the geomagnetic field in the Middle Devonian and Lower Ordovician: southern Mugodjary ophiolites (Urals). Phys. Earth Planet. Inter. 58, 289–306. https://doi.org/10.1016/0031-9201(89)90101-5.
Doubrovine, P.V., Veikkolainen, T., Pesonen, L.J., Piispa, E., Ots, S., Smirnov, A.V., Kulakov, E.V., Biggin, A.J., 2019. Latitude dependence of geomagnetic paleosecular variation and its relation to the frequency of magnetic reversals: observations from the cretaceous and Jurassic. Geochem. Geophys. Geosyst. 20, 1240–1279. https://doi.org/10.1029/2018GC007863.
Driscoll, P.E., 2016. Simulating 2 Ga of geodynamo history. Geophys. Res. Lett. 43, 5680–5687. https://doi.org/10.1002/2016GL068858.
Driscoll, P., Olson, P., 2011. Superchron cycles driven by variable core heat flow. Geophys. Res. Lett. 38 (9) https://doi.org/10.1029/2011gl046808.
Dunlop, D.J., 2002. Theory and application of the Day plot (Mrs/Ms versus Hcr/Hc) 2. Application to data for rocks, sediments, and soils. J. Geophys. Res. 107, 1–15. https://doi.org/10.1029/2001jb000487.
Dunlop, D.J., 2011. Physical basis of the Thellier – Thellier and related paleointensity methods. Phys. Earth Planet. Inter. 187, 118–138. https://doi.org/10.1016/j.pepi.2011.03.006.
Dunlop, D.J., 2014. High-temperature susceptibility of magnetite: A new pseudo-single-domain effect. Geophys. J. Int. 199, 707–716. https://doi.org/10.1093/gji/ggu247.
Dunlop, D.J., Özdemir, Ö., 1997. Rock Magnetism - Fundamentals and Frontiers. Cambridge University Press.
Dvorák, J., Galle, A., Herbig, H.-G., Krejci, Z., Malec, J., Paszkowski, M., Racki, G., Skompski, S., Szulczewski, M., Zakowa, H., 1995. Guide to Excursion B4: Evolution of the Polish-Moravian carbonate platform in the Late Devonian and Early Carboniferous: Holy Cross Mts., Kraków Upland, Moravian Karst, in: International Congress on Carboniferous-Permian. Polish Geological Institute, Krakow, Poland, p. 35.
Ellwood, B.B., Crick, R.E., El Hassani, A., 1999. The Magneto-Susceptibility Event and Cyclostratigraphy (MSEC) method used in geological correlation of Devonian rocks from Anti-Atlas Morocco. Am. Assoc. Pet. Geol. Bull. 83, 1119–1134. https://doi.org/10.1306/e4fd2e8d-1732-11d7-8645000102c1865d.
Elmore, R.D., Kelley, J., Evans, M., Lewchuk, M.T., 2001. Remagnetization and orogenic fluids: Testing the hypothesis in the central Appalachians. Geophys. J. Int. 144, 568–576. https://doi.org/10.1046/j.0956-540X.2000.01349.x.
Elmore, R.D., Muxworthy, A.R., Aldana, M., 2012. Remagnetization and chemical alteration of sedimentary rocks. Geol. Soc. Spec. Publ. 371, 1–21. https://doi.org/10.1144/SP371.15.
Epstein, A.G., Epstein, J.B., Harris, L.D., 1977. Conodont color alteration - an index to organic metamorphism. USGS Prof. Pap. 995, 27pp.
Ernst, R.E., Rodygin, S.A., Grinev, O.M., 2020. Age correlation of Large Igneous Provinces with Devonian biotic crises. Glob. Planet. Chang. 185, 103097 https://doi.org/10.1016/j.gloplacha.2019.103097.
Ernst, R.E., Bond, D.P.G., Zhang, S., Buchan, K.L., Grasby, S.E., Youbi, N., El Bilali, H., Bekker, A., Doucet, L.S., 2021. Large igneous province record through time and implications for secular environmental changes and geological time-scale boundaries. In: Ernst, R.E., Dickson, A.J., Bekker, A. (Eds.), Large Igneous Provinces: A Driver of Global Environmental and Biotic Changes, pp. 1–26. https://doi.org/10.1002/9781119507444.ch1.

Evans, D.A.D., 2006. Proterozoic low orbital obliquity and axial-dipolar geomagnetic field from evaporite palaeolatitudes. Nature 444, 51–55. https://doi.org/10.1038/nature05203.
Fallas, K.M., McNaughton, R.B., 2013. Geology, Norman Wells (southeast), Northwest Territories. Geol. Surv. Canada, Can. Geosci. Map, p. 100. https://doi.org/10.4095/292292.
Fanelli, D., 2012. Negative results are disappearing from most disciplines and countries. Scientometrics 90, 891–904. https://doi.org/10.1007/s11192-011-0494-7.
Feist, R., Flajs, G., Girard, C., 2000. The stratotype section of the Devonian-Carboniferous boundary. Cour. Forschungsinstitut Senckenb. 77–82.
Fields, B.D., Melott, A.L., Ellis, J., Ertel, A.F., Fry, B.J., Lieberman, B.S., Liu, Z., Miller, J. A., Thomas, B.C., 2020. Supernova triggers for end-Devonian extinctions. PNAS 117, 21008–21010. https://doi.org/10.1073/pnas.2013774117.
Fisher, R., 1953. Dispersion on a sphere. Proc. R. Soc. Lond. 217, 295–305. https://doi.org/10.1098/rspa.1953.0064.
Gallet, Y., Pavlov, V., Korovnikov, I., 2019. Extreme geomagnetic reversal frequency during the Middle Cambrian as revealed by the magnetostratigraphy of the Khorbusuonka section (northeastern Siberia). Earth Planet. Sci. Lett. 528 https://doi.org/10.1016/j.epsl.2019.115823.
Garcia, A.S., Thomas, D.N., Liss, D., Shaw, J., 2006. Low geomagnetic field intensity during the Kiaman superchron: Thellier and microwave results from the Great Whin Sill intrusive complex, northern United Kingdom. Geophys. Res. Lett. 33, 3–7. https://doi.org/10.1029/2006GL026729.
García-Alcalde, J.L., 1997. North Gondwanan Emsian events. Episodes 20, 241–246. https://doi.org/10.18814/epiiugs/1997/v20i4/006.
García-Alcalde, J.L., Ellwood, B.B., Soto, F., Truyóls-Massoni, M., Tomkin, J.H., 2012. Precise timing of the Upper Taghanic Biocrisis, Geneseo Bioevent, in the Middle-Upper Givetian (Middle Devonian) boundary in Northern Spain using biostratigraphic and magnetic susceptibility data sets. Palaeogeogr. Palaeoclimatol. Palaeoecol. 313–314, 26–40. https://doi.org/10.1016/j.palaeo.2011.10.006.
Garza, R.S.M., Zijderveld, J.D.A., 1996. Paleomagnetism of Paleozoic strata, Brabant and Ardennes Massifs, Belgium: Implications of prefolding and postfolding Late Carboniferous secondary magnetizations for European apparent polar wander. J. Geophys. Res. Solid Earth 101, 15799–15818. https://doi.org/10.1029/96jb00325.
Gouwy, S.A., 2006. Report on 15 conodont samples from the Horn river group (Hare Indian and Canol formations). Prohibition Creek. Geol. Surv. Canada, Paleontol. Rep, 1–15.
Gouwy, S.A., Pedder, E.A.H., Uyeno, T.T., MacKenzie, W.S., 2021. Description of five Devonian sections (Hume River, Gayna River Gorge, Powell Creek Tributary, Powell Creek, and Prohibition Creek) from the northern front of the Mackenzie Mountains and the Franklin Mountains (Northwest Territories, Canada). GSC Open File 8802. https://doi.org/10.4095/328354.
Gouwy, S.A., Uyeno, T.T., 2018. Lower and lower Middle Devonian Conodont biostratigraphy in the Northern Mackenzie Mountains and adjacent areas (NWT, Canada): Graphic Correlation applied to the Middle Devonian Hume Formation and reassessment of the time-rock chart. In: Canadian Paleontology Conference Abstract Book. Saskatoon, pp. 12–13.
Gouwy, S.A., 2022. Paper 6. Devonian conodont biostratigraphy of the Mackenzie Mountains (NWT, Canada). In: Lavoie, D., Dewing, K. (Eds.), Sedimentary Basins of the Canadian North - Contributions to a 1000 Ma Geological Journay and Insight on Resource Potential. Geological Survey of Canada. Bulletin 609.
Grabowski, J., Nawrocki, J., 1996. Multiple remagnetizations in the Devonian carbonates in the northwestern part of the Kielce region (Holy Cross Mts., southern part). Kwartalnik Geol. 40, 47–64.
Grabowski, J., Nawrocki, J., 2001. Palaeomagnetism of some Devonian carbonates from the Holy Cross Mts. (Central Poland): Large pre-Permian rotations or strain modified palaeomagnetic directions? Geol. Q. 45, 165–178.
Gradstein, F.M., Ogg, J.G., Schmitz, M.D., Ogg, G.M., 2020. Geologic Time Scale 2020. Elsevier.
Green, T., Slotznick, S.P., Jaqueto, P., Raub, T.D., Tohver, E., Playton, T.E., Haines, P.W., Kirschvink, J.L., Hocking, R.M., Montgomery, P., 2021. High-resolution Late Devonian magnetostratigraphy from the Canning Basin, Western Australia: A re-evaluation. Front. Earth Sci. 9, 1–12. https://doi.org/10.3389/feart.2021.757749.
Gromczakiewicz-Łomnicka, A., 1974. Upper Visean conodont fauna from the Carboniferous limestone north of Krzeszowice (environs of Cracow, Poland). Rocz. Pol. Tow. Geol. la Soc. Geol. Pologne XLIV 475–481.
Guzhikov, A.Y., 2019. General magnetostratigraphic scale: present status and outlook of development. In: Recent Adv. Rock Magn. Environ. Magn. Paleomagn, pp. 343–351. https://doi.org/10.1007/978-3-319-90437-5_24.
Hance, L., Poty, E., 2006. Hastarian. Geol. Belgica 9, 111–116.
Hansma, J., Tohver, E., Yan, M., Trinajstic, K., Roelofs, B., Peek, S., Slotznick, S.P., Kirschvink, J., Playton, T., Haines, P., Hocking, R., 2015. Late Devonian carbonate magnetostratigraphy from the Oscar and Horse Spring Ranges, Lennard Shelf, Canning Basin, Western Australia. Earth Planet. Sci. Lett. 409, 232–242. https://doi.org/10.1016/j.epsl.2014.10.054.
Hargraves, R.B., Dawson, E.M., Van Houten, F.B., 1987. Palaeomagnetism and age of mid-Palaeozoic ring complexes in Niger, West Africa, and tectonic implications. Geophys. J. R. Astron. Soc. 90, 705–729. https://doi.org/10.1111/j.1365-246X.1987.tb00750.x.
Hartenfels, S., Becker, R.T., 2009. Timing of the global Dasberg crisis - implications for Famennian eustasy and chronostratigraphy. Palaeontogr. Am. 63, 71–97.
Hartenfels, S., Becker, R.T., 2016. The global Annulata Events: Review and new data from the Rheris Basin (northern Tafilalt) of SE Morocco, in: Geological Society. Special Publications, London, pp. 291–354. https://doi.org/10.1144/SP423.14.
Hawkins, L., 2018. A Mid-Paleozoic Dipole Low defined from new paleointensity estimates from Russia and the UK. University of Liverpool.
Hawkins, L.M.A., Anwar, T., Shcherbakova, V.V., Biggin, A.J., Kravchinsky, V.A., Shatsillo, A.V., Pavlov, V.E., 2019. An exceptionally weak Devonian geomagnetic field recorded by the Viluy Traps, Siberia. Earth Planet. Sci. Lett. 506, 134–145. https://doi.org/10.1016/j.epsl.2018.10.035.
Hawkins, L.M.A., Grappone, J.M., Sprain, C.J., Saengduean, P., Sage, E.J., Thomas-Cunningham, S., Kugabalan, B., Biggin, A.J., 2021. Intensity of the Earth's magnetic field: Evidence for a Mid-Paleozoic dipole low. Proc. Natl. Acad. Sci. U. S. A. 118 https://doi.org/10.1073/pnas.2017342118.
Helsen, S., Königshof, P., 1994. Conodont thermal alteration patterns in Palaeozoic rocks from Belgium, northern France and western Germany. Geol. Mag. 131, 369–386. https://doi.org/10.1017/S0016756800011122.
Henderson, C.M., Shen, S.Z., Gradstein, F.M., Agterberg, F.P., 2020. The Permian period. In: Geologic Time Scale 2020. Elsevier, pp. 875–902. https://doi.org/10.1016/b978-0-12-824360-2.00024-3.
Heslop, D., Roberts, A.P., 2018. A Bayesian approach to the paleomagnetic conglomerate test. J. Geophys. Res. Solid Earth 123, 1132–1142. https://doi.org/10.1002/2017JB014526.
Hounslow, M.W., 2021. A geomagnetic polarity timescale for the Carboniferous. Geol. Soc. London Spec. Publ. 512 https://doi.org/10.1144/sp512-2020-102. SP512-2020–102.
Hounslow, M.W., Balabanov, Y.P., 2018. A geomagnetic polarity timescale for the Permian, calibrated to stage boundaries. Geol. Soc. Spec. Publ. 450, 61–103. https://doi.org/10.1144/SP450.8.
Hounslow, M.W., Domeier, M., Biggin, A.J., 2018. Subduction flux modulates the geomagnetic polarity reversal rate. Tectonophysics 742–743, 34–49. https://doi.org/10.1016/j.tecto.2018.05.018.
Hounslow, M.W., Harris, S.E., Wójcik, K., Nawrocki, J., Ratcliffe, K.T., Woodcock, N.H., Montgomery, P., 2021. A geomagnetic polarity stratigraphy for the Middle and Upper Ordovician. Palaeogeogr. Palaeoclimatol. Palaeoecol. 567 https://doi.org/10.1016/j.palaeo.2021.110225.
House, M.R., 2002. Strength, timing, setting and cause of mid-Palaeozoic extinctions. Palaeogeogr. Palaeoclimatol. Palaeoecol. 181, 5–25. https://doi.org/10.1016/S0031-0182(01)00471-0.
House, M.R., Gradstein, F.M., 2004. The Devonian period. A Geol. Time Scale 2004, 202–221. https://doi.org/10.1017/CBO9780511536045.015.
House, M.R., Kirchgasser, W.T., 1993. Devonian goniatite biostratigraphy and timing of facies movements in the Frasnian of eastern North America. Geol. Soc. London Spec. Publ. 70, 267–292.
Huang, B., Otofuji, Y.I., Yang, Z., Zhu, R., 2000. New Silurian and Devonian palaeomagnetic results from the Hexi Corridor terrane, northwest China, and their tectonic implications. Geophys. J. Int. 140, 132–146. https://doi.org/10.1046/j.1365-246X.2000.00983.x.
Hurley, N.F., Van Der Voo, R., 1987. Paleomagnetism of Upper Devonian reefal limestones, Canning basin, Western Australia. Geol. Soc. Am. Bull. 98, 138–146. https://doi.org/10.1130/0016-7606(1987)98<138:POUDRL>2.0.CO;2.
Iosifidi, A.G., Khramov, A.N., 2013. Paleomagnetism of Paleozoic Sediments from the Kozhim River section: On the Problem of Palinspastic Reconstructions of the Subpolar Urals and Pai-Khoi. Izv. Phys. Solid Earth 49, 63–76. https://doi.org/10.1134/S1069351313010059.
Irving, E., Strong, D.F., 1984. Evidence against large-scale Carboniferous strike-slip faulting in the Appalachian-Caledonian orogen. Nature 310, 762–764. https://doi.org/10.1038/310762a0.
Irving, E., Strong, D.F., 1985. Paleomagnetism of rocks from Burin Peninsula, Newfoundland: Hypothesis of Late Paleozoic displacement of Acadia criticized. J. Geophys. Res. 90, 1949. https://doi.org/10.1029/jb090ib02p01949.
Jackson, M., Swanson-Hysell, N.L., 2012. Rock magnetism of remagnetized carbonate rocks: another look. Geol. Soc. Spec. Publ. 371, 229–251. https://doi.org/10.1144/SP371.3.
Jeleńska, M., Kadzialko-Hofmokl, M., Edel, J.B., Jamrozik, L., Petersen, N., Soffel, H., 1995. Palaeomagnetic investigations of the Palaeozoic circum-Sowie Góry Mountains ophiolitic belt in the Sudetes Poland. Geophys. J. Int. 122, 658–674. https://doi.org/10.1111/j.1365-246X.1995.tb07018.x.
Jeleńska, M., Kadziałko-Hofmokl, M., Bakhmutov, V., Poliachenko, I., Ziółkowski, P., 2015. Palaeomagnetic and rock magnetic study of Lower Devonian sediments from Podolia, SW Ukraine: Remagnetization problems. Geophys. J. Int. 200, 557–573. https://doi.org/10.1093/gji/ggu411.
Joachimski, M.M., Breisig, S., Buggisch, W., Talent, J.A., Mawson, R., Gereke, M., Morrow, J.R., Day, J., Weddige, K., 2009. Devonian climate and reef evolution: Insights from oxygen isotopes in apatite. Earth Planet. Sci. Lett. 284, 599–609. https://doi.org/10.1016/j.epsl.2009.05.028.
Kabanov, P., 2022. Devonian of the Mackenzie. In: Lavoie, D., Dewing, K. (Eds.), Sedimentary Basins of the Canadian North - Contributions to a 1000 Ma Geological Journey and Insight on Resource Potential, 609. Geological Survey of Canada Bulletin. In press.
Kabanov, P., Jiang, C., 2020. Photic-zone euxinia and anoxic events in a Middle-Late Devonian shelfal sea of Panthalassan continental margin, NW Canada: Changing paradigm of Devonian ocean and sea level fluctuations. Glob. Planet. Chang. 188, 103153 https://doi.org/10.1016/j.gloplacha.2020.103153.
Kabanov, P., Vandenberg, R., Gouwy, S., van der Boon, A., Thallner, D., Biggin, A., 2019. Geological and geochemical data from Mackenzie corridor. In: Part X: reference sections of Middle-Upper Devonian strata at Prohibition Creek, Norman Range, Northwest Territories. Geol. Surv. Canada Open File 8648.
Kadziałko-Hofmokl, M., Jeleńska, M., Aïfa, T., Edel, J.B., Zelaźniewicz, A., 1999. Paleomagnetism and remagnetization of Upper Devonian synorogenic clastic

sediments from the Pogorzała Formation (Świebodzice Depression, West Sudetes, Poland). Geol. Sudet. 32, 113–126.
Kaiho, K., Miura, M., Tezuka, M., Hayashi, N., Jones, D.S., Oikawa, K., Casier, J.G., Fujibayashi, M., Chen, Z.Q., 2021. Coronene, mercury, and biomarker data support a link between extinction magnitude and volcanic intensity in the Late Devonian. Glob. Planet. Chang. 199 https://doi.org/10.1016/j.gloplacha.2021.103452.
Kaiser, S.I., Aretz, M., Becker, R.T., 2016. The global Hangenberg Crisis (Devonian-Carboniferous transition): Review of a first-order mass extinction. Geol. Soc. Spec. Publ. 423, 387–437. https://doi.org/10.1144/SP423.9.
Katz, B., Elmore, R.D., Cogoini, M., Ferry, S., 1998. Widespread chemical remagnetization: Orogenic fluids or burial diagenesis of clays? Geology 26 (7), 603–606.
Kent, D.V., 1979. Paleomagnetism of the Devonian Onondaga limestone revisited. J. Geophys. Res. 84, 3576–3588. https://doi.org/10.1029/JB084iB07p03576.
Kent, D.V., 1985. Thermoviscous remagnetization in some Appalachian limestones. Geophys. Res. Lett. 12, 805–808. https://doi.org/10.1029/GL012i012p00805.
Kent, D.V., Dia, O., Sougy, J.M.A., 1984. Paleomagnetism of Lower-Middle Devonian and Upper Proterozoic-Cambrian(?) rocks from Mejeria (Mauritania, West Africa). Plate Reconstruct. From Paleozoic Paleomag. 99–115. https://doi.org/10.1029/gd012p0099.
Kent, D.V., Olsen, P.E., Lepre, C., Rasmussen, C., Mundil, R., Gehrels, G.E., Giesler, D., Irmis, R.B., Geissman, J.W., Parker, W.G., 2019. Magnetochronology of the entire Chinle Formation (Norian Age) in a scientific drill core from petrified forest National Park (Arizona, USA) and implications for regional and global correlations in the Late Triassic. Geochem. Geophys. Geosyst. 20, 4654–4664. https://doi.org/10.1029/2019GC008474.
Khramov, A.N., 1967. Importance of palaeomagnetic data for Devonian stratigraphy and palaeogeography in the USSR. In: Oswald, D.H. (Ed.), International Symposium of the Devonian System, II. Canadian Society of Petroleum Geologists, pp. 1363–1370. Calgary.
Khramov, A.N., Rodionov, V.P., 1980. The geomagnetic field during Palaeozoic time. Journal of geomagnetism and geoelectricity 32 (Supplement3), SIII99–SIII115.
Khramov, A.N., Shkatova, V.K., 2000. Phanerozoic general magnetostratigraphic scale of polarity. Adj. 9 (in Russian). In: Addit. to Stratigr. Codes Russ, pp. 24–45.
Kiessling, W., Flügel, E., Golonka, J., 2003. Patterns of Phanerozoic carbonate platform sedimentation. Lethaia. 36, 195–226. https://doi.org/10.1080/00241160310004648.
Kirschvink, J.L., 1980. The least-squares line and plane and the analysis of palaeomagnetic data. Geophys. J. Int. 62, 699–718. https://doi.org/10.1111/j.1365-246X.1980.tb02601.x.
Knight, K.B., Nomade, S., Renne, P.R., Marzoli, A., Bertrand, H., Youbi, N., 2004. The Central Atlantic Magmatic Province at the Triassic–Jurassic boundary: paleomagnetic and 40Ar/39Ar evidence from Morocco for brief, episodic volcanism. Earth Planet. Sci. Lett. 228, 143–160. https://doi.org/10.1016/j.epsl.2004.09.022.
Kodama, K.P., 2021. Combined Magnetostratigraphy From Three Localities of the Rainstorm Member of the Johnnie Formation in California and Nevada, United States Calibrated by Cyclostratigraphy: A 13 R/Ma Reversal Frequency for the Ediacaran. Front. Earth Sci. 9, 1–11. https://doi.org/10.3389/feart.2021.764714.
Kodama, K.P., Carnes, L.K., Tarduno, J.A., Berti, C., 2019. Palaeointensity of the 1.3 billion-yr-old Gardar basalts, southern Greenland revisited: No evidence for onset of inner core growth. Geophys. J. Int. 217, 1974–1987. https://doi.org/10.1093/gji/ggz126.
Kolesov, Y.V., 1984. Paleomagnetic stratigraphy of the Devonian-Carboniferous boundary beds in the Soviet north-east and in the Franco-Belgian basin. Ann. la Société Géologique Belgique 107, 135–136.
Kolesov, Y.V., 2005. Magnetostratigraphy of Paleozoic in North-East of Russia (in Russian). NESC FEB RAS, Magdan.
Kolesov, E.V., 2007. A Palaeozoic magnetostratigraphic scale for North-East Russia and a trans-regional correlation of its reference magnetozones. Bull. North-Eastern Sci. Cent. 4, 31–42.
Königshof, P., 2003. Conodont deformation patterns and textural alteration in Paleozoic conodonts: examples from Germany and France. Senckenb. Lethaea 83, 149–156. https://doi.org/10.1007/bf03043310.
Königshof, P., Da Silva, A.-C.C., Suttner, T.J., Kido, E., Waters, J., Carmichael, S.K., Jansen, U., Pas, D., Spassov, S., 2016. Shallow-water facies setting around the Kačák Event: A multidisciplinary approach. Geol. Soc. London Spec. Publ. 423, 171–199. https://doi.org/10.1144/SP423.4.
Koymans, M.R., Langereis, C.G., Pastor-Galán, D., van Hinsbergen, D.J.J., 2016. Paleomagnetism.org: an online multi-platform open source environment for paleomagnetic data analysis. Comput. Geosci. 93, 127–137. https://doi.org/10.1016/j.cageo.2016.05.007.
Koymans, M.R., van Hinsbergen, D.J.J., Pastor-Galán, D., Vaes, B., Langereis, C.G., 2020. Towards FAIR paleomagnetic data management through Paleomagnetism.org 2.0. Geochem. Geophys. Geosyst. 21, 1–7. https://doi.org/10.1029/2019GC008838.
Kravchinsky, V.A., 2012. Paleozoic large igneous provinces of Northern Eurasia: correlation with mass extinction events. Glob. Planet. Chang. 86–87, 31–36. https://doi.org/10.1016/j.gloplacha.2012.01.007.
Kravchinsky, V.A., Konstantinov, K.M., Courtillot, V., Savrasov, J.I., Valet, J.P., Cherniy, S.D., Mishenin, S.G., Parasotka, B.S., 2002. Paleomagnetism of East Siberian traps and kimberlites: Two new poles and palaeogeographic reconstructions at about 360 and 250 Ma. Geophys. J. Int. 148, 1–33. https://doi.org/10.1046/j.0956-540x.2001.01548.x.
Kulakov, E.V., Sprain, C.J., Doubrovine, P.V., Smirnov, A.V., Paterson, G.A., Hawkins, L., Fairchild, L., Piispa, E.J., Biggin, A.J., 2019. Analysis of an Updated Paleointensity Database (QPI-PINT) for 65–200 Ma: Implications for the Long-Term History of Dipole Moment Through the Mesozoic. J. Geophys. Res. Solid Earth 124, 9999–10022. https://doi.org/10.1029/2018JB017287.
Kutterolf, S., Hansteen, T.H., Appel, K., Freundt, A., Krüger, K., Pérez, W., Wehrmann, H., 2013. Combined bromine and chlorine release from large explosive volcanic eruptions: a threat to stratospheric ozone? Geology 41, 707–710. https://doi.org/10.1130/G34044.1.
Lakin, J.A., Marshall, J.E.A., Troth, I., Harding, I.C., 2016. Greenhouse to icehouse: A biostratigraphic review of latest Devonian-Mississippian glaciations and their global effects. Geol. Soc. Spec. Publ. 423, 439–464. https://doi.org/10.1144/SP423.12.
Łaptaś, A., 1982. Sedimentation of the Middle Devonian carbonates in the Dębnik region. Stud. Geol. Pol. 75, 59–100.
Le Hir, G., Donnadieu, Y., Goddéris, Y., Meyer-Berthaud, B., Ramstein, G., Blakey, R.C., 2011. The climate change caused by the land plant invasion in the Devonian. Earth Planet. Sci. Lett. 310, 203–212. https://doi.org/10.1016/j.epsl.2011.08.042.
Lenton, T.M., Daines, S.J., Mills, B.J.W., 2018. COPSE reloaded: An improved model of biogeochemical cycling over Phanerozoic time. Earth-Science Rev. 178, 1–28. https://doi.org/10.1016/j.earscirev.2017.12.004.
Leonhardt, R., 2006. Analyzing rock magnetic measurements: The RockMagAnalyzer 1.0 software. Comput. Geosci. 32, 1420–1431. https://doi.org/10.1016/j.cageo.2006.01.006.
Levashova, N.M., Mikolaichuk, A.V., McCausland, P.J.A., Bazhenov, M.L., Van der Voo, R., 2007. Devonian paleomagnetism of the North Tien Shan: Implications for the middle-Late Paleozoic paleogeography of Eurasia. Earth Planet. Sci. Lett. 257, 104–120. https://doi.org/10.1016/j.epsl.2007.02.025.
Lewandowski, M., 1995. Palaeomagnetic constraints for Variscan mobilism of the Upper Silesian and Malopolska Massifs, southern Poland - reply. Kwartalnik Geol. 39, 211–229.
Liu, H., Bai, Z., Wang, H., Yaskawa, K., 1991. Search for the geomagnetic reversal near the Devonian-Carboniferous boundary. J. Geomagn. Geoelectr. 43, 755–764. https://doi.org/10.5636/jgg.43.755.
Livermore, R.A., Smith, A.G., Briden, J.C., 1985. Palaeomagnetic constraints on the distribution of continents in the late Silurian and early Devonian. Philos. Trans. R. Soc. Lond. Ser. B Biol. Sci. 309, 29–56. https://doi.org/10.1098/rstb.1985.0069.
Lloyd, S.J., Biggin, A.J., Halls, H., Hill, M.J., 2021. First palaeointensity data from the cryogenian and their potential implications for inner core nucleation age. Geophys. J. Int. 226, 66–77. https://doi.org/10.1093/gji/ggab090.
Lottmann, J., 1990. The Middle Givetian pumilio-Events a tool for high time resolution and event-stratigraphical correlation. In: Kauffman, E.G., Walliser, O.H. (Eds.), Lecture Notes in Earth Sciences. Springer, Berlin, Heidelberg, pp. 145–149. https://doi.org/10.1007/bfb0011142.
Løvlie, R., Torsvik, T., Jelenska, M., Levandowski, M., 1984. Evidence for detrital remanent magnetization carried by hematite in Devonian red beds from Spitsbergen; palaeomagnetic implications. Geophys. J. R. Astron. Soc. 79, 573–588. https://doi.org/10.1111/j.1365-246X.1984.tb02242.x.
Mac Niocaill, C., Smethurst, M.A., 1994. Palaeozoic palaeogeography of Laurentia and its margins: a reassessment of palaeomagnetic data. Geophys. J. Int. 116, 715–725. https://doi.org/10.1111/j.1365-246X.1994.tb03292.x.
Małkowski, K., Racki, G., 2009. A global biogeochemical perturbation across the Silurian-Devonian boundary: Ocean-continent-biosphere feedbacks. Palaeogeogr. Palaeoclimatol. Palaeoecol. https://doi.org/10.1016/j.palaeo.2009.03.010.
Marcilly, C.M., Torsvik, T.H., Domeier, M., Royer, D.L., 2021. New paleogeographic and degassing parameters for long-term carbon cycle models. Gondwana Res. 97, 176–203. https://doi.org/10.1016/j.gr.2021.05.016.
Maron, M., Muttoni, G., Rigo, M., Gianolla, P., Kent, D.V., 2019. New magnetobiostratigraphic results from the Ladinian of the Dolomites and implications for the Triassic geomagnetic polarity timescale. Palaeogeogr. Palaeoclimatol. Palaeoecol. 517, 52–73. https://doi.org/10.1016/j.palaeo.2018.11.024.
Marshall, J.E.A., 2021. A terrestrial Devonian-Carboniferous boundary section in East Greenland. Palaeobiodiversity and Palaeoenvironments 101, 541–559. https://doi.org/10.1007/s12549-020-00448-x.
Marshall, J.E.A., Lakin, J., Troth, I., Wallace-Johnson, S.M., 2020. UV-B radiation was the Devonian-Carboniferous boundary terrestrial extinction kill mechanism. Sci. Adv. 6, 1–9.
Martin, D.L., 1975. Devonian Columbus limestone of Ohio: a possible stratigraphic tool. Tectonophysics 28, 125–134.
McCabe, C., Elmore, R.D., 1989. The occurrence and origin of Late Paleozoic remagnetization in the sedimentary rocks of North America. Rev. Geophys. 27, 471–494. https://doi.org/10.1029/RG027i004p00471.
McFadden, P.L., McElhinny, M.W., 1988. The combined analysis of remagnetization circles and direct observations in palaeomagnetism. Earth Planet. Sci. Lett. 87, 161–172.
McFadden, P.L., Merrill, R.T., 1984. Lower mantle convection and geomagnetism. J. Geophys. Res. 89, 3354–3362. https://doi.org/10.1029/JB089iB05p03354.
McGhee, G.R., Racki, G., 2021. Extinction: Late Devonian mass extinction. In: Encyclopedia of Life Sciences. John Wiley & Sons, pp. 1–12. https://doi.org/10.1002/9780470015902.a0029301.
McGhee, G.R., Clapham, M.E., Sheehan, P.M., Bottjer, D.J., Droser, M.L., 2013. A new ecological-severity ranking of major Phanerozoic biodiversity crises. Palaeogeogr. Palaeoclimatol. Palaeoecol. 370, 260–270. https://doi.org/10.1016/j.palaeo.2012.12.019.
Meert, J.G., van der Voo, R., Powell, C.M., Li, Z.-X., McElhinny, M.W., Chen, Z., Symons, D.T.A., 1993. A plate-tectonic speed limit ? Nature 363, 216–217.
Meert, J.G., Levashova, N.M., Bazhenov, M.L., Landing, E., 2016. Rapid changes of magnetic Field polarity in the late Ediacaran: Linking the Cambrian evolutionary radiation and increased UV-B radiation. Gondwana Res. 34, 149–157. https://doi.org/10.1016/j.gr.2016.01.001.

Middleton, M.F., Schmidt, P.W., 1982. Paleothermometry of the Sydney Basin. J. Geophys. Res. 87, 5351–5359. https://doi.org/10.1029/JB087iB07p05351.
Minguez, D., Kodama, K.P., Engelder, T., 2016. Paleomagnetism of the Oatka Creek Member of the Marcellus Formation: A Devonian paleopole for North America. Geol. Soc. Am. Bull. 128, 707–718. https://doi.org/10.1130/b31291.1.
Morel, P., Irving, E., 1978. Tentative Paleocontinental Maps for the Early Phanerozoic and Proterozoic. J. Geol. 86, 535–561. https://doi.org/10.1086/649724.
Mullender, T.A.T., Velzen, A.J., Dekkers, M.J., 1993. Continuous drift correction and separate identification of ferrimagnetic and paramagnetic contributions in thermomagnetic runs. Geophys. J. Int. 114, 663–672. https://doi.org/10.1111/j.1365-246X.1993.tb06995.x.
Mullender, T.A.T., Frederichs, T., Hilgenfeldt, C., de Groot, L.V., Fabian, K., Dekkers, M. J., 2016. Automated paleomagnetic and rock magnetic data acquisition with an in-line horizontal "2G" system. Geochem. Geophys. Geosyst. 17, 3546–3559. https://doi.org/10.1002/2016GC006436.
Narkiewicz, M., Racki, G., 1984. Stratigraphy of the Devonian of the Debnik anticline. Kwartalnik Geol. 28, 513–546.
Nawrocki, J., 1993. The Devonian-Carboniferous platform paleomagnetic directions from the Silesian-Cracow area and their importance for Variscan paleotectonic reconstructions. Kwartalnik Geol. 37, 397–430.
Nawrocki, J., 1995. Palaeomagnetic constraints for Variscan mobilism of the Upper Silesian and Malopolska Massifs, southern Poland - discussion. Kwartalnik Geol. 39, 211–229.
Nawrocki, J., Fanning, M., Lewandowska, A., Polechońska, O., Werner, T., 2008. Palaeomagnetism and the age of the Cracow volcanic rocks (S Poland). Geophys. J. Int. 174, 475–488. https://doi.org/10.1111/j.1365-246X.2008.03804.x.
Niedźwiedzki, G., Szrek, P., Narkiewicz, K., Narkiewicz, M., Ahlberg, P.E., 2010. Tetrapod trackways from the early Middle Devonian period of Poland. Nature 463, 43–48. https://doi.org/10.1038/nature08623.
Nysæther, E., Torsvik, T.H., Feist, R., Walderhaug, H.J., Eide, E.A., 2002. Ordovician palaeogeography with new palaeomagnetic data from the Montagne Noire (Southern France). Earth Planet. Sci. Lett. 203, 329–341. https://doi.org/10.1016/S0012-821X(02)00847-6.
Ogg, J.G., Smith, A.G., 2004. The geomagnetic polarity time scale. A Geol. Time Scale 2004, 63–86. https://doi.org/10.1017/CBO9780511536045.006.
Ogg, J.G., Ogg, G.M., Gradstein, F.M., 2016a. Devonian. A Concise Geol. Time Scale 1996, 85–103. https://doi.org/10.1002/9781444313413.ch3.
Ogg, J.G., Ogg, G.M., Gradstein, F.M., 2016b. Carboniferous. A Concise Geol. Time Scale 99–113. https://doi.org/10.1007/BF00812525.
Oliver, J., 1992. The spots and stains of plate tectonics. Earth Sci. Rev. 32, 77–106. https://doi.org/10.1016/0012-8252(92)90013-J.
Paschall, O., Carmichael, S.K., Königshof, P., Waters, J.A., Ta, P.H., Komatsu, T., Dombrowski, A., 2019. The Devonian-Carboniferous boundary in Vietnam: Sustained ocean anoxia with a volcanic trigger for the Hangenberg Crisis? Glob. Planet. Chang. 175, 64–81. https://doi.org/10.1016/j.gloplacha.2019.01.021.
Pastor-Galán, D., Ursem, B., Meere, P.A., Langereis, C., 2015. Extending the Cantabrian Orocline to two continents (from Gondwana to Laurussia). Paleomagnetism from South Ireland. Earth Planet. Sci. Lett. 432, 223–231. https://doi.org/10.1016/j.epsl.2015.10.019.
Pavlov, V.E., Gallet, Y., 2005. A third superchron during the Early Paleozoic. Episodes 28, 1–7.
Pedder, A.E.H., 2017. Benthic biostratigraphy of the upper Eifelian (Devonian) Hume Formation at Hume River (type locality), northern Mackenzie Mountains, Northwest Territories, Canada. Stratigraphy 14, 349–364.
Percival, L.M.E., Selby, D., Bond, D.P.G., Rakociński, M., Racki, G., Marynowski, L., Adatte, T., Spangenberg, J.E., Föllmi, K.B., 2019. Pulses of enhanced continental weathering associated with multiple Late Devonian climate perturbations: Evidence from osmium-isotope compositions. Palaeogeogr. Palaeoclimatol. Palaeoecol. 524, 240–249. https://doi.org/10.1016/j.palaeo.2019.03.036.
Perrin, M., Prévot, M., 1988. Uncertainties about the Proterozoic and Paleozoic polar wander path of the West African craton and Gondwana: evidence for successive remagnetization events. Earth Planet. Sci. Lett. 88, 337–347. https://doi.org/10.1016/0012-821X(88)90090-8.
Peters, K.E., Cassa, M.R., 1994. Applied source rock geochemistry: chapter 5: part II. essential elements. In: Magoon, L.B., Dow, W.G. (Eds.), The Petroleum System–From Source to Trap: AAPG Memoir 60. AAPG, pp. 93–120.
Piper, J.D.A., 2006. A ~ 90° Late Silurian-Early Devonian apparent polar wander loop: The latest inertial interchange of planet earth? Earth Planet. Sci. Lett. 250, 345–357. https://doi.org/10.1016/j.epsl.2006.08.001.
Piper, J.D.A., 2007. Palaeomagnetism of the Loch Doon Granite Complex, Southern Uplands of Scotland: the Late Caledonian palaeomagnetic record and an Early Devonian episode of True Polar Wander. Tectonophysics 432, 133–157. https://doi.org/10.1016/j.tecto.2006.12.009.
Pisarzowska, A., Rakociński, M., Marynowski, L., Szczerba, M., Thoby, M., Paszkowski, M., Perri, M.C., Spalletta, C., Schönlaub, H.P., Kowalik, N., Gereke, M., 2020. Large environmental disturbances caused by magmatic activity during the Late Devonian Hangenberg Crisis. Glob. Planet. Chang. 190, 103155 https://doi.org/10.1016/j.gloplacha.2020.103155.
Poty, E., Berkowski, B., Chevalier, E., Hance, L., 2007. Biostratigraphic and sequence stratigraphic correlations between the Dinantian deposits of Belgium and Southern Poland (Krakow area). In: Proceedings of the XVth International Congress on Carboniferous and Permian Stratigraphy. Utrecht, the Netherlands, 10-16 August 2003, pp. 97–107.
Powerman, V., Shatsillo, A., Coe, R., Zhao, X., Gladkochub, D., Buchwaldt, R., Pavlov, V., 2013. Palaeogeography of the Siberian platform during middle Palaeozoic Times (~450-400 Ma): New palaeomagnetic evidence from the Lena and Nyuya rivers. Geophys. J. Int. 194, 1412–1440. https://doi.org/10.1093/gji/ggt197.
Prestianni, C., Gerrienne, P., 2010. Early seed plant radiation: An ecological hypothesis. Geol. Soc. Spec. Publ. 339, 71–80. https://doi.org/10.1144/SP339.7.
Pullaiah, G., Irving, E., Buchan, K.L., Dunlop, D.J., 1975. Magnetization changes caused by burial and uplift. Earth Planet. Sci. Lett. 28, 133–143. https://doi.org/10.1016/0012-821X(75)90221-6.
Racki, G., 2020. A volcanic scenario for the Frasnian–Famennian major biotic crisis and other Late Devonian global changes: More answers than questions? Glob. Planet. Chang. 189 https://doi.org/10.1016/j.gloplacha.2020.103174.
Racki, G., Piechota, A., Bond, D., Wignall, P.B., 2004. Geochemical and ecological aspects of lower Frasnian pyrite-ammonoid level at Kostomłoty (Holy Cross Mountains, Poland). Geol. Q. 48, 267–282.
Racki, G., Rakocinski, M., Marynowski, L., Wignall, P.B., 2018. Mercury enrichments and the Frasnian-Famennian biotic crisis: A volcanic trigger proved? Geology 46, 543–546. https://doi.org/10.1130/G40233.1.
Rejebian, V.A., Harris, A.G., Huebner, J.S., 1987. Conodont color and textural alteration: An index to regional metamorphism, contact metamorphism and hydrothermal alteration. Bull. Geol. Soc. Am. 99, 471–479. https://doi.org/10.1130/0016-7606(1987)99<471:CCATAA>2.0.CO;2.
Ribbert, K.-H., 1983. Geologische Karte von Nordrhein-Westfalen 1:25000 Erlauterungen 5505 Blankenheim. Geologische Karte von Nordrhein-Westfalen 1:25000.
Roberts, A.P., 2015. Magnetic mineral diagenesis. Earth-Science Rev. 151, 1–47. https://doi.org/10.1016/j.earscirev.2015.09.010.
Roberts, A.P., Almeida, T.P., Church, N.S., Harrison, R.J., Heslop, D., Li, Y., Li, J., Muxworthy, A.R., Williams, W., Zhao, X., 2017. Resolving the Origin of Pseudo-Single Domain Magnetic Behavior. J. Geophys. Res. Solid Earth 122, 9534–9558. https://doi.org/10.1002/2017JB014860.
Rosenqvist, L., Opgenoorth, H., Buchert, S., McCrea, I., Amm, O., Lathuillere, C., 2005. Extreme solar-terrestrial events of October 2003: High-latitude and Cluster observations of the large geomagnetic disturbances on 30 October. J. Geophys. Res. Sp. Phys. 110 https://doi.org/10.1029/2004JA010927.
Sallomy, J.T., Piper, J.D.A., 1973. Palaeomagnetic Studies in the British Caledonides—II The Younger Gabbros of Aberdeenshire. Scotland. Geophys. J. R. Astron. Soc. 34, 13–25. https://doi.org/10.1111/j.1365-246X.1973.tb02383.x.
Sandberg, C.A., Morrow, J.R., Ziegler, W., 2002. Late Devonian sea-level changes, catastrophic events, and mass extinctions. Spec. Pap. Geol. Soc. Am. 356, 473–487. https://doi.org/10.1130/0-8137-2356-6.473.
Schätz, M., Zwing, A., Tait, J., Belka, Z., Soffel, H.C., Bachtadse, V., 2006. Paleomagnetism of Ordovician carbonate rocks from Malopolska Massif, Holy Cross Mountains, SE Poland - Magnetostratigraphic and geotectonic implications. Earth Planet. Sci. Lett. 244, 349–360. https://doi.org/10.1016/j.epsl.2006.01.061.
Schmidt, P.W., Embleton, B.J.J., Cudahy, T.J., Powell, C.M.A., 1986. Prefolding and premegakinking magnetizations from the Devonian Comerong Volcanics, New South Wales, Australia, and their bearing on the Gondwana Pole Path. Tectonics 5, 135–150. https://doi.org/10.1029/TC005i001p00135.
Scotese, C.R., Song, H., Mills, B.J.W., van der Meer, D.G., 2021. Phanerozoic paleotemperatures: The earth's changing climate during the last 540 million years. Earth Sci, Rev, p. 215.
Self, S., 2015. Explosive Super-Eruptions and Potential Global Impacts, Volcanic Hazards, Risks, and Disasters. Elsevier Inc. https://doi.org/10.1016/B978-0-12-396453-3.00016-2
Shatsillo, A.V., Pavlov, V.E., 2019. Systematics of Paleomagnetic Directions from Early–Middle Devonian Rocks of Minusa Troughs: New Data and Old Problems. Izv. Phys. Solid Earth 55, 471–487. https://doi.org/10.1134/S1069351319030091.
Shcherbakova, V.V., Biggin, A.J., Veselovskiy, R.V., Shatsillo, A.V., Hawkins, L.M.A., Shcherbakov, V.P., Zhidkov, G.V., 2017. Was the Devonian geomagnetic field dipolar or multipolar? Palaeointensity studies of Devonian igneous rocks from the Minusa Basin (Siberia) and the Kola Peninsula dykes. Russia. Geophys. J. Int. 209, 1265–1286. https://doi.org/10.1093/gji/ggx085.
Shcherbakova, V.V., Bakhmutov, V.G., Thallner, D., Shcherbakov, V.P., Zhidkov, G.V., Biggin, A.J., 2020. Ultra-low palaeointensities from East European Craton, Ukraine support a globally anomalous palaeomagnetic field in the Ediacaran. Geophys. J. Int. 220, 1920–1946. https://doi.org/10.1093/gji/ggz566.
Shcherbakova, V.V., Zhidkov, G.V., Shcherbakov, V.P., Golovanova, I.V., Danukalov, K. N., Salmanova, R.Y., 2021. Ultra-low geomagnetic field intensity in the Devonian obtained from the Southern Ural Rock Studies. Izv. Phys. Solid Earth 57, 900–912. https://doi.org/10.1134/s1069351321060070.
Siscoe, G.L., Chen, C.-K., 1975. The paleomagnetosphere. J. Geophys. Res. 80, 4675–4680. https://doi.org/10.1029/ja080i034p04675.
Smethurst, M.A., Khramov, A.N., 1992. A new Devonian palaeomagnetic pole for the Russian platform and Baltica, and related apparent polar wander. Geophys. J. Int. 108, 179–192. https://doi.org/10.1111/j.1365-246X.1992.tb00848.x.
Smirnov, A.V., Tarduno, J.A., Kulakov, E.V., McEnroe, S.A., Bono, R.K., 2016. Palaeointensity, core thermal conductivity and the unknown age of the inner core. Geophys. J. Int. 205, 1190–1195. https://doi.org/10.1093/gji/ggw080.
Smirnov, A.V., Kulakov, E.V., Foucher, M.S., Bristol, K.E., 2017. Intrinsic paleointensity bias and the long-term history of the geodynamo. Sci. Adv. 3, 1–8. https://doi.org/10.1126/sciadv.1602306.
Sprain, C.J., Swanson-Hysell, N.L., Fairchild, L.M., Gaastra, K., 2018. A field like today's? The strength of the geomagnetic field 1.1 billion years ago. Geophys. J. Int. 213, 1969–1983. https://doi.org/10.1093/gji/ggy074.
Stadelmann, A., 2004. Globale Effekte einer Erdmagnetfeldumkehrung: Magnetosphärenstruktur und kosmische Teilchen. Technischen Universität Carolo-Wilhelmina zu Braunschweig, Braunschweig.

Stearns, C., Van Der Voo, R., Abrahamsen, N., 1989. A new Siluro-Devonian paleopole from Early Paleozoic rocks of the Franklinian Basin, North Greenland Fold Belt. J. Geophys. Res. 94, 669–683. https://doi.org/10.1029/jb094ib08p10669.

Strother, P.K., Servais, T., Vecoli, M., 2010. The effects of terrestrialization on marine ecosystems: The fall of CO2. Geol. Soc. Spec. Publ. 339, 37–48. https://doi.org/10.1144/SP339.4.

Suttner, T.J., Kido, E., Joachimski, M.M., Vodrážková, S., Pondrelli, M., Corradini, C., Corriga, M.G., Simonetto, L., Kubajko, M., 2021. Paleotemperature record of the Middle Devonian Kačák Episode. Sci. Rep. 11, 1–10. https://doi.org/10.1038/s41598-021-96013-3.

Tarduno, J.A., Cottrell, R.D., Smirnov, A.V., 2002. The Cretaceous superchron geodynamo: Observations near the tangent cylinder. Proc. Natl. Acad. Sci. U. S. A. 99, 14020–14025. https://doi.org/10.1073/pnas.222373499.

Tarduno, J.A., Cottrell, R.D., Watkeys, M.K., Hofmann, A., Doubrovine, P.V., Mamajek, E.E., Liu, D., Sibeck, D.G., Neukirch, L.P., Usui, Y., 2010. Geodynamo, solar wind, and magnetopause 3.4 to 3.45 billion years ago. Science 327, 1238–1240. https://doi.org/10.1126/science.1183445.

Tauxe, L., 2010. Essentials of paleomagnetism. In: *Essentials of Paleomagnetism*. University of California Press.

Tauxe, L., Yamazaki, T., 2007. Paleointensities. In: Treatise on Geophysics. https://doi.org/10.1016/B978-044452748-6.00098-5.

Thallner, D., Biggin, A.J., Halls, H.C., 2021. An extended period of extremely weak geomagnetic field suggested by palaeointensities from the Ediacaran Grenville dykes (SE Canada). Earth Planet. Sci. Lett. 568, 117025 https://doi.org/10.1016/j.epsl.2021.117025.

Thébault, E., Finlay, C.C., Beggan, C.D., Alken, P., Aubert, J., Barrois, O., Bertrand, F., Bondar, T., Boness, A., Brocco, L., Canet, E., Chambodut, A., Chulliat, A., Coïsson, P., Civet, F., Du, A., Fournier, A., Fratter, I., Gillet, N., Hamilton, B., Hamoudi, M., Hulot, G., Jager, T., Korte, M., Kuang, W., Lalanne, X., Langlais, B., Léger, J.M., Lesur, V., Lowes, F.J., Macmillan, S., Mandea, M., Manoj, C., Maus, S., Olsen, N., Petrov, V., Ridley, V., Rother, M., Sabaka, T.J., Saturnino, D., Schachtschneider, R., Sirol, O., Tangborn, A., Thomson, A., Tøffner-Clausen, L., Vigneron, P., Wardinski, I., Zvereva, T., 2015. International geomagnetic reference field: The 12th generation. Earth, Planets Sp. 67 https://doi.org/10.1186/s40623-015-0228-9.

Thominski, H.P., Wohlenberg, J., Bleil, U., 1993. The remagnetization of Devono-Carboniferous sediments from the Ardenno-Rhenish Massif. Tectonophysics 225, 411–431. https://doi.org/10.1016/0040-1951(93)90307-6.

Thorning, L., 1974. Palaeomagnetic Results from Lower Devonian Rocks of the Cheviot Hills, Northern England. Geophys. J. R. Astron. Soc. 36, 487–496. https://doi.org/10.1111/j.1365-246X.1974.tb03650.x.

Tonarová, P., Vodrážková, S., Ferrová, L., de la Puente, G.S., Hints, O., Frýda, J., Kubajko, M., 2017. Palynology, microfacies and biostratigraphy across the Daleje Event (Lower Devonian, lower to upper Emsian): new insights from the offshore facies of the Prague Basin, Czech Republic. Palaeobiodiversity and Palaeoenvironments 97, 419–438. https://doi.org/10.1007/s12549-017-0274-3.

Torsvik, T.H., 2019. Earth history: A journey in time and space from base to top. Tectonophysics 760, 297–313. https://doi.org/10.1016/j.tecto.2018.09.009.

Torsvik, T.H., Cocks, L.R.M., 2013. New global palaeogeographical reconstructions for the Early Palaeozoic and their generation. Geol. Soc. Mem. 38, 5–24. https://doi.org/10.1144/M38.2.

Torsvik, T.H., van der Voo, R., Preeden, U., Mac Niocaill, C., Steinberger, B., Doubrovine, P.V., van Hinsbergen, D.J.J., Domeier, M., Gaina, C., Tohver, E., Meert, J.G., McCausland, P.J.A., Cocks, L.R.M., 2012. Phanerozoic polar wander, palaeogeography and dynamics. Earth-Science Rev. https://doi.org/10.1016/j.earscirev.2012.06.002.

Torsvik, T.H., Van Der Voo, R., Doubrovine, P.V., Burke, K., Steinberger, B., Ashwal, L.D., Trønnes, R.G., Webb, S.J., Bull, A.L., 2014. Deep mantle structure as a reference frame for movements in and on the Earth. Proc. Natl. Acad. Sci. U. S. A. 111, 8735–8740. https://doi.org/10.1073/pnas.1318135111.

Tsandev, I., Slomp, C.P., 2009. Modeling phosphorus cycling and carbon burial during Cretaceous Oceanic Anoxic Events. Earth Planet. Sci. Lett. 286, 71–79. https://doi.org/10.1016/j.epsl.2009.06.016.

Uyeno, T.T., Pedder, A.E.H., Uyeno, T.A., 2017. Conodont biostratigraphy and T-R cycles of the Middle Devonian Hume Formation at Hume River (type locality), northern Mackenzie Mountains, Northwest Territories, Canada. Stratigraphy 14, 391–404. https://doi.org/10.29041/strat.14.1-4.391-404.

van der Boon, A., Kuiper, K.F., Villa, G., Renema, W., Meijers, M.J.M., Langereis, C.G., Aliyeva, E., Krijgsman, W., 2017. Onset of Maikop sedimentation and cessation of Eocene arc volcanism in the Talysh Mountains, Azerbaijan. Geol. Soc. London. Spec. Publ. 428, 145–169. https://doi.org/10.1144/sp428.3.

Van der Voo, R., 1990. The reliability of paleomagnetic data. Tectonophysics 184, 1–9. https://doi.org/10.1016/0040-1951(90)90116-P.

van der Voo, R., 1994. True polar wander during the middle Paleozoic? Earth Planet. Sci. Lett. 122, 239–243.

van der Voo, R., Torsvik, T.H., 2012. The history of remagnetization of sedimentary rocks: Deceptions, developments and discoveries. Geol. Soc. Spec. Publ. 371, 23–53. https://doi.org/10.1144/SP371.2.

van Velzen, A.J., Zijderveld, J.D.A., 1995. Effects of weathering on single-domain magnetite in Early Pliocene marine marls. Geophys. J. Int. 121, 267–278. https://doi.org/10.1111/j.1365-246X.1995.tb03526.x.

Vérard, C., 2004. Palaeozoic Palaeomagnetism of South-Eastern Australia: Implications for the APW path of Gondwana. University of Munich.

Vogt, J., Zieger, B., Glassmeier, K.H., Stadelmann, A., Kallenrode, M.B., Sinnhuber, M., Winkler, H., 2007. Energetic particles in the paleomagnetosphere: Reduced dipole configurations and quadrupolar contributions. J. Geophys. Res. Sp. Phys. 112, 1–13. https://doi.org/10.1029/2006JA012224.

Voigt, G.H., 1995. Magnetospheric configuration. In: Handbook of Atmospheric Electrodynamics. Taylor & Francis, Boca Raton. https://doi.org/10.1201/9780203713297.

Walliser, O.H., 1996. Global Events in the Devonian and Carboniferous. In: Global Events and Event Stratigraphy in the Phanerozoic, pp. 225–250. https://doi.org/10.1007/978-3-642-79634-0_11.

Weil, A.B., Van der Voo, R., 2002. Insights into the mechanism for orogen-related carbonate remagnetization from growth of authigenic Fe-oxide: A scanning electron microscopy and rock magnetic study of Devonian carbonates from northern Spain. J. Geophys. Res. Solid Earth 107. https://doi.org/10.1029/2001jb000200. EPM 1-1-EPM 1-14.

Witzke, B.J., 1990. Palaeoclimates constrains for palaeozoic Palaeolatitudes of Laurentia and Euramerica. Geol. Soc. Mem. 12, 57–73. https://doi.org/10.1144/GSL.MEM.1990.012.01.05.

Witzke, B.J., Heckel, P.H., 1988. Paleoclimatic indicators and inferred Devonian paleolatitudes of Euramerica. In: Devonian of the World: Proceedings of the 2nd International Symposium on the Devonian System - Memoir, 14, pp. 49–63.

Wójcik, K., 2012. Famennian Fusulinina (Foraminifera) from the Holy Cross Mountains (central Poland). Geol. J. 47, 594–615. https://doi.org/10.1002/gj.2419.

Wolniewicz, P., 2009. Late Famennian Stromatoporoids from Dębnik Anticline, Southern Poland. Acta Palaeontol. Pol. 54, 337–350. https://doi.org/10.4202/app.2007.0096.

Zahirovic, S., Müller, R.D., Seton, M., Flament, N., 2015. Tectonic speed limits from plate kinematic reconstructions. Earth Planet. Sci. Lett. 418, 40–52. https://doi.org/10.1016/j.epsl.2015.02.037.

Zegers, T.E., Dekkers, M.J., Bailly, S., 2003. Late Carboniferous to Permian remagnetization of Devonian limestones in the Ardennes: Role of temperature, fluids, and deformation. J. Geophys. Res. Solid Earth 108, n/a-n/a. https://doi.org/10.1029/2002JB002213.

Zhang, Y., Hou, M., Liu, G., Zhang, C., Prakapenka, V.B., Greenberg, E., Fei, Y., Cohen, R. E., Lin, J.F., 2020. Reconciliation of experiments and theory on transport properties of iron and the geodynamo. Phys. Rev. Lett. 125, 78501. https://doi.org/10.1103/PhysRevLett.125.078501.

Ziegler, W., Sandberg, C.A., 1997. Proposal of boundaries for a Late Frasnian Substage and for subdivision of the Famennian Stage into three Substages. SDS Newsl. 14, 11–12.

Zijderveld, J.D.A., 1967. AC demagnetization of rocks: analysis of results. In: Collinson, D.W., Creer, K.M. (Eds.), Methods in Paleomagnetism. Elsevier, Amsterdam, pp. 254–286.

Zwing, A., 2003. Causes and mechanisms of remagnetisation in Palaeozoic sedimentary rocks. In: A Multidisciplinary Approach. Ludwig-Maximilians-Universitat Munchen.

Zwing, A., Bachtadse, V., 2000. Paleoposition of the northern margin of Armorica in Late Devonian times: Paleomagnetic and rock magnetic results from the Frankenstein Intrusive Complex (Mid-German Crystalline Rise). J. Geophys. Res. Solid Earth 105, 21445–21456. https://doi.org/10.1029/2000jb900167.

Zwing, A., Matzka, J., Bachtadse, V., Soffel, H.C., 2005. Rock magnetic properties of remagnetized Palaeozoic clastic and carbonate rocks from the NE Rhenish massif. Germany. Geophys. J. Int. 160, 477–486. https://doi.org/10.1111/j.1365-246X.2004.02493.x.